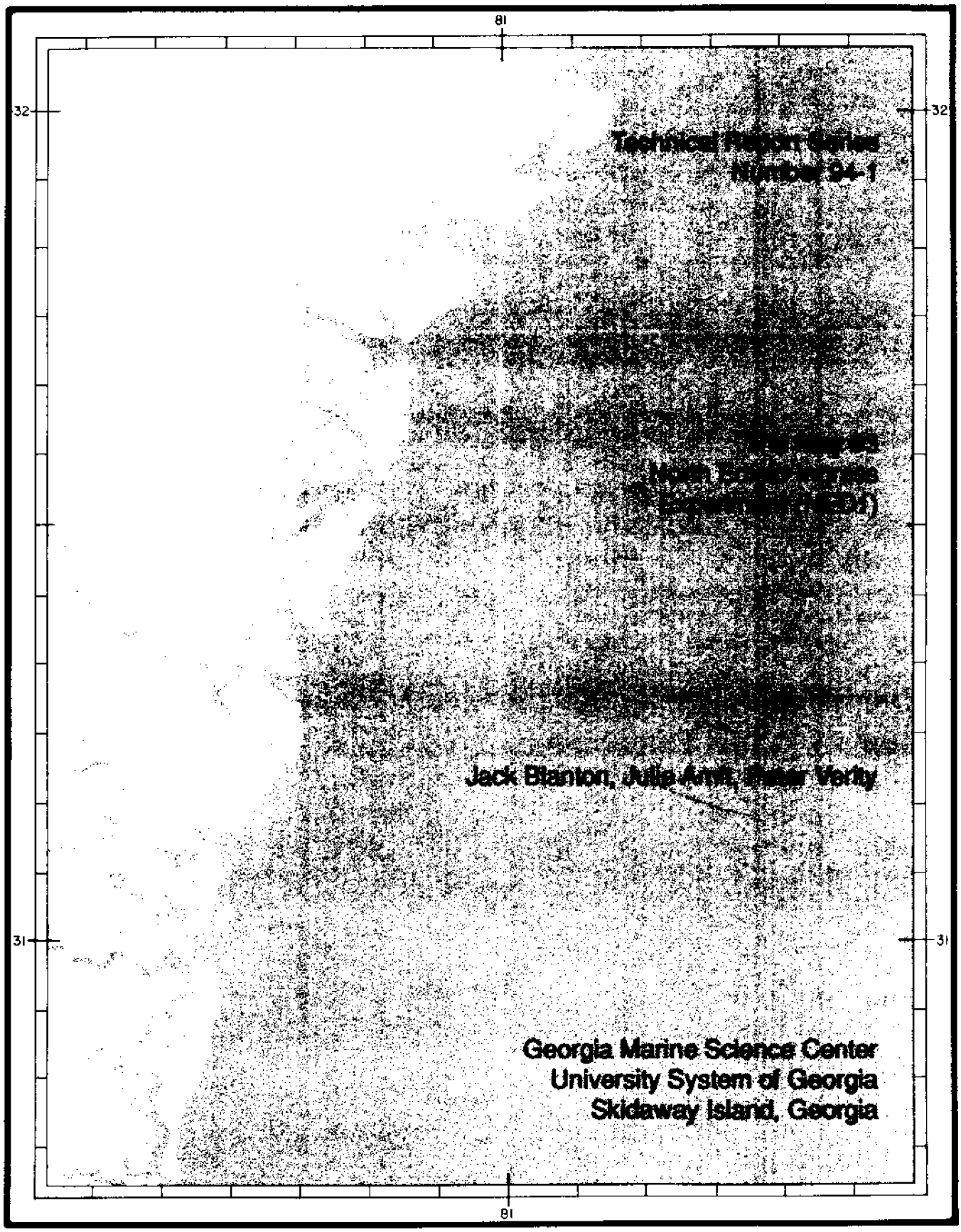

Technical Report Series
Number 94-1

Jack Blanton, Julie Amft, Sheer Verity

Georgia Marine Science Center
University System of Georgia
Skidaway Island, Georgia

The May 93 North Edisto Ingress Experiment (NED1)

Technical Report 94-1

J. Blanton, J. Amft, and P. Verity

Skidaway Institute of Oceanography
10 Ocean Science Circle
Savannah, Georgia 31411

The Technical Report Series of the Georgia Marine Science Center is issued by the Georgia Sea Grant College Program and the Marine Extension Service of the University of Georgia on Skidaway Island (30 Ocean Science Circle, Savannah, Georgia 31411). It was established to provide dissemination of technical information and progress reports resulting from marine studies and investigations mainly by staff and faculty of the University System of Georgia. In addition, it is intended for the presentation of techniques and methods, reduced data, and general information of interest to industry, local, regional, and state governments and the public. Information contained in these reports is in the public domain. If this pre-publication copy is cited, it should be sited as an unpublished manuscript. This work was sponsored by joint grants from the Georgia Sea Grant Program (Grant No. R/EA-15) to the Skidaway Institute of Oceanography and the South Carolina Sea Grant Consortium (Grant No. 93277) to the South Carolina Marine Resource Research Institute.

ACKNOWLEDGEMENTS

We wish to express our appreciation to the several individuals without whose help this project would not have been possible. First, our thanks go to Marsha Ward who participated in the cruises and Lane Mitcham of Skidaway Institute who developed much of the instrumentation and software used in the ODIS system aboard the BLUE FIN. Next, we thank Charlie Barans, Betty Wenner, Bruce Stender and David Knott of the South Carolina Marine Resources Research Institute, our scientific partners in this project. We also appreciate the able support of Captain Jay Fripp and crew Raymond Sweatte and Chris Knight of the R/V BLUE FIN, and Captain Paul Tucker of the R/V ANITA.

This work was sponsored by joint grants from the Georgia Sea Grant Program (Grant No. R/EA-15) to the Skidaway Institute of Oceanography and the South Carolina Sea Grant Consortium (Grant No. 93277) to the SC Marine Resource Research Institute.

ABSTRACT

The ingress of postlarval crustaceans through inlets is a potential bottleneck to recruitment. A joint oceanographic and fishery program was designed to identify the physical oceanographic transport processes that control the ingress of postlarval blue crab and white shrimp through an inlet. A 14-day experiment was conducted in and off the South Carolina coast utilizing a combination of moored instrumentation and shipboard surveys. Two research vessels operated in the inlet and offshore to measure vertical profiles of conductivity, temperature, depth, and chl *a* as well as larval abundance.

The estuary was essentially well-mixed during upwelling with stratified water offshore. The abrupt salinity disconnection from vertically well-mixed to stratified between offshore waters and estuarine waters suggests weak coupling between estuarine and coastal waters. The estuary was also well-mixed during downwelling but chl *a* concentrations were higher. Salinity on the shelf was vertically uniform, consistent with strong vertical mixing. Coupling of coastal and estuarine waters was optimized during this period when downwelling-favorable winds plus spring tides efficiently transported oceanic water into the estuary. Both salinity and chlorophyll *a* increased most rapidly in the inlet during downwelling winds and the onset of spring tidal conditions. Chl *a* concentration generally increased with depth suggesting a benthic source. A near-bottom chl *a* maxima was present along the ebb tide delta between the inlet mouth and the coastal front. It was positively correlated with salinity reflecting higher chl *a* in the more-saline water where the coastal front intersects the bottom along the offshore portion of the inlet delta.

Abundances of postlarval *Penaeus* were usually greatest in surface samples. Peaks abundances in the inlet coincided with downwelling conditions suggesting that larval ingress is enhanced then.

Keywords: Shrimp, Coastal, Estuaries, Fisheries, South Carolina, Hydrodynamics, Hdyrography, Inlet, Larvae, Meteorology, Oceanography, Plankton, Recruitment, Upwelling, Downwelling, Fronts

LIST OF TABLES

Table 1. Moored instrumentation used during NED1 in May 1993. p. 31

Table 2a. R/V BLUE FIN station log for NED1. p. 32

Table 2b. R/V ANITA station log for NED1. p. 34

Table 3. First order statistics for parameters measured during NED1. The station location and depth above bottom are designated for each sensor. All parameters with x- and y-components have been rotated 50 degrees counter-clockwise. Series with a length of 15.25 days begin 13 May 1993 at 18 GMT and end 29 May 1993 at 00 GMT; series with a length of 11.75 days begin 15 May 1993 at 00 GMT and end 26 May 1993 at 18 GMT. (a) 3hlp data; (b) 40hlp data. p. 36

Table 4. First order statistics using 3hlp data for parameters measured for 2 tidal cycles each during the neap and spring tide of NED1. The station location and depth above bottom are designated for each sensor. All parameters with x- and y-components have been rotated 50 degrees counter-clockwise. (a) Neap tide

data begin 15 May 1993 at 09 GMT and end 16 May 1993 at 09 GMT; (b) spring tide data begin 22 May 1993 at 14 GMT and end 23 May 1993 at 14 GMT. p. 37

Table 5. First order statistics using 40hlp data for parameters measured for two events (one upwelling and one downwelling) during NED1. The station location and depth above bottom are designated for each sensor. All parameters with x- and y-components have been rotated 50 degrees counter-clockwise.
(a) The upwelling event begins 16 May 1993 at 12 GMT and ends 19 May 1993 at 12 GMT;
(b) the downwelling event begins 21 May 1993 at 00 GMT and ends 23 May 1993 at 00 GMT. p. 38

LIST OF FIGURES

Fig. 1. Location maps showing bathymetry and station locations for moorings and ship sampling. (a) Offshore domain covered by R/V BLUE FIN; (b) inlet domain covered primarily by R/V ANITA. p. 39

Fig. 2. Mooring design for stations M1 and M2 during NED1. p. 41

Fig. 3. Sampling times of offshore and inlet surveys in relation to cycles of tide and darkness. Predicted flood currents are positive and time is Eastern Daylight Savings Time. p. 42

Fig. 4. Calibration curves of CTD fluorometer voltage versus extracted chlorophyll *a*. (a) R/V ANITA; (b) R/V BLUE FIN. p. 43

Fig. 5. Time series of rotated wind stress at FBIS1. Hourly data have been smoothed with a 40-hour low-pass filter and rotated 50 degrees counter-clockwise. (a) Alongshelf and cross-shelf components; (b) vector plot. p. 44

Fig. 6. Time series of 3hlp current data from M1. (a) Wind stress component at FBIS1; (b) along-inlet current component (positive seaward); (c) cross-inlet current component (positive northeastward). p. 45

Fig. 7. Time series of 3hlp current data from M2. (a) Wind stress components at FBIS1; (b) cross-shelf component (positive offshore); (c) alongshelf component

(positive northeastward). p. 46

Fig. 8. Time series of 3hlp data from M1 and M2. (a) Temperature; (b) salinity; (c) σ_t; (d) subsurface pressure. p. 47

Fig. 9. Vector plots of 40hlp wind stress at FBIS1 and coastal currents at M2. p. 49

Fig. 10. Component plots of 40hlp wind stress at FBIS1 and coastal currents at M2. p. 50

Fig. 11. Time series plots of 40hlp data from M1 and M2. (a) Temperature; (b) salinity; (c) σ_t; (d) subsurface pressure. p. 51

Fig. 12. Oceanographic and larval survey OS1: 14-15 May 1993. (a) Salinity; b) chlorophyll *a*; (c) temperature (d) σ_t. See Figure 1 for station locations. p. 53

Fig. 13. Oceanographic and larval survey OS2: 15-16 May 1993. (a) Salinity; (b) chlorophyll *a*; (c) temperature (d) σ_t. See Figure 1 for station locations. p. 54

Fig. 14. Oceanographic and larval survey OS3: 20 May 1993. (a) Salinity; (b) chlorophyll *a*; (c) temperature (d) σ_t. See Figure 1 for station location. p. 55

Fig. 15. Oceanographic and larval survey OS4: 20-21 May 1993. (a) Salinity; (b) chlorophyll *a*; (c) temperature (d) σ_t. See Figure 1 for station locations. p. 56

Fig. 16. Oceanographic and larval survey OS5: 22 May 1993. (a) Salinity; (b) not available; (c) temperature (d) not available. See Figure 1 for station locations. Note: The InterOcean Systems S4 CTD used for this survey did not have a fluorometer and salinities for this survey have not yet been calibrated. p. 57

Fig. 17. Oceanographic and larval survey OS6: 23 May 1993. (a) Salinity; (b) chlorophyll *a*; (c) temperature (d) σ_t. See Figure 1 for station locations. p. 58

Fig. 18. Oceanographic and larval survey OS7: 24 May 1993. (a) Salinity; (b) chlorophyll *a*; (c) temperature (d) σ_t. See Figure 1 for station locations. p. 59

Fig. 19 Oceanographic and larval survey OS8: 25 May 1993. (a) Salinity; (b) chlorophyll *a*; (c) temperature (d) σ_t. See Figure 1 for station locations. p. 60

Fig. 20. Oceanographic and larval survey OS9: 25-26 May 1993. (a) Salinity; (b) chlorophyll *a*; (c) temperature (d) σ_t. See Figure 1 for station locations. p. 61

Fig. 21. Oceanographic and larval survey OS10: 26 May 1993. (a) Salinity; (b) chlorophyll *a*; (c) temperature (d) σ_t. See Figure 1 for station locations. p. 62

Fig. 22. Offshore oceanographic surveys conducted during high water and low water neap tide of 15 May 1993. See Figure 1 for station locations. p. 63

Fig. 23. Estuarine survey in the North Edisto River during low water neap tide of 15 May 1993. See Figure 1 for station locations. p. 64

Fig. 24. Estuarine surveys in the North Edisto River during high water and low water spring tide of 22 May 1993. See Figure 1 for station locations. p. 65

Fig. 25. Time versus depth plots during nighttime maximum flood current in the throat of North Edisto Inlet. (a) Salinity; (b) chlorophyll *a*; (c) temperature (d) σ_t. p. 66

Fig. 26. (a) Chlorophyll *a* versus salinity; (b) chlorophyll *a* versus σ_t and (c) chlorophyll *a* versus optical backscatter (400*volts) for all offshore stations. p. 67

Fig. 27. (a) Chlorophyll *a* versus salinity; (b) chlorophyll *a* versus σ_t and (c) chlorophyll *a* versus optical backscatter (400*volts) for all North Edisto Inlet stations. p. 68

Fig. 28. Density (No./100 m^3) of postlarval Penaeus from surface and bottom plankton samples taken during NED1, May 1993. Collections were made at night during flood tide. p. 69

Fig. 29. Composite sections of salinity and chlorophyll a during (a) neap tide on 15 May and (b) spring tide on 22 May. The shallow inlet delta is in the break between zones covered by the R/V ANITA in the estuary and those covered by R/V BLUE FIN offshore. See Figure 1 for station locations. p. 70

Fig. 30. Near-surface salinity and temperature data on 5 traverses between M1 and A6 using the ODIS flow-through system. The numbers for each line denote the May date of the survey. See Figure 1 for location of M1 and A6. p. 72

Table of Contents

Acknowledgements i

Abstract ii

List of Tables iv

List of Figures vi

Table of Contents xi

1.0 Purpose and Objectives 1

2.0 Oceanographic Methods Used 2

3.0 Results and Discussion 8

4.0 Summary 24

References 29

The May 93 North Edisto Ingress Experiment (NED1)

by

J. Blanton, J. Amft, and P. Verity

1.0 Purpose and Objectives

This report summarizes data and results from NED1, the May 1993 North Edisto Ingress Experiment. This was the first of a series of cruises designed to relate the spatial and temporal distribution of postlarval blue crab and white shrimp in inner shelf water entrained through an inlet to periodic (tidal, diel, lunar) and stochastic (wind, current) events. Our hypothesis is that the physical flow field interacts with the behavior and population biology of white shrimp and blue crab larvae to discontinuously transport developmental larval stages from offshore sites to estuarine nurseries. From a conceptual perspective, we view this transport as comprising two steps, each likely dominated by a different mechanism: (1) transport from seaward spawning or larval development sites into the coastal frontal zone (as for blue crab), and (2) transport from the coastal frontal region into the estuary.

Postlarvae are entrained into an inlet by an interaction of the alongshore coastal current with a landward influx of coastal water caused by alongshore wind stress and tidal currents. Determination of the portion of the coastal current from which landward withdrawal occurs requires a study of the configuration and extent of the coastal frontal zone. Circulation will differentially influence ingress of blue crab and white shrimp depending upon the vertical distribution of the postlarvae. The strength of the tidal current

over the lunar cycle has a neap-spring modulation. The ability of larvae to maintain themselves at a certain depth can be nullified by strong vertical mixing induced by strong tidal currents. The degree of vertical mixing encountered by the larvae will depend upon current friction at the seabed and the degree of vertical density stratification. The vertical density stratification is imposed by the ambient density structure of the coastal frontal zone and local freshwater discharges.

NED1 was designed to determine: (1) the hydrography of the coastal frontal zone adjacent to a study site and corresponding abundances of larvae or megalopae, (2) the hydrographic state of the inlet water and corresponding abundances of larvae or megalopae, and (3) the response of shelf and inlet waters to wind and tides.

NED1 was conducted in and off the North Edisto Inlet on the South Carolina coast (Fig. 1a) in May 1993. During spring, prevailing winds favor upwelling, and the coastal frontal zone is vertically stratified because of seasonally high freshwater discharge. White shrimp postlarvae are usually present in coastal waters at this time. The sampling period covered 14 days. Because the tidal cycle is 12.48 hrs (2 cycles in 24.96 hrs) and the diurnal cycle is 24 hrs, a sampling of the same tidal stage over the 14-day period covers a full cycle of spring-neap tides and half-cycle of sunlight.

2.0 Oceanographic methods used

We utilized a combination of moored instrumentation and shipboard sampling. One mooring was was positioned on the inner continental shelf to assess the response of the alongshelf current to wind forcing and another mooring was deployed within the deep inlet

channel to monitor the strong tidal currents there. Instruments at both moorings were placed in the lower half of the water column to measure currents, temperature, salinity and density, and subsurface pressure.

The temporal resolution of currents and water masses at a few discrete points was supplemented by frequent hydrographic and larval abundance surveys both in the inlet and offshore. Thus, the combined synthesis of *in situ* data and shipboard data from NED1 provided us the means to determine: (1) the temporal variations in coastal water advected into the inlet; (2) the location of larval populations relative to the coastal front; and (3) temporal variations in larval abundance advected into the inlet during flood tide.

2.1 Moored instruments

Oceanographic information was collected from two moored instrument arrays, designated as 'M1' and 'M2' (Fig. 1a) for approximately two weeks in May 1993. M1 was placed on a relatively flat ledge to the south of the main channel of the North Edisto River in water 14.5 meters deep (the main channel is 21 meters deep). M2 was located about 10 nautical miles (18 km) offshore at the 14-meter isobath.

Two InterOcean Systems, Inc. S4 current meters and two Sea-Bird Electronics, Inc. SEACAT data loggers were deployed at each site to measure currents, temperature and conductivity at 2 levels in the vertical and subsurface pressure at the bottom (Fig. 2; Table 1). Salinity and density (σ_t) were derived from conductivity, temperature and pressure values. The sampling rate for all the moored instruments was six minutes (0.1 hour). The temperature and conductivity values recorded by the S4 current meters were excluded from this data report because the quality of the signals tended to degrade over time and were

inferior to those of the SEACAT sensors.

Wind speed and direction, barometric pressure, and air temperature were monitored hourly at Folly Beach (FBIS1), a nearby C-MAN (Coastal-Marine Automated Network) station which was maintained by the National Oceanic and Atmospheric Administration (NOAA). FBIS1 is about 30 kilometers east-northeast of the North Edisto River study area. The meteorological information obtained at this station should represent local conditions. The wind speed and direction files were converted to x and y components. The corresponding surface wind stress components were calculated by an iterative technique which adjusted the wind speed to a 10-meter level and used a variable drag coefficient depending on the magnitude of the wind speed.

2.2 Shipboard sampling

Several hydrographic and larval abundance surveys were carried out on board the R/V BLUE FIN of the Skidaway Institute of Oceanography, and the R/V ANITA of the South Carolina Marine Resources Research Institute for a 14-day period in May 1993.

The BLUE FIN generally occupied offshore stations on the adjacent continental shelf (Fig. 1a) in an attempt to map the structure of the coastal frontal zone and the distribution of larval abundance perpendicular to the shore (stations T13 to T1) and then parallel to the ebb tide delta (arc stations A11 to A1). The timing of the offshore surveys was set to reach station A6 at the maximum flood tide which best coincided with the nighttime surveys in the throat.

The ANITA was stationed in the North Edisto throat and sampled during nighttime flood tides at three positions across the throat designated "N" (north), "M" (middle) and

"S" (south). These station locations are depicted as three short parallel lines near mooring M1 on Figure 1b. The throat surveys were designed to measure oceanographic properties of temperature, salinity, density and larval abundance entering the inlet and ascertain lateral variability in these parameters.

2.2.1 Hydrographic sampling

Each ship was equipped with an instrument called a CTD which recorded vertical profiles of conductivity (C), temperature (T), and depth (D). All the vertical profiles (or casts) were taken with a Sea-Bird Electronics, Inc. Model 25 Sealogger CTD, except those for Offshore Survey #5 which were taken with an InterOcean Systems, Inc. S4 CTD. Salinity and density were calculated from the conductivity, temperature and depth values using standard algorithms. An optional fluorometer was installed on each unit and the CTD on the BLUE FIN also had an optical backscatter (OBS) sensor. The fluorometer was designed to measure chlorophyll *a* fluorescence (Fl) and the OBS sensor measured turbidity by detecting infrared radiation scattered from suspended matter. The OBS values were not calibrated with suspended sediment samples, so they represent relative turbidity only.

All the sensors on the CTD were manufactured by Sea-Bird Electronics, Inc. (SBE), except the fluorometer, the Model OBS-3 sensor and the 0-100 psia strain gauge pressure sensor which were manufactured by SEA TECH Inc., D & A Instrument Company and Paine Corporation, respectively.

The CTD unit was lowered through the water column and real-time data were displayed on a personal computer. The SBE Sealogger CTD was set up to sample all the

above parameters (C, T, D, Fl, OBS and calculated salinity and density) at 1 Hz in real-time mode. Thus, the vertical structure of the water column could immediately be ascertained. The CTD cast information was also stored as a binary data file (with a sample rate of 4 Hz) on the personal computer. Software provided by SBE allowed several ways to view the data, including graphical or tabular display of the variables.

As part of the post-deployment processing, data from each CTD downcast were averaged by depth into 1.0 meter bins. This allowed hundreds of data points to be summarized into relatively few values and still keep the vertical resolution of various features. The bin-averaged data were then grouped appropriately to create contour plots of selected parameters, such as temperature, salinity and fluorescence.

The station log (Table 2) indicates the timing and position for the 114 CTD casts taken on the BLUE FIN and the 78 casts from the ANITA. A more graphical representation shows the relative schedules for the various offshore and throat surveys for each vessel (Fig. 3).

The throat and offshore surveys were intended to simultaneously sample the inlet and nearshore regions. However, since the nighttime flood tide was about one hour later every day (2 semi-diurnal tidal cycles ~ 25 hours), the offshore surveys gradually progressed out of the nighttime hours and many offshore stations were sampled during the day. The original schedule was also disrupted by occasional bad weather which precluded the BLUE FIN from going offshore. Additionally, we experienced mechanical problems with the ANITA for several days near the beginning of the study period and two throat surveys were conducted on the BLUE FIN.

There were a couple of surveys labeled "lw" and "hw" (Fig. 3) which represent hydrographic sampling only (no larval sampling) along offshore and estuarine transects centered in time at consecutive Low Water and High Water periods. They were designed to show how far water masses were translated during one-half of a semi-diurnal tidal cycle and to see if conditions changed during the neap to spring tidal cycle. These surveys will be described in a later section.

2.2.2 Continuous mapping of near-surface ocean properties

An Oceanographic Data Interface System (ODIS) aboard the BLUE FIN was designed to interface with an assortment of instruments. A primary navigation interface consisted of a Global Positioning System (GPS) and a fathometer. Near-surface ocean water was continuously pumped through a suite of sensors interfaced to ODIS that included temperature, conductivity, and fluorescence sensors. The fluorescence output of a Turner Designs fluorometer was calibrated by periodically collecting subsamples downstream of the fluorometer and measuring their chlorophyll *a* (chl *a*) content in the lab. These calibrations are still underway. ODIS data were logged automatically onto disk during most of the BLUE FIN cruises at sampling intervals ranging from 2 min to 15 min.

2.2.3 Phytoplankton biomass sampling

Vertical profiles of fluorescence representing phytoplankton biomass were measured aboard each ship. The two Sea-Bird CTDs used aboard the BLUE FIN and ANITA were both equipped with SEA TECH *in situ* fluorometers. Prior to the spring cruises, both were calibrated against the same phytoplankton cultures. These tests showed that the fluorescence output of both instruments was linear over their maximum range. During the

cruises, natural plankton samples were collected by bucket immediately adjacent to the CTD at the surface during selected vertical profiles. Subsamples were concentrated on filters, extracted later in acetone, and chl *a* was measured in the lab using a Turner Designs Fluorometer. These data were used to derive a calibration curve to convert *in situ* fluorescence from CTD vertical profiles into chl *a* (Fig. 4).

2.2.4 Larval sampling

Net tows in the offshore domain were taken at stations outside the coastal front, inside the coastal front and 3 arc stations (A9, A6, and A3); A6 was sampled near the time of maximum flood current. Tows in the inlet were done in the North Edisto throat (near M1; see Fig. 1b) and sampled during nighttime flood tide at three positions across the throat designated "N" (north), "M" (middle) and "S" (south). This plan complements the hydrographic sampling plan in the inlet described at the beginning of Section 2.2. Inboard and outboard nets were set at surface and bottom at each station using 0.6m bongo nets (0.505 mesh) fitted with an opening and closing device. Tow duration was approximately 5 minutes in the throat and 10 minutes offshore.

3.0 Results and Discussion

Results from NED1 are described by a series of tables and plots that come from moored and shipboard instrumentation. The main forces that affect estuarine and coastal waters are bottom friction induced by tidal and wind-generated currents and surface wind stress. These forces affect the degree of stratification imposed by buoyancy sources from freshwater discharges along the coast and surface heating, as well as govern the strength

and direction of currents. The role of these interacting forces will become obvious in the results that follow.

3.1 Wind stress events

The alongshelf component of wind stress is the principal forcing for coastal currents and wind-driven sea level fluctuations. Figure 5 shows the rotated component and vector plots of wind stress that have been subjected to a 40-hour low-pass filter. (Filtered data sets are discussed in the next section.) The wind stress direction was predominantly upwelling-favorable (positive alongshelf; i.e., northeastward along the coast) with the exception of two downwelling events (negative alongshelf). One downwelling event began on 20 May and lasted about 3 days; the other began late on 26 May and lasted for 2 days.

When wind stress is upwelling-favorable (local wind blowing from the southwest), water near the surface is advected offshore and replaced by deeper water from farther offshore. The coastal front is spread seaward and the strength of vertical stratification increases. When wind stress is downwelling-favorable (local wind blowing from the northeast) water near the surface is advected shoreward, near bottom water is carried seaward, the front is strengthed close to shore, and vertical stratification diminishes. The significance of the upwelling- and downwelling-favorable wind stress is evident in the offshore transect contour plots of temperature, salinity, density and chlorophyll *a* described in a later section.

3.2 Moored instrument statistics

All moored instruments at M1 and M2 had a sample rate of six minutes, but for this analysis every tenth value was selected to create hourly records. Then the hourly values

for both the oceanographic and meteorological data were independently filtered with a 3-hour and 40-hour low-pass digital filter. The 3-hour filter (3hlp) removes the high frequency noise from the record and the 40-hour filter (40hlp) removes variations associated with phenomena with periodicities of less than 40 hours (i.e. mainly tides). The 3hlp values have a delta-t of 1 hour, while the 40hlp files have been decimated to have a delta-t of 6 hours.

We determined the principal axes along which current and wind vectors had their maximum variance. All 3hlp and 40hlp data had principal axes within 25 degrees of the local shoreline orientation of 50 degrees east of north. Thus, for simplicity, all current and wind stress vectors were rotated 50 degrees counter-clockwise, so the principal axes would be closely parallel to the local shoreline and isobaths. For this rotated coordinate system, positive x-components are directed offshore and positive y-components are alongshore toward the north.

Three tables of statistics present first order properties for the filtered data sets (Tables 3, 4 and 5). Table 3 shows 3hlp and 40hlp statistics for the complete data sets. The effect of the low-pass filter is most evident in the currents where the 40hlp standard deviations are significantly smaller than the corresponding 3hlp values. Reductions in the other ocean parameters are not so large. Hourly wind data are least affected by the filters.

Note that under the vector rotations used, 3hlp currents (which contain most of their variance in the semi-diurnal tide) mostly fluctuate along the axis of the inlet and perpendicular to the shoreline (the x-axis). When the tidal variances are excluded by the 40hlp filter, most of the variance in the inlet is still along the x-axis (the inlet's axis), while that of the coastal currents offshore is more shore-parallel.

Statistics during neap and spring tide periods illustrate the effects of the larger spring tides on tidal currents (Table 4). The x-axis tidal currents increased by 25 and 11 percent in the inlet throat at mid-water and bottom, respectively. Similar increases of 7 and 21 percent were measured in the coastal waters offshore. Subsurface pressure fluctuations (which represent tidal height elevations) were 40%/30% higher at M2/M1 during spring tides than for neap tides.

An upwelling and downwelling event was defined for 16-19 May and 21-23 May, respectively (Table 5). Both offshore current meters were located below the pycnocline for the upwelling event in a zone of onshore flow that strengthed toward the bottom, a feature that has been seen off Georgia during upwelling (Blanton, 1986). Presumably, above the pycnocline, a current meter would have measured an offshore component.

The reversal of alongshelf currents from an upwelling to a downwelling regime is apparent at the offshore station. The water column was well mixed during the downwelling event, and both meters measured an onshore flow that decreased with depth. Continuity demands that a compensating offshore flow take place somewhere, presumably either in a bottom boundary layer or at some other location north or south of M2.

The 40hlp currents in the inlet are difficult to interpret. If we had been able to locate M1 in mid-channel, we would have expected to measure influx of ocean water during the downwelling event. The fact that sea level rose at the onset of downwelling (discussed later) suggests that was indeed the case. Since M1 was, in fact, located off the main axis channel on a ledge with complex surrounding topography, the 40hlp data probably are reflecting a more complex wind and pressure-generated circulation. Therefore, we will not discuss further the 40hlp current meter data from M1.

3.3 Time series of winds, currents, and water mass properties

Plots of the 3hlp and 40hlp moored data display the rotated wind stress and current vectors, as well as temperature, salinity, σ_t and subsurface pressure data (Figs. 6 - 11). The plots of 3hlp current meter data at M1 (Fig. 6) show strong tidal currents along the axis of the inlet (x-component). Positive x-component currents ebb toward the ocean. Currents are only slightly diminished at the near-bottom meter. The fluctuations in the cross-inlet (y) direction are very small (note differences in scale) when compared to the axial fluctuations. These components are difficult to interpret because a slight change in the coordinate rotation would change the algebraic sign of the cross-inlet component. Therefore, we place no significance on the cross-axis components in the inlet until further analyses are completed.

Offshore tidal currents at mooring M2 are strongest in the cross-shelf (x) component (Fig. 7). They are also embedded in the alongshelf (y) component to a smaller degree, a characteristic that illustrates that tidal current vectors trace out an ellipse in coastal waters. Note the positive and negative trends in the alongshelf component that will be discussed for the 40hlp data.

Temperature, salinity, and σ_t at mooring M1 in the inlet show the effects of the tidal current as it advects horizontal gradients of properties past the sensors (Fig. 8). The similarity in the top and bottom data indicates that the water column is essentially vertically homogeneous.

The situation is different offshore. The decreased magnitude of the cross-shelf (x-component) tidal currents does not advect large fluctuations in temperature, salinity and σ_t

by the sensors (Fig. 8). However, the presence of vertical gradients of these parameters is evident from the fact that the "TOP" and "BOT" are vertically stratified until 22 May, after which they become well mixed. This becomes clearer in plots of the 40hlp data and in the hydrographic section plots from the BLUE FIN that follow.

The 40hlp data for wind stress and currents off the coast at mooring M2 (Fig. 9) show the effects of wind on coastal currents. The long episode of upwelling-favorable wind stress from 15 to 20 May was matched by positive alongshelf (y-component) current, except for a brief 18-hr interlude of weak downcoast currents beginning just before 16 May. There are short period fluctuations in wind stress evident in the 3hlp data that are filtered out in the 40hlp data (compare Fig. 6a to Fig. 11a). These fluctuations can reverse currents if they last more than 6 hours and may account for short-term reversals in the 40hlp current that do not match the 40hlp wind. Thus the 18-hr interlude of downcoast currents before positive alongshelf currents set in may have been triggered by a strong onshore wind component (Fig. 6a) that was filtered out of the 40hlp wind data. When the wind stress reversed on 20 May, alongshelf currents also reversed and remained so until upwelling-favorable winds resumed just before 24 May.

In general, the 40hlp alongshelf (y-component) currents at bottom are less than those measured about 6 m above bottom (Fig. 10). The opposite is true for the cross-shelf (x) components. During the first upwelling-favorable wind event, the near-bottom component is onshore at about 5 cm/s as predicted in the discussion under wind measurements. As the water mass section plots will show, coastal waters at M2 were vertically stratified and the baroclinic pressure gradient associated with such a regime predicts onshore flow in a bottom layer at this time.

Note that during the downwelling event and the following upwelling one, offshore flow and subsequent onshore flow near bottom does not develop. Vertical stratification at M2 had disappeared by this time. The cross-shelf component 6 meters above bottom swings onshore during downwelling and offshore during upwelling. We interpret the onshore flow as a manifestation of the flow required to raise sea level at the coast, and the following offshore flow as a similar manifestation of the flow that lowers sea level during upwelling. The distribution of cross-shelf flow in the vertical is dependent upon vertical stratification which governs the internal pressure gradient affecting such flows. Our vertical resolution of currents is not sufficient to offer more precise interpretation of cross-shelf components, and expectations derived from stratified fluids do not necessarily follow from such poorly resolved data.

The evolution of temperature, salinity and density fields at M1 and M2 is easily seen in the 40hlp data (Fig. 11). At the offshore station, mid-water column and bottom temperatures rose during the upwelling event as northward currents brought in warmer shelf waters from the south. Temperature in the inlet fell during the downwelling event and began increasing again during the second upwelling event. Actually, temperatures at M1 began falling about 1 day before the wind reversed. The 3hlp wind data, which are more representative of the instantaneous winds (Fig. 6a), were the strongest during this event. Falling inlet temperatures at this time suggest that cooler water from offshore was brought into the inlet. Simultaneous temperatures at M1 and M2 showed an overall increase in temperature, but a temperature gradient between inlet and coastal waters that diminished over time. Thermal stratification offshore had disappeared by 22 May.

Salinities in the inlet were 3 to 4 PSU fresher than those in coastal waters (Fig. 11b). An early dip in inlet salinity coincided with a lull in wind stress. Salinities rose more or less steadily during the study, but the rate of increase was greatest during the downwelling event. Afterward, salinity was practically steady. The salinity difference between inlet and coastal water decreased to about 2 PSU after 22 May.

Subsurface pressure (SSP) fluctuations (Fig. 11d) reflect the combined effects of changing sea level elevation and barometric pressure. SSP fluctuations were characterized by three rapid increases in pressure followed by slower decreases. The abrupt increases occurred near times of change in wind stress, but SSP was generally higher during downwelling and lower during upwelling, indicating an influx of water into the inlet during downwelling periods.

3.4 Offshore hydrographic sections

The following figures consist of cross-shelf versus depth plots of salinity, chlorophyll *a*, temperature and σ_t for each of the offshore surveys. Tables of bin-averaged data from which these plots are drawn are available from the authors upon request. We also used a flowthrough system that pumped water from 1.6m below the surface along the ship track and recorded salinity, temperature, and fluorescence. The flow-through system allowed us to tie in the near-surface estuarine data to similar data offshore as well as help resolve scales of variation. We have divided this section into surveys that were done under upwelling-favorable wind stress conditions and compared them to those conducted during downwelling-favorable wind stress.

3.4.1 Offshore surveys OS1 through OS4 (14-22 May 1993)

These surveys (Figs. 12-15) were done under upwelling-favorable winds that diminished at the time of OS3 and shifted to downwelling-favorable during OS4. During OS1 and OS2, the front (see the salinity plot) was spread seaward. It outcropped near T13 during OS1 but had moved farther offshore during OS2. Vertical stratification was quite strong, and the two-layered nature of the coastal front is most apparent at this time. Note that the nose of the front (seen near T3 on OS1) shows up as a high-salinity subsurface zone at A6 along the arc. The offshore transect was always done near the time of low water, but the tide was flooding by the time the ship cruised along the arc. Thus, the nose of the front containing the 34-PSU isohaline was apparently advected shoreward by the flooding tide so that it intersected the arc below the surface during the first three surveys.

Wind stress had diminished significantly during OS3. The higher salinity subsurface water had progressed shoreward to station T3, and a strong coastal front appeared between T3 and T5. A shallow lens of low salinity water extended shoreward and shows up along the arc through A6. (The water mass structure along the arc must be interpreted with the flooding tide in mind.) Through the time of OS3, the shallow water along the arc was vertically stratified to varying degrees because the coastal front was advected over the arc during flood tide. Vertical mixing was not strong enough to destroy the front at this time.

By the time of OS4, the halocline and pycnocline depth *increased* seaward of T5 which reflects strong upwelling of deeper water from farther offshore. The water mass above the pycnocline was relatively warm and fresh and may have been part of the coastal front at one time. We were unable to define the offshore extent of this warm and relatively low salinity patch during OS4, which extended out an additional 9 nautical miles

from T13 (which was usually our most offshore station location). There was no evidence that the density gradient was becoming positive (which it should as the outer shelf was approached) at T22 indicating that the patch size of the low density lens was greater than 6 nautical miles in the cross-shelf extent.

During OS4, the 34-PSU isohaline had either upwelled or mixed to the surface at T7 forming a relative high salinity zone with a weak coastal front (weakness indicated primarily by the σ_t gradient) situated between T7 and T1. Winds had reversed to a downwelling-favorable direction at the time of the T1 - T5 stations, and the water there had become well mixed. Also, OS4 was conducted only one day before maximum spring tide.

3.4.2 Offshore surveys OS5 and OS6 (22-24 May 1993)

These two surveys (Figs. 16 and 17) were completed during downwelling-favorable winds and coincidentally at the time of spring tide. Downwelling circulation and spring tide conditions provide the most efficient vertical mixing. Vertically stratified water previously appearing between T7 and T10 during upwelling-favorable winds was no longer present. Instead, the water here was vertically mixed to salinities greater than 34 PSU. The coastal front between T1 and T3 was still present for OS5 but water had mixed vertically by the time of OS6 and the front appeared to be destroyed. The water along the arc was essentially well mixed for both surveys, although there was some evidence of lower salinity water (< 33.6 PSU) being advected by the flood tide from offshore.

Data from OS6 suggest that some of the water mass structure in shallow water reflects alongshelf advection. The coastal front between T1 and T3 was quite weak with salinities

between 33.8 and 34.0 PSU. We cannot rule out the possibility of a stronger front being present closer to shore than T1. Advection of lower salinity water around the arc could form weak stratification on the arc but leave water farther offshore unaffected.

OS6 was conducted as downwelling-favorable winds had diminished considerably before changing to an upwelling-favorable mode. We presume that the low salinity lens observed during OS1 through OS4 was advected seaward during upwelling. During downwelling, the vertical gradient was destroyed in the relatively shallow water close to the coast, but probably survived as a lens farther offshore (~ T10 and T13). Upon relaxation of downwelling wind, the cross-shelf forces in this water mass structure are out of balance, and there is a tendency for near-surface water in the lens to be advected onshore. This would explain the reappearance at T13 of the strongly stratified water, evident during OS4.

3.4.3 Offshore surveys OS7 through OS10 (24-27 May 1993)

These surveys (Figs. 18-21) were conducted during upwelling-favorable winds, but these had diminished by the time of OS10 to the beginning of a downwelling episode that would last for two days (Fig. 5). Upwelling winds had blown for almost one day at the time of OS7. The low salinity lens offshore at T13 was still present but had weakened in vertical stratification. This feature remained in place for OS8 and OS9, but was not present for OS10. The water from T1 to T10 was essentially well-mixed during all these surveys, but there is a suggestion of more stratified conditions shoreward of T1. For example, there was a weak coastal front between T1 and T7 during OS2 but stratification was much stronger along the arc at A9, suggesting advection of low salinity surface water

into the area along the arc. Salinities along the arc had increased slightly by the time of OS10 suggesting that the low salinity source was patchy. A low salinity source from along the coast is also suggested in one of the surveys in the inlet and will be described in Section 3.5 of this report.

3.4.4 Offshore comparisons at neap and spring tide

Neap and spring tides occurred on 15 May and 22 May, respectively. We conducted two quick hydrographic surveys along the "S" line of stations (Fig. 1a) on 15 May to define the changes in coastal water masses between high and low water at neap tide. The sections (Fig. 22) showed the same high degree of vertical stratification as observed during OS1 and OS2 which immediately preceded and followed the neap tide surveys. The low salinity lens was a relatively broad feature during slack low water extending from A1 to S10 (right panels on Fig. 22). At the end of flood tide, however, the vertical density gradient was considerably stronger beneath the lens which was somewhat more compact with a well-mixed surface layer. Due to the horizontal nature of the isohalines and other properties, we were unable to estimate a horizontal tidal excursion for the neap tide survey.

No comparable survey was done at spring tide, but the OS5 survey (Fig. 16) showed well-mixed conditions offshore of the coastal front which was a relatively compact feature close to shore. This undoubtedly reflects the result of both the higher tidal current strengths at spring tide and the more efficient vertical mixing of coastal regions during downwelling conditions (Blanton and Atkinson, 1983; Blanton et al., 1989; Blanton et al., in press).

In summary, neap tide and upwelling-favorable winds represented relatively weak

vertical mixing conditions that allowed coastal waters to be vertically stratified. Spring tide, on the other hand, occurred during downwelling conditions and was quite effective in erasing vertical stratification except near the coast.

3.5 Estuarine longitudinal sections

A low water survey from the North Edisto inlet mouth to 13 nautical miles inland was conducted at neap tide on 15 May (Fig. 23). A similar high and low water survey was conducted at spring tide on 22 May (Fig. 24). The low water survey showed a weakly stratified (almost well-mixed) estuary with salinities of about 30 PSU at the mouth decreasing to about 23 PSU at the upstream survey limit. By the time of spring tide, low water salinities had increased by 1 PSU throughout the inlet. The high water survey indicated the presence of relatively low salinity water that had intruded from offshore on the flood tide. This water was stratified and produced a relative maxima in density slightly upriver in the region of maximum water depth. This is further evidence of a low salinity coastal source near the inlet mouth (see Section 3.4.3).

The almost vertical nature of the isohalines allowed an estimate of the excursion of water from its high water to low water position (Fig. 24). Using the 31-PSU isohaline as an indicator, the tidal excursion through the inlet throat was approximately 5 nautical miles. The same excursion occurred for the 26 PSU isohaline farther inland. These distances apply to spring tide, and they would presumably be somewhat smaller for neap tide.

3.6 Throat surveys

South (S), Middle (M) and North (N) inlet stations (near M1 in Fig. 1a) were sampled as quickly as possible for each of the 13 throat surveys. All CTD casts and plankton tows were taken only during nighttime flood conditions. The order of station selection was random and if time permitted, the three stations were repeated. A preliminary look at the hydrographic data suggests slight variability of the water mass properties in the throat cross-section. However, we need to examine the data more closely since the casts were taken at different times relative to maximum flood, and tidal aliasing (especially with such strong tidal currents) may confound the relevant features.

An additional CTD cast (without a plankton tow) was taken at the middle throat station at maximum flood tide whenever possible. A time series plot of these CTD measurements (Fig. 25) displays the temporal variability in salinity, temperature and fluorescence in the water column. These data confirm that salinities near the mouth were about 30 PSU on May 13 - 15 (neap tide) and increased from that time until 26 May to a level of about 32 PSU. The rate of increase was greatest between 20 May and 22 May, which coincided with downwelling winds and the onset of spring tidal conditions. It is likely that weakly stratified water present from 13-20 May was erased by mixing from the faster spring tidal currents on 22 May, but further analyses are needed to confirm this.

3.7 Biology results

3.7.1 Offshore surveys

The spatial distribution of chlorophyll *a* (chl *a*) was quite similar throughout the study period, with variations apparently induced by the combination of wind reversals and tidal

mixing. Generally, chl *a* was highest in the deeper samples at the arc stations, and decreased with distance offshore and at shallower depths (e.g., Fig. 17). Concentrations typically ranged from 4-5 µg/l nearshore to 0.5-1 µg/l offshore. Under downwelling-favorable winds, chl *a* was vertically stratified only in the arc stations (Fig. 17). Under upwelling-favorable conditions, chl *a* was vertically stratified at offshore stations as well (Fig. 12). The highest chl *a* concentrations occurred in waters of intermediate salinities (33-34 PSU; Fig. 26a). Since salinity was the major contributor to water column stability, chl *a* fluorescence was also correlated with intermediate values of σ_t (22.5-23.5; Fig. 26b). Optical backscatter (OBS) measured by the CTD was highly correlated with chl *a* fluorescence (Fig. 26c).

3.7.2 Estuarine longitudinal transects

Three surveys downstream from NED6 to NED1 were conducted, one during high water and two during low water (Figs. 23 and 24). The spatial distribution of chl *a* was similar in each survey, with highest concentrations (4-5 µg/l) near the estuary mouth, and low concentrations (2-3 µg/l) at intermediate river stations. Upriver stations (NED 3-6) typically showed weak or little vertical stratification of chl *a*, whereas fluorescence increased with depth at the downriver stations (NED 1-2). At a given station, chl *a* concentrations were greater at high water than low water.

3.7.3 Throat surveys

The middle throat station was sampled at the time of maximum flood tide coinciding with darkness. Chl *a* exhibited a pattern of increasing concentration with depth (Fig. 25b). Nearbottom concentrations often saturated the sensor at 10 volts (~ 5.6 µg/l) and are thus

minimum estimates of chl *a*. Beginning on 22 May, chl *a* increased rapidly to saturated values throughout the water column. Surface values gradually declined over the next 2-3 days.

Patterns in the temporal and spatial distribution of salinity were similar to those of chl *a* (Fig. 25), increasing with depth and over time. As a result, salinity and chl *a* exhibited a highly significant positive correlation (Fig. 27a). The most appropriate regression model to fit the data cannot be determined because of the samples which saturated the fluorometer output, but it appears that approximately half of the variance in chl *a* distribution in space and time can be explained by changes in salinity. As observed in offshore waters, patterns in water column stability reflected changes in salinity, so that chl *a* was also highly correlated with σ_t (Fig. 27b). Chl *a* was again highly correlated with optical backscatter (Fig. 27c).

3.7.4 Larval results

Counting of postlarval samples has been finished for the middle and southern stations in the inlet (Fig. 28). The northern and offshore samples will be counted during the second year. Postlarval quantities of *Penaeus* were, in general, most abundant in surface samples. The key result is that the two peaks on 22 May and 24 May and the two larger peaks on 27 May and 28 May occurred during downwelling conditions. Even the small peak on 15 May occurred during a brief downwelling-favorable wind event.

There are some details in the abundance curve that raise questions. Note that abundances of *Penaeus* began to increase at the beginning of the downwelling event which began on 20 May to a peak density on 22 May. There was a brief decrease on 23 May

then another peak on 24 May when upwelling-favorable winds occurred. These questions have prompted us to sample more frequently when the wind shifts from upwelling-favorable to downwelling-favorable so that temporal variability is better resolved.

4.0 Summary

The upwelling/downwelling cycles observed during NED1 clearly affect the oceanography of coastal waters [compare Fig. 12 (upwelling) with Fig. 17 (downwelling)]. Coastal currents were northward at M2 during upwelling and changed to southward during downwelling. Sea level as represented by subsurface pressure decreased/increased in the inlet and offshore during upwelling/downwelling. Salinity at the inlet throat rose most rapidly during the downwelling event of 21-23 May. Coupling of coastal waters with those of an estuarine nursery was optimized during the downwelling events which transported oceanic water into the estuary and raised sea level.

4.1 Preliminary interpretation

We have two sets of sections done within one day of each other in which we can compare the hydrographic and chl *a* distributions in both the estuary and across the shelf (Fig. 29). The low water neap tide survey on 15 May (Fig. 29a) shows an essentially well-mixed estuary in the lower reaches between stations NED1 and NED3. Once the inlet delta is crossed, stratified water characteristic of upwelling conditions is encountered offshore. Note the strong decrease in chl *a* away from the bottom and offshore. This gradient is also reflected in the inlet with high values of chl *a* along the bottom adjoining the ocean and in the inlet basin as a whole, which has chl *a* values only slightly below 3 µg/l.

The next simultaneous survey was done at spring tide low water on 22 May during downwelling conditions. Salinity and chl *a* concentrations in the estuary (Fig. 29b) were similar with maximum chl *a* along the inlet bottom next to the ebb delta. A similar maximum occurred on the shelf at the bottom adjacent to the delta. Salinity on the shelf was vertically uniform, consistent with high vertical mixing (downwelling winds plus spring tides). There was a 2-PSU salinity difference across the inlet delta.

Low salinity stratified water along the arc showed up several times in our surveys (e.g., Fig. 20). A stratified low salinity source also showed up at HIGH water at the ocean end of the estuary (Fig. 24), a feature that could only have come from the shelf. The origin of the low salinity source is quite speculative at this time. We have data from the ODIS flow-through system as a means to extrapolate CTD surface salinities between M1 in the inlet to A6 along the arc. (Cross-calibration between CTDs and the flow-through sensor has not been completed.) Five high water traverses across the ebb-tide delta (Fig. 30) show that lowest salinities along this track occurred near Deveaux Banks between 2 and 3 nautical miles seaward of M1. The low salinity water was relatively warm. We speculate that it represents low salinity water advected along the coast into the region of the inlet delta. Note the wide range of salinities observed at A6 (Fig. 30). These correlate with upwelling/downwelling conditions that have advected low/high salinity water into the arc from other sources.

In summary, the lowest salinity water along the arc was often relatively warm (as in OS7 through OS10), consistent with heating in shallow water. More observations of tidal and wind-generated currents on the ebb tide delta and along the arc are required before we can understand their temporal and spatial variability. Since this water mass may provide a

food source for the larvae, it is important to understand its origin.

4.2 Concluding remarks

The primary food for early planktonic stages of shrimp larvae is phytoplankton. As the larvae age and increase in size, their diet also includes protozoan and metazoan microzooplankton (Dobkin, 1961; Cook and Murphy, 1969; Christmas and Etzold, 1977). Since spatial and temporal patterns in the distribution of herbivorous microzooplankton in coastal waters are related to those of their prey (Verity et al., 1993), phytoplankton biomass (chl *a*) represents either a direct food source for shrimp larvae or a tracer of that food source. Thus, the distribution of chl *a* relative to more conservative properties (salinity, temperature, density) provides an indicator of water masses or hydrographic regions which may be nutritionally beneficial to shrimp larvae during their transport from offshore spawning sites to estuarine nursery grounds.

The key to understanding the processes influencing the mesoscale distribution of plankton during May is to resolve the apparent paradox in the relationship between salinity and chl *a* in the mouth of the estuary, and that observed seaward. Chl *a* peaked at intermediate salinities in coastal waters but was positively correlated with salinity in the estuary (Fig. 29). The decline in chl *a* in waters of 34 PSU or greater is due to increasing nutrient limitation of phytoplankton growth with distance offshore (Verity et al., 1993; Yoder et al., 1993). The decline in chl *a* in coastal waters of <33.5 PSU (Fig. 26a) is similar to that which occurred in estuarine waters of <33.5 PSU (Fig. 27a). Since the source of new nutrients for phytoplankton growth is freshwater, one would expect a negative correlation between salinity and chl *a*, as observed farther upstream in the North

Edisto river transects (Figs. 23 and 24) and nearby waters (Verity et al. 1993), but contrary to that observed at the middle throat station over time (Fig. 25). The positive correlation reflects higher chl *a* in deeper waters, which are also more saline. Since fresher water at the surface should contain more nutrients and also provide more light for algal photosynthesis, the increase in chl *a* with depth is provocative. This increase with depth was also observed at arc stations (Figs. 12-15; 17-21) as well as in the estuary.

Explanations for this near-bottom chl *a* maximum include enhanced production at depth, sinking of phytoplankton from surface waters, and epibenthic sources. Several observations are instructive in this regard. First, the North Edisto estuary is tidally dominated, with tidal current velocities often exceeding 100 cm/s (2 knots) and occasionally exceeding 150 cm/s (3 knots) on the spring tide ebb. Second, a region of enhanced chl *a* concentrations coincides with the mouth of the estuary, which is shallow (Fig. 29) and thus susceptible to wind- and tide-induced scouring of surface sediments. Third, the temporal peak in chl *a* near station M1 coincides with the time of spring tides, which flood larger areas of the marshes and increase the amount of bottom material pumped or scoured out. Fourth, the elevated chl *a* in nearbottom waters occurs in both stratified and non-stratified (i.e., vertically mixed) waters (e.g., Fig. 29). If the subsurface maximum in chl *a* was due to enhanced production at depth or settling from above, then mixing sufficient to produce homogeneous salinity distributions should result in homogeneous phytoplankton distributions. However, if the source of chl *a* is epibenthic phytoplankton, then a near-bottom peak should expand upwards from the bottom as observed in the inlet throat (Fig. 25). The increase in water column chl *a* would be further stimulated by addition of previously sessile algae flushed from the marshes by high water.

Thus, we hypothesize that hydrography and meteorology combine to regulate the temporal and spatial distribution of phytoplankton in the North Edisto estuary and adjacent coastal waters. In turn, these distributions may affect how larvae are distributed in coastal waters.

A tidal excursion of approximately 5 nautical miles has implications for future sampling plans. A particle located on the arc at the beginning of flood tide would be advected across the delta and into the inlet throat, a situation that was not expected at the beginning of the study. Thus, larvae sampled on the arc may show up in samples taken in the throat allowing us to better link data found along the arc to data in the inlet. This motivates us to devote some of our future sampling efforts to the delta itself, although such efforts will be somewhat restricted due to shoals and other hazards.

Preliminary *Penaeid* abundance data in the inlet throat suggest that ingress increases during downwelling events, which is consistent with one of the hypotheses we advanced at the beginning of this study. However, some critical questions arise. In the first of two large ingress events on 22 May and 24 May (Fig. 28), downwelling winds had diminished on the 23rd. So why did abundances peak again on 24 May when upwelling conditions had begun? While downwelling conditions push coastal water into the inlet and carry any larvae present at the mouth into the inlet, there are other plausible mechanisms that could carry larvae in coastal waters to the inlet during the onset of upwelling. Since bottom water is carried shoreward as downwelling relaxes and upwelling begins, larvae near bottom could be advected toward the inlet during the initial stages of upwelling.

Clearly more information is required to understand how larvae "pool" in coastal waters in the vicinity of the inlet, and how fluctuating oceanographic conditions optimize the communication of coastal waters with inlet waters. This requires a better determination

of temporal fluctuations in circulation and larval abundances at the onset and through a downwelling event before mechanisms operating on the scale of an upwelling/downwelling cycle can be understood and put in proper context with larval ingress.

5.0 References

Blanton, J. O. 1986. Coastal frontal zones as barriers to offshore fluxes of contaminants. Rapp. P. -v. Reun. Cons. int. Explor. Mer 186: 18-30.

Blanton, J. O. and L. P. Atkinson. 1983. Transport and fate of river discharge on the continental shelf of the southeastern United States. J. Geophys. Res., 88(C8): 4730-4738.

Blanton, J. O., L.-Y. Oey, J. Amft, and T. N. Lee. 1989. Advection of momentum and buoyancy in a coastal frontal zone. J. Phys. Oceanogr. 19: 98-115.

Blanton, J. O., F. Werner, C. Kim, L. Atkinson, T. Lee and D. Savidge. Transport and fate of low-density water in a coastal frontal zone. Cont. Shelf Res: in press.

Christmas, J. Y. and D. J. Etzold. 1977. The shrimp fishery of the Gulf of Mexico United States; a regional management plan. Gulf Coast Res. Lab. Tech. Rep. Ser. No. 2. 125 pp.

Cook, H. L. and M. A. Murphy. 1969. The culture of larval penaeid shrimp. Trans. Am. Fish. Soc. 98(4): 751-754.

Dobkin, S. 1961. Early developmental stages of pink shrimp, *Penaeus duorarum*, from Florida waters. U.S. Fish Wildl. Serv. Fish. Bull. 190(61): 321-349.

Verity, P. G., J. A. Yoder, S. S. Bishop, J. R. Nelson, D. B. Craven, J. O. Blanton, C. Y. Robertson, and C. R. Tronzo. 1993. Composition, productivity and nutrient chemistry of a coastal ocean planktonic food web. Cont. Shelf Res. 13: 741-776.

Yoder, J. A., P. G. Verity, S. S. Bishop, and F. E. Hoge. 1993. Phytoplankton chl *a*, primary production, and nutrient distributions across a coastal frontal zone off Georgia, USA. Cont. Shelf Res. 13: 131-141.

6.0 Acknowledgments

We wish to express our appreciation to the several individuals without whose help this project would not have been possible. First, our thanks go to Marsha Ward who participated in the cruises and Lane Mitcham of Skidaway Institute who developed much of the instrumentation and software used in the ODIS system aboard the BLUE FIN. Next, we thank Charlie Barans, Betty Wenner, Bruce Stender and David Knott of the South Carolina Marine Resources Research Institute, our scientific partners in this project. We also appreciate the able support of Captain Jay Fripp and crew Raymond Sweatte and Chris Knight of the R/V BLUE FIN, and Captain Paul Tucker of the R/V ANITA.

This work was sponsored by joint grants from the Georgia Sea Grant Program (Grant No. R/EA-15) to the Skidaway Institute of Oceanography and the South Carolina Sea Grant Consortium (Grant No. 93277) to the SC Marine Resource Research Institute.

Table 1. Moored instrumentation used during NED1 in May 1993.

STATION	INSTRU. DEPTH (m)	WATER DEPTH (m)	INSTRUMENT	PARAMETERS MEASURED	DEPLOYMENT DATES (1993)	LATITUDE (deg N)	LONGITUDE (deg W)
M1	-6.5	-14.5	SEACAT 295	C,T	05/13 - 05/29	32.569	80.195
M1	-8.0	-14.5	S4 706	C,T,V	05/13 - 05/29	32.569	80.195
M1	-12.0	-14.5	S4 1530	C,T,V	05/13 - 05/29	32.569	80.195
M1	-13.5	-14.5	SEACAT 849	C,P,T	05/13 - 05/29	32.569	80.195
M2	-7.0	-14.0	SEACAT 327	C,T	05/15 - 05/26	32.417	80.073
M2	-8.0	-14.0	** S4 908 **	C,T,V	05/15 - 05/26	32.417	80.073
M2	-11.5	-14.0	S4 909	C,T,V	05/15 - 05/26	32.417	80.073
M2	-13.0	-14.0	SEACAT 848	C,P,T	05/15 - 05/26	32.417	80.073
FBIS1	+9.8	land	C-MAN	A,B,W	05/13 - 05/29	32.68	79.89

Instrument:

SEACAT serial# = Sea-Bird Electronics SEACAT data logger
S4 serial# = InterOcean Systems S4 current meter

Weather Stations:

FBIS1 = Folly Beach (C-MAN)

C-MAN = Coastal-Marine Automated Network (NOAA)

Parameters:

A = air temperature
B = barometric pressure
C = conductivity
P = subsurface pressure
T = water temperature
V = current velocity
W = wind velocity

** S4-908 had a data gap from 22 May 1993 at 1754 GMT to 23 May 1993 at 0006 GMT; it was filled in with information from S4-909

Table 2a. R/V BLUE FIN station log for NED1.

	Cruise	Cast #	Sta	Date mm dd yy	Time (GMT)	Water Depth (m)	Latitude (N) deg min	Longitude (W) deg min
Offshore Transect Survey #1: (os1)								
*	B1	001	T13	05/15/93	0028	15.6	32 22.72	80 01.29
*	B1	002	T10	05/15/93	0219	11.5	32 25.63	80 02.10
	B1	003	T7	05/15/93	0331	10.2	32 28.71	80 03.29
	B1	004	T5	05/15/93	0411	9.6	32 30.64	80 03.49
	B1	005	T3	05/15/93	0439	10.5	32 32.56	80 03.91
	B1	006	T1	05/15/93	0505	7.1	32 34.45	80 04.47
*	B1	007	A9	05/15/93	0555	7.0	32 33.22	80 07.32
*	B1	008	A6	05/15/93	0655	7.0	32 30.60	80 09.01
*	B1	009	A3	05/15/93	0738	7.5	32 30.37	80 12.44
Offshore Low Water Neap Tide Survey: (lw)								
	B1	010	A1	05/15/93	1341	5.0	32 31.02	80 14.70
	B1	011	S3	05/15/93	1406	9.0	32 29.37	80 13.16
	B1	012	S5	05/15/93	1425	10.4	32 27.72	80 11.97
	B1	013	S7	05/15/93	1450	11.0	32 26.07	80 10.67
	B1	014	S10	05/15/93	1523	15.9	32 23.65	80 08.71
Offshore High Water Neap Tide Survey: (hw)								
	B1	015	S10	05/15/93	2043	17.0	32 23.75	80 08.68
	B1	016	S7	05/15/93	2118	11.1	32 26.19	80 10.79
	B1	017	S5	05/15/93	2142	11.4	32 27.80	80 12.11
	B1	018	S3	05/15/93	2205	10.1	32 29.41	80 13.26
	B1	019	A1	05/15/93	2232	5.5	32 31.01	80 14.70
Offshore Transect Survey #2: (os2)								
*	B1	020	T13	05/16/93	0102	14.3	32 22.90	80 01.55
	B1	021	T10	05/16/93	0201	12.1	32 25.64	80 02.35
*	B1	022	T7	05/16/93	0234	9.6	32 28.68	80 03.07
	B1	023	T5	05/16/93	0321	8.8	32 30.65	80 03.48
	B1	024	T3	05/16/93	0345	9.5	32 32.49	80 03.91
	B1	025	T1	05/16/93	0410	6.6	32 34.49	80 04.50
*	B1	026	A9	05/16/93	0445	6.5	32 33.14	80 07.36
*	B1	027	A6	05/16/93	0546	6.5	32 30.71	80 08.98
*	B1	028	A3	05/16/93	0646	7.5	32 30.32	80 12.58
Throat Survey #3: (ts3)								
*	B1	029	N	05/17/93	0440	12.5	32 34.32	80 11.59
*	B1	030	M	05/17/93	0516	21.8	32 34.19	80 11.70
*	B1	031	S	05/17/93	0557	12.5	32 34.18	80 11.84
	B1	032	M	05/17/93	0648	21.8	32 34.17	80 11.64
*	B1	033	S	05/17/93	0708	12.5	32 34.18	80 11.82
*	B1	034	N	05/17/93	0745	13.9	32 34.26	80 11.57
*	B1	035	M	05/17/93	0825	20.0	32 34.20	80 11.80
Throat Survey #4: (ts4)								
*	B1	036	M	05/18/93	0521	22.0	32 34.21	80 11.68
*	B1	037	N	05/18/93	0617	14.0	32 34.31	80 11.65
*	B1	038	S	05/18/93	0654	12.6	32 34.25	80 11.91
*	B1	039	M	05/18/93	0723	20.4	32 34.26	80 11.76
*	B1	040	N	05/18/93	0755	13.5	32 34.31	80 11.62
*	B1	041	S	05/18/93	0831	14.2	32 34.25	80 11.91
Offshore Transect Survey #3: (os3)								
*	B1	042	T13	05/20/93	1510	15.8	32 22.70	80 01.29
*	B1	043	T10	05/20/93	1555	11.4	32 25.62	80 02.51
*	B1	044	T7	05/20/93	1645	9.5	32 28.76	80 03.06
	B1	045	T5	05/20/93	1715	9.2	32 30.69	80 03.51
	B1	046	T3	05/20/93	1741	8.8	32 32.38	80 03.78
	B1	047	T1	05/20/93	1811	6.0	32 34.57	80 04.53
*	B1	048	A9	05/20/93	1838	6.0	32 33.13	80 07.33
*	B1	049	A6	05/20/93	2050	6.5	32 30.62	80 09.00
*	B1	050	A3	05/20/93	2243	8.0	32 30.38	80 12.51
Offshore Transect Survey #4: (os4)								
	B1	051	A1	05/21/93	0001	6.2	32 31.01	80 14.67
	B1	052	S10	05/21/93	0119	17.0	32 23.53	80 08.53
	B1	053	T22	05/21/93	0313	21.5	32 16.18	79 54.20
	B1	054	T19	05/21/93	0401	21.0	32 18.01	79 57.28
	B1	055	T16	05/21/93	0502	15.0	32 20.40	79 59.32
	B1	056	T10	05/21/93	0701	11.5	32 25.57	80 02.39
*	B1	057	T7	05/21/93	0745	9.4	32 28.56	80 03.07
*	B1	058	T5	05/21/93	0904	9.0	32 30.54	80 03.47
*	B1	059	T3	05/21/93	1013	11.0	32 32.54	80 03.93
	B1	060	T1	05/21/93	1057	7.5	32 34.38	80 04.53
*	B1	061	A6	05/21/93	1147	7.5	32 30.62	80 09.06

Table 2a (continued)

Offshore Transect Survey #5: (os5)

	B1	062	T13	05/22/93	0528	14.0	32 22.50	80 01.65
	B1	063	T10	05/22/93	0607	11.8	32 25.71	80 02.29
+	B1	064	T7	05/22/93	0645	9.0	32 28.61	80 03.01
	B1	065	T5	05/22/93	0748	9.2	32 30.63	80 03.49
+	B1	066	T3	05/22/93	0811	9.5	32 32.51	80 03.96
	B1	067	T1	05/22/93	0909	6.7	32 34.49	80 04.47
+	B1	068	A9	05/22/93	0938	6.7	32 33.17	80 07.33
+	B1	069	A6	05/22/93	1103	6.5	32 30.65	80 09.01
+	B1	070	A3	05/22/93	1145	7.7	32 30.41	80 12.47

Offshore Transect Survey #6: (os6)

	B1	071	T13	05/23/93	0545	13.5	32 22.68	80 01.61
+	B1	072	T10	05/23/93	0634	11.4	32 25.72	80 02.41
	B1	073	T7	05/23/93	0740	9.7	32 28.76	80 03.12
+	B1	074	T5	05/23/93	0835	8.5	32 30.52	80 03.49
	B1	075	T3	05/23/93	0940	9.9	32 32.58	80 04.00
	B1	076	T1	05/23/93	1020	6.5	32 34.49	80 04.47
+	B1	077	A9	05/23/93	1050	6.8	32 33.10	80 07.31
+	B1	078	A6	05/23/93	1148	7.0	32 30.65	80 08.97
+	B1	079	A3	05/23/93	1256	7.5	32 30.37	80 12.51

Offshore Transect Survey #7: (os7)

	B1	080	T13	05/24/93	0635	13.5	32 22.83	80 01.61
	B1	081	T10	05/24/93	0724	12.0	32 25.69	80 02.35
+	B1	082	T7	05/24/93	0830	9.5	32 28.86	80 03.04
	B1	083	T5	05/24/93	0930	8.8	32 30.61	80 03.22
+	B1	084	T3	05/24/93	1000	10.0	32 32.57	80 03.98
	B1	085	A9	05/24/93	1110	7.0	32 33.13	80 07.13
+	B1	086	A6	05/24/93	1150	8.5	32 30.58	80 08.78
+	B1	087	A3	05/24/93	1245	6.5	32 30.38	80 12.16

Offshore Transect Survey #8: (os8)

	B1	088	T13	05/25/93	0706	14.3	32 22.75	80 01.35
	B1	089	T10	05/25/93	0740	11.5	32 25.60	80 02.02
+	B1	090	T7	05/25/93	0819	9.9	32 28.73	80 02.75
	B1	091	T5	05/25/93	0959	8.5	32 30.57	80 03.22
+	B1	092	T3	05/25/93	1054	9.3	32 32.42	80 03.45
	B1	093	T1	05/25/93	1123	6.6	32 34.45	80 04.07
+	B1	094	A9	05/25/93	1159	5.2	32 33.13	80 06.87
+	B1	095	A6	05/25/93	1323	7.9	32 30.59	80 08.63

Offshore Transect Survey #9: (os9)

	B1	096	T13	05/25/93	1935	14.9	32 22.83	80 01.34
	B1	097	T10	05/25/93	2011	11.5	32 25.60	80 02.10
+	B1	098	T7	05/25/93	2047	10.2	32 28.54	80 02.72
	B1	100	T5	05/25/93	2155	8.5	32 30.46	80 03.05
	B1	101	T3	05/25/93	2219	10.1	32 32.56	80 03.50
	B1	102	T1	05/25/93	2302	6.9	32 34.33	80 04.12
+	B1	103	A9	05/26/93	0005	7.1	32 33.00	80 07.05
+	B1	104	A6	05/26/93	0103	8.5	32 30.59	80 08.63
+	B1	105	A3	05/26/93	0212	8.3	32 30.32	80 12.18

Offshore Transect Survey #10: (os10)

	B1	106	T13	05/26/93	2156	14.5	32 22.65	80 01.19
	B1	107	T10	05/26/93	2225	11.4	32 25.73	80 02.15
	B1	108	T7	05/26/93	2317	9.8	32 28.68	80 02.66
	B1	109	T5	05/26/93	2337	8.9	32 30.62	80 03.14
	B1	110	T3	05/26/93	2354	9.7	32 32.50	80 03.56
	B1	111	T1	05/27/93	0020	6.9	32 34.39	80 04.09
+	B1	112	A9	05/27/93	0102	7.0	32 33.08	80 07.02
+	B1	113	A6	05/27/93	0211	7.5	32 30.59	80 08.70
+	B1	114	A3	05/27/93	0313	7.8	32 30.34	80 12.08

\+ = plankton net tows were taken at this station

Cruise:

B1 = R/V BLUE FIN (May 93 cruise)

Station:

S = south side of channel (near Edisto Island)
M = middle of channel (in throat)
N = north side of channel (near Privateer Point)

T# = offshore transect station (North)
S# = offshore transect station (South)
A# = offshore arc station

Table 2b. R/V ANITA station log for NED1.

	Cruise	Cast #	Sta	Date mm dd yy	Time (GMT)	Water Depth (m)	Latitude (N) deg min	Longitude (W) deg min
Throat Survey #1: (ts1)								
+	A1	001	N	05/14/93	0236	17.0	32 34.24	80 11.39
+	A1	002	M	05/14/93	0334	17.0	32 34.17	80 11.45
+	A1	003	S	05/14/93	0421	14.0	32 34.14	80 11.56
+	A1	004	S	05/14/93	0504	13.0	32 34.10	80 11.57
Throat Survey #2: (ts2)								
+	A1	005	M	05/15/93	0230	14.5	32 34.32	80 11.61
+	A1	006	N	05/15/93	0318	16.5	32 34.38	80 11.56
+	A1	007	S	05/15/93	0415	16.5	32 34.24	80 11.66
	A1	008	M	05/15/93	0444	22.5	32 34.06	80 11.34
+	A1	009	S	05/15/93	0509	16.5	32 34.28	80 11.69
+	A1	010	M	05/15/93	0558	15.7	32 34.28	80 11.68
+	A1	011	N	05/15/93	0656	17.5	32 34.35	80 11.52
Inshore Low Water Neap Tide Survey: (lw)								
	A1	012	NED1	05/15/93	1320	10.5	32 32.68	80 09.50
	A1	013	NED2	05/15/93	1352	16.2	32 34.34	80 11.61
	A1	014	NED3	05/15/93	1426	11.3	32 36.33	80 13.96
	A1	015	NED4	05/15/93	1450	6.5	32 37.67	80 15.88
	A1	016	NED5	05/15/93	1511	11.5	32 39.15	80 14.16
	A1	017	NED6	05/15/93	1534	6.7	32 40.91	80 13.37
CTD time-series: (ctdts)								
	A1	018	N	05/19/93	0457	18.0	32 34.18	80 11.34
	A1	019	M	05/19/93	0505	22.0	32 34.09	80 11.34
	A1	020	S	05/19/93	0512	12.5	32 34.07	80 11.48
	A1	021	M	05/19/93	0625	21.5	32 34.12	80 11.36
	A1	022	M	05/19/93	0828	16.0	32 34.21	80 11.57
	A1	023	M	05/19/93	0956	16.0	32 34.27	80 11.57
	A1	024	N	05/19/93	1130	17.5	32 34.19	80 11.32
	A1	025	M	05/19/93	1135	17.5	32 34.11	80 11.42
	A1	026	S	05/19/93	1141	12.8	32 34.06	80 11.49
Throat Survey #5: (ts5)								
+	A1	027	N	05/20/93	0612	20.3	32 34.20	80 11.43
+	A1	028	S	05/20/93	0701	13.5	32 34.13	80 11.53
+	A1	029	N	05/20/93	0750	17.1	32 34.28	80 11.48
	A1	030	M	05/20/93	0834	17.7	32 34.16	80 11.38
Throat Survey #6: (ts6)								
+	A1	031	N	05/21/93	0708	19.4	32 34.15	80 11.42
+	A1	032	N	05/21/93	0800	15.8	32 34.32	80 11.49
+	A1	033	S	05/21/93	0843	13.5	32 34.19	80 11.67
	A1	034	M	05/21/93	0930	22.0	32 34.17	80 11.41
Throat Survey #7: (ts7)								
+	A1	035	M	05/22/93	0750	15.2	32 34.22	80 11.53
+	A1	036	S	05/22/93	0838	15.5	32 34.22	80 11.63
+	A1	037	N	05/22/93	0915	16.7	32 34.27	80 11.43
	A1	038	M	05/22/93	1000	16.3	32 34.15	80 11.47
Inshore High Water Spring Tide Survey: (hw)								
	A1	039	NED1	05/22/93	1228	11.5	32 32.68	80 09.50
	A1	040	NED2	05/22/93	1247	20.5	32 34.21	80 11.45
	A1	041	NED3	05/22/93	1311	10.4	32 36.07	80 13.96
	A1	042	NED4	05/22/93	1335	7.5	32 37.58	80 15.87
	A1	043	NED5	05/22/93	1355	12.5	32 39.16	80 14.18
	A1	044	NED6	05/22/93	1425	12.2	32 40.91	80 13.32
Inshore Low Water Spring Tide Survey: (lw)								
	A1	045	NED1	05/22/93	1816	8.7	32 32.59	80 09.50
	A1	046	NED2	05/22/93	1849	21.5	32 34.18	80 11.40
	A1	047	NED3	05/22/93	1913	10.5	32 36.11	80 13.80
	A1	048	NED4	05/22/93	1947	6.6	32 37.72	80 15.90
	A1	049	NED5	05/22/93	2003	6.5	32 39.14	80 14.21
	A1	050	NED6	05/22/93	2025	10.2	32 40.91	80 13.33
Throat Survey #8: (ts8)								
	A1	051	M	05/22/93	2215	21.0	32 34.08	80 11.34
+	A1	052	M	05/23/93	0048	15.5	32 34.22	80 11.55
+	A1	053	N	05/23/93	0133	15.8	32 34.28	80 11.39
+	A1	054	S	05/23/93	0208	14.5	32 34.20	80 11.63

Table 2b (continued)

Throat Survey #9: (ts9)

	A1	055	M	05/24/93	0012	16.1	32 34.22	80 11.54
+	A1	056	M	05/24/93	0107	17.0	32 34.18	80 11.49
+	A1	057	S	05/24/93	0148	15.5	32 34.12	80 11.51
+	A1	058	N	05/24/93	0246	18.5	32 34.28	80 11.42

Throat Survey #10: (ts10)

	A1	059	M	05/25/93	0039	22.0	32 34.10	80 11.39
+	A1	060	M ** NO CTD CAST		0111	17.0	32 34.19	80 11.58 **
+	A1	061	S	05/25/93	0159	15.5	32 34.08	80 11.49
+	A1	062	N	05/25/93	0243	23.0	32 34.17	80 11.36

Throat Survey #11: (ts11)

	A1	063	M	05/26/93	0046	17.0	32 34.12	80 11.44
+	A1	064	S	05/26/93	0054	13.5	32 34.07	80 11.50
+	A1	065	M	05/26/93	0141	21.8	32 34.11	80 11.40
+	A1	066	N	05/26/93	0230	17.4	32 34.26	80 11.38

Throat Survey #12: (ts12)

+	A1	067	M	05/27/93	0120	22.8	32 34.09	80 11.34
+	A1	068	N	05/27/93	0155	18.2	32 34.19	80 11.36
+	A1	069	S	05/27/93	0235	12.1	32 34.08	80 11.53
+	A1	070	N	05/27/93	0310	17.0	32 34.31	80 11.45
+	A1	071	M	05/27/93	0345	16.7	32 34.12	80 11.44
+	A1	072	S	05/27/93	0425	13.5	32 34.10	80 11.56

Throat Survey #13: (ts13)

+	A1	073	N	05/28/93	0116	17.5	32 34.20	80 11.35
+	A1	074	M	05/28/93	0222	17.5	32 34.05	80 11.36
+	A1	075	S	05/28/93	0300	13.5	32 34.04	80 11.48
+	A1	076	M	05/28/93	0336	20.5	32 34.20	80 11.34
+	A1	077	S	05/28/93	0420	13.4	32 34.10	80 11.56
+	A1	078	N	05/28/93	0456	17.5	32 34.26	80 11.41

+ = plankton net tows were taken at this station

Cruise:

A1 = R/V ANITA (May 93 cruise)

Station:

S = south side of channel (near Edisto Island)
M = middle of channel (in throat)
N = north side of channel (near Privateer Point)

NED0 = estuarine station in North Edisto River

Table 3. First order statistics for parameters measured during NED1. The station location and depth above bottom are designated for each sensor. All parameters with x- and y-components have been rotated 50 degrees counter-clockwise. Series with a length of 15.25 days begin 13 May 1993 at 18 GMT and end 29 May 1993 at 00 GMT; series with a length of 11.75 days begin 15 May 1993 at 00 GMT and end 26 May 1993 at 18 GMT. (a) 3hlp data; (b) 40hlp data.

Parameter	Min	Max	Mean	Stan. Dev.	Length (days)
(a) 3-HOUR LOW-PASS (3hlp) DATA					
FBIS1 x-comp wind stress (Pa * 10)	-0.54	0.60	-0.06	0.14	15.25
FBIS1 y-comp wind stress (Pa * 10)	-0.73	0.72	0.09	0.23	15.25
FBIS1 barometric pressure (mb)	1003.96	1023.49	1014.85	5.75	15.25
FBIS1 air temperature (deg C)	14.03	26.02	22.07	2.37	15.25
M1 8.0m temperature (deg C)	21.51	25.23	23.64	0.76	15.25
M1 8.0m salinity (PSU)	28.03	33.46	31.19	1.48	15.25
M1 8.0m sigma-t (kg/m^3)	18.13	22.94	20.87	1.26	15.25
M1 6.5m x-comp current (cm/s)	-115.06	157.99	2.80	80.83	15.25
M1 6.5m y-comp current (cm/s)	-10.82	11.85	2.07	3.62	15.25
M1 2.5m x-comp current (cm/s)	-100.85	120.28	-1.35	60.16	15.25
M1 2.5m y-comp current (cm/s)	-18.59	22.29	-2.59	7.89	15.25
M1 1.0m temperature (deg C)	21.45	25.26	23.53	0.77	15.25
M1 1.0m salinity (PSU)	28.43	33.46	31.38	1.36	15.25
M1 1.0m sigma-t (kg/m^3)	18.40	22.96	21.04	1.17	15.25
M1 1.0m pressure (dbar)	12.57	14.84	13.67	0.60	15.25
M2 7.0m temperature (deg C)	20.01	22.16	21.20	0.59	11.75
M2 7.0m salinity (PSU)	32.58	34.99	34.27	0.35	11.75
M2 7.0m sigma-t (kg/m^3)	22.34	24.62	23.89	0.29	11.75
M2 6.0m x-comp current (cm/s)	-38.89	36.31	-0.06	17.51	11.75
M2 6.0m y-comp current (cm/s)	-39.31	31.01	4.08	11.96	11.75
M2 2.5m x-comp current (cm/s)	-25.94	22.18	-2.63	13.65	11.75
M2 2.5m y-comp current (cm/s)	-25.22	22.66	2.43	8.80	11.75
M2 1.0m temperature (deg C)	20.25	22.10	21.02	0.66	11.75
M2 1.0m salinity (PSU)	33.98	35.09	34.47	0.28	11.75
M2 1.0m sigma-t (kg/m^3)	23.68	24.69	24.09	0.30	11.75
M2 1.0m pressure (dbar)	11.54	13.79	12.56	0.57	11.75
(b) 40-HOUR LOW-PASS (40hlp) DATA					
FBIS1 x-comp wind stress (Pa * 10)	-0.29	0.14	-0.05	0.10	15.25
FBIS1 y-comp wind stress (Pa * 10)	-0.35	0.48	0.09	0.19	15.25
FBIS1 barometric pressure (mb)	1005.31	1022.45	1014.84	5.77	15.25
FBIS1 air temperature (deg C)	18.15	23.91	22.08	1.72	15.25
M1 8.0m temperature (deg C)	22.60	24.71	23.64	0.59	15.25
M1 8.0m salinity (PSU)	29.97	32.23	31.19	0.71	15.25
M1 8.0m sigma-t (kg/m^3)	19.98	21.60	20.87	0.63	15.25
M1 6.5m x-comp current (cm/s)	-4.56	8.99	2.16	3.37	15.25
M1 6.5m y-comp current (cm/s)	-0.27	3.67	2.07	0.94	15.25
M1 2.5m x-comp current (cm/s)	-7.16	4.43	-1.75	2.76	15.25
M1 2.5m y-comp current (cm/s)	-8.34	1.31	-2.57	2.39	15.25
M1 1.0m 849 temperature (deg C)	22.54	24.48	23.54	0.57	15.25
M1 1.0m salinity (PSU)	30.17	32.32	31.38	0.63	15.25
M1 1.0m sigma-t (kg/m^3)	20.17	21.67	21.03	0.56	15.25
M1 1.0m pressure (dbar)	13.49	13.85	13.67	0.10	15.25
M2 7.0m temperature (deg C)	20.48	22.05	21.20	0.56	11.75
M2 7.0m salinity (PSU)	33.73	34.62	34.27	0.27	11.75
M2 7.0m sigma-t (kg/m^3)	23.57	24.31	23.89	0.20	11.75
M2 6.0m x-comp current (cm/s)	-8.38	5.10	-0.02	3.20	11.75
M2 6.0m y-comp current (cm/s)	-15.61	15.43	4.13	8.00	11.75
M2 2.5m x-comp current (cm/s)	-7.77	1.67	-2.60	2.65	11.75
M2 2.5m y-comp current (cm/s)	-11.50	10.37	2.45	5.62	11.75
M2 1.0m temperature (deg C)	20.28	22.05	21.03	0.66	11.75
M2 1.0m salinity (PSU)	34.10	34.99	34.47	0.27	11.75
M2 1.0m sigma-t (kg/m^3)	23.69	24.66	24.09	0.29	11.75
M2 1.0m pressure (dbar)	12.40	12.71	12.56	0.09	11.75

Table 4. First order statistics using 3hip data for parameters measured for 2 tidal cycles each during the neap and spring tide of NED1. The station location and depth above bottom are designated for each sensor. All parameters with x- and y-components have been rotated 50 degrees counter-clockwise. (a) Neap tide data begin 15 May 1993 at 09 GMT and end 16 May 1993 at 09 GMT; (b) spring tide data begin 22 May 1993 at 14 GMT and end 23 May 1993 at 14 GMT.

Parameter	Min	Max	Mean	Stan. Dev.	Length (hours)
(a) NEAP TIDE DATA					
FBIS1 x-comp wind stress (Pa * 10)	-0.39	0.04	-0.13	0.12	25
FBIS1 y-comp wind stress (Pa * 10)	0.00	0.38	0.18	0.12	25
FBIS1 barometric pressure (mb)	1011.44	1014.87	1013.89	0.84	25
FBIS1 air temperature (deg C)	18.61	24.33	22.53	1.64	25
M1 8.0m temperature (deg C)	22.30	24.20	23.42	0.55	25
M1 8.0m salinity (PSU)	28.17	32.06	30.51	1.28	25
M1 8.0m sigma-t (kg/m^3)	18.49	21.73	20.41	1.10	25
M1 6.5m x-comp current (cm/s)	-87.71	106.60	-2.23	72.65	25
M1 6.5m y-comp current (cm/s)	-4.51	11.53	1.81	3.85	25
M1 2.5m x-comp current (cm/s)	-71.36	90.53	-4.74	58.01	25
M1 2.5m y-comp current (cm/s)	-16.04	20.41	0.39	9.56	25
M1 1.0m temperature (deg C)	22.20	24.09	23.28	0.49	25
M1 1.0m salinity (PSU)	28.66	32.23	30.77	1.15	25
M1 1.0m sigma-t (kg/m^3)	18.89	21.88	20.65	0.99	25
M1 1.0m pressure (dbar)	12.92	14.41	13.72	0.49	25
M2 7.0m temperature (deg C)	20.30	20.82	20.54	0.15	25
M2 7.0m salinity (PSU)	33.46	34.15	33.84	0.21	25
M2 7.0m sigma-t (kg/m^3)	23.37	23.98	23.74	0.18	25
M2 6.0m x-comp current (cm/s)	-27.13	29.08	2.12	16.47	25
M2 6.0m y-comp current (cm/s)	-10.83	12.85	-0.94	6.31	25
M2 2.5m x-comp current (cm/s)	-19.44	15.48	-1.97	12.12	25
M2 2.5m y-comp current (cm/s)	-10.73	12.83	-1.11	6.41	25
M2 1.0m temperature (deg C)	20.25	20.46	20.34	0.07	25
M2 1.0m salinity (PSU)	33.98	34.22	34.11	0.07	25
M2 1.0m sigma-t (kg/m^3)	23.89	24.09	23.99	0.05	25
M2 1.0m pressure (dbar)	11.88	13.29	12.60	0.46	25
(b) SPRING TIDE DATA					
FBIS1 x-comp wind stress (Pa * 10)	0.00	0.12	0.06	0.03	25
FBIS1 y-comp wind stress (Pa * 10)	-0.22	0.05	-0.06	0.09	25
FBIS1 barometric pressure (mb)	1017.61	1022.32	1019.48	1.38	25
FBIS1 air temperature (deg C)	15.44	22.72	19.50	2.40	25
M1 8.0m temperature (deg C)	21.51	23.59	22.64	0.57	25
M1 8.0m salinity (PSU)	29.38	33.28	31.79	1.36	25
M1 8.0m sigma-t (kg/m^3)	19.55	22.94	21.60	1.17	25
M1 6.5m x-comp current (cm/s)	-110.06	157.99	7.25	90.59	25
M1 6.5m y-comp current (cm/s)	-4.89	7.58	2.00	3.04	25
M1 2.5m x-comp current (cm/s)	-90.44	106.11	1.10	64.62	25
M1 2.5m y-comp current (cm/s)	-15.67	9.28	-3.64	6.48	25
M1 1.0m temperature (deg C)	21.45	23.64	22.59	0.57	25
M1 1.0m salinity (PSU)	29.50	33.24	31.86	1.30	25
M1 1.0m sigma-t (kg/m^3)	19.64	22.96	21.67	1.12	25
M1 1.0m pressure (dbar)	12.86	14.81	13.79	0.65	25
M2 7.0m temperature (deg C)	21.37	21.66	21.55	0.08	25
M2 7.0m salinity (PSU)	34.42	34.52	34.46	0.03	25
M2 7.0m sigma-t (kg/m^3)	23.89	23.97	23.94	0.02	25
M2 6.0m x-comp current (cm/s)	-30.91	25.12	-1.40	17.64	25
M2 6.0m y-comp current (cm/s)	-17.98	14.79	0.01	10.67	25
M2 2.5m x-comp current (cm/s)	-22.13	22.18	-0.79	14.65	25
M2 2.5m y-comp current (cm/s)	-13.21	10.71	-1.10	7.49	25
M2 1.0m temperature (deg C)	21.37	21.62	21.53	0.07	25
M2 1.0m salinity (PSU)	34.44	34.52	34.47	0.03	25
M2 1.0m sigma-t (kg/m^3)	23.90	23.98	23.95	0.02	25
M2 1.0m pressure (dbar)	11.79	13.79	12.68	0.64	25

Table 5. First order statistics using 40hlp data for parameters measured for two events (one upwelling and one downwelling) during NED1. The station location and depth above bottom are designated for each sensor. All parameters with x- and y-components have been rotated 50 degrees counter-clockwise. (a) The upwelling event begins 16 May 1993 at 12 GMT and ends 19 May 1993 at 12 GMT; (b) the downwelling event begins 21 May 1993 at 00 GMT and ends 23 May 1993 at 00 GMT.

Parameter	Min	Max	Mean	Stan. Dev.	Length (days)
(a) UPWELLING EVENT					
FBIS1 x-comp wind stress (Pa * 10)	-0.11	-0.03	-0.06	0.02	3
FBIS1 y-comp wind stress (Pa * 10)	0.20	0.48	0.30	0.10	3
FBIS1 barometric pressure (mb)	1007.85	1014.80	1012.44	2.21	3
FBIS1 air temperature (deg C)	23.25	23.91	23.76	0.18	3
M1 8.0m temperature (deg C)	23.71	24.71	24.39	0.33	3
M1 8.0m salinity (PSU)	30.39	30.68	30.51	0.10	3
M1 8.0m sigma-t (kg/m^3)	20.02	20.37	20.13	0.10	3
M1 6.5m x-comp current (cm/s)	-4.56	-0.07	-1.89	1.75	3
M1 6.5m y-comp current (cm/s)	1.02	2.69	1.86	0.56	3
M1 2.5m x-comp current (cm/s)	-7.16	-3.23	-5.27	1.34	3
M1 2.5m y-comp current (cm/s)	-1.18	1.31	-0.12	0.92	3
M1 1.0m temperature (deg C)	23.64	24.48	24.26	0.27	3
M1 1.0m salinity (PSU)	30.68	31.08	30.80	0.13	3
M1 1.0m sigma-t (kg/m^3)	20.28	20.60	20.39	0.11	3
M1 1.0m pressure (dbar)	13.49	13.71	13.59	0.06	3
M2 7.0m temperature (deg C)	20.65	20.99	20.79	0.11	3
M2 7.0m salinity (PSU)	33.73	34.51	34.12	0.31	3
M2 7.0m sigma-t (kg/m^3)	23.57	24.20	23.88	0.24	3
M2 6.0m x-comp current (cm/s)	-3.32	1.15	-0.75	1.61	3
M2 6.0m y-comp current (cm/s)	0.38	15.43	10.69	4.27	3
M2 2.5m x-comp current (cm/s)	-7.62	-2.63	-5.28	1.26	3
M2 2.5m y-comp current (cm/s)	1.18	10.37	7.83	2.66	3
M2 1.0m temperature (deg C)	20.40	20.66	20.53	0.11	3
M2 1.0m salinity (PSU)	34.15	*34.88	34.43	0.26	3
M2 1.0m sigma-t (kg/m^3)	24.00	24.50	24.18	0.17	3
M2 1.0m pressure (dbar)	12.40	12.59	12.49	0.06	3
(b) DOWNWELLING EVENT					
FBIS1 x-comp wind stress (Pa * 10)	0.05	0.14	0.09	0.03	2
FBIS1 y-comp wind stress (Pa * 10)	-0.11	-0.06	-0.09	0.02	2
FBIS1 barometric pressure (mb)	1007.49	1019.30	1013.37	4.03	2
FBIS1 air temperature (deg C)	18.15	20.65	18.98	0.80	2
M1 8.0m temperature (deg C)	22.60	23.75	23.02	0.43	2
M1 8.0m salinity (PSU)	31.33	31.78	31.65	0.16	2
M1 8.0m sigma-t (kg/m^3)	20.94	21.60	21.39	0.24	2
M1 6.5m current (cm/s)	1.82	6.77	4.33	1.80	2
M1 6.5m y-comp current (cm/s)	0.81	3.07	1.94	0.94	2
M1 2.5m x-comp current (cm/s)	-1.49	0.67	0.01	0.70	2
M1 2.5m y-comp current (cm/s)	-8.34	-4.72	-6.14	1.21	2
M1 1.0m temperature (deg C)	22.54	23.62	22.94	0.40	2
M1 1.0m salinity (PSU)	31.49	31.85	31.76	0.12	2
M1 1.0m sigma-t (kg/m^3)	21.10	21.66	21.50	0.20	2
M1 1.0m pressure (dbar)	13.66	13.84	13.78	0.06	2
M2 7.0m temperature (deg C)	20.84	21.52	21.32	0.24	2
M2 7.0m salinity (PSU)	34.41	34.51	34.45	0.03	2
M2 7.0m sigma-t (kg/m^3)	23.94	24.17	23.99	0.08	2
M2 6.0m x-comp current (cm/s)	-8.38	1.69	-4.39	3.44	2
M2 6.0m y-comp current (cm/s)	-15.61	0.03	-8.71	5.89	2
M2 2.5m x-comp current (cm/s)	-4.28	1.67	-1.43	2.29	2
M2 2.5m y-comp current (cm/s)	-11.50	0.14	-6.23	4.27	2
M2 1.0m temperature (deg C) p	20.39	21.53	21.09	0.46	2
M2 1.0m salinity (PSU) 40hlp	34.42	34.98	34.64	0.22	2
M2 1.0m sigma-t (kg/m^3)	23.91	24.65	24.20	0.30	2
M2 1.0m pressure (dbar)	12.57	12.71	12.67	0.05	2

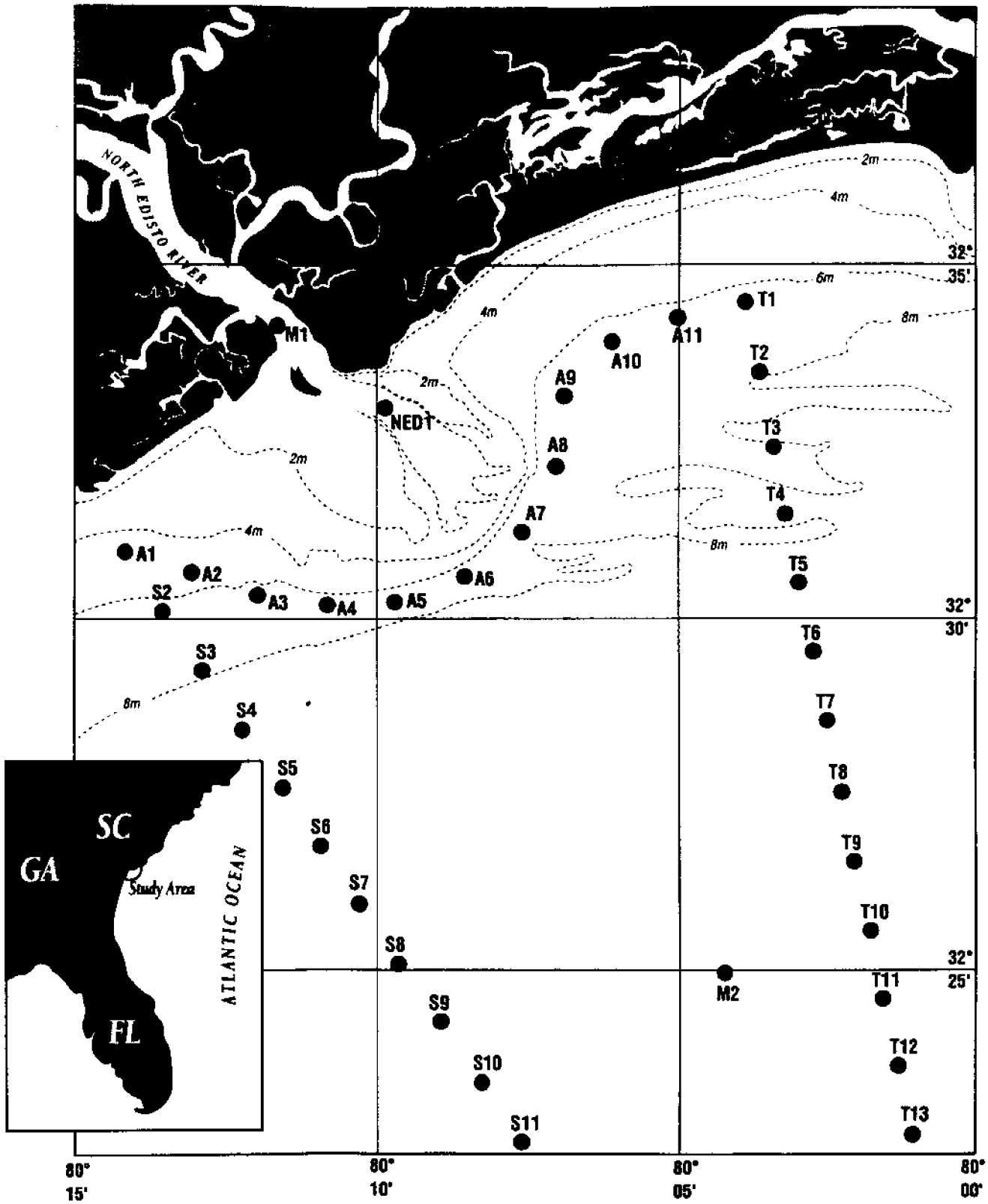
NORTH EDISTO RIVER
2m
4m
6m
8m
32°
35'
M1
NED1
A1
A2
A3
A4
A5
A6
A7
A8
A9
A10
A11
T1
T2
T3
T4
T5
S2
S3
S4
S5
S6
S7
S8
S9
S10
S11
T6
T7
T8
T9
T10
T11
T12
T13
M2
30'
25'
SC
GA
FL
Study Area
ATLANTIC OCEAN
80° 15'
80° 10'
80° 05'
80° 00'

Figure 1A

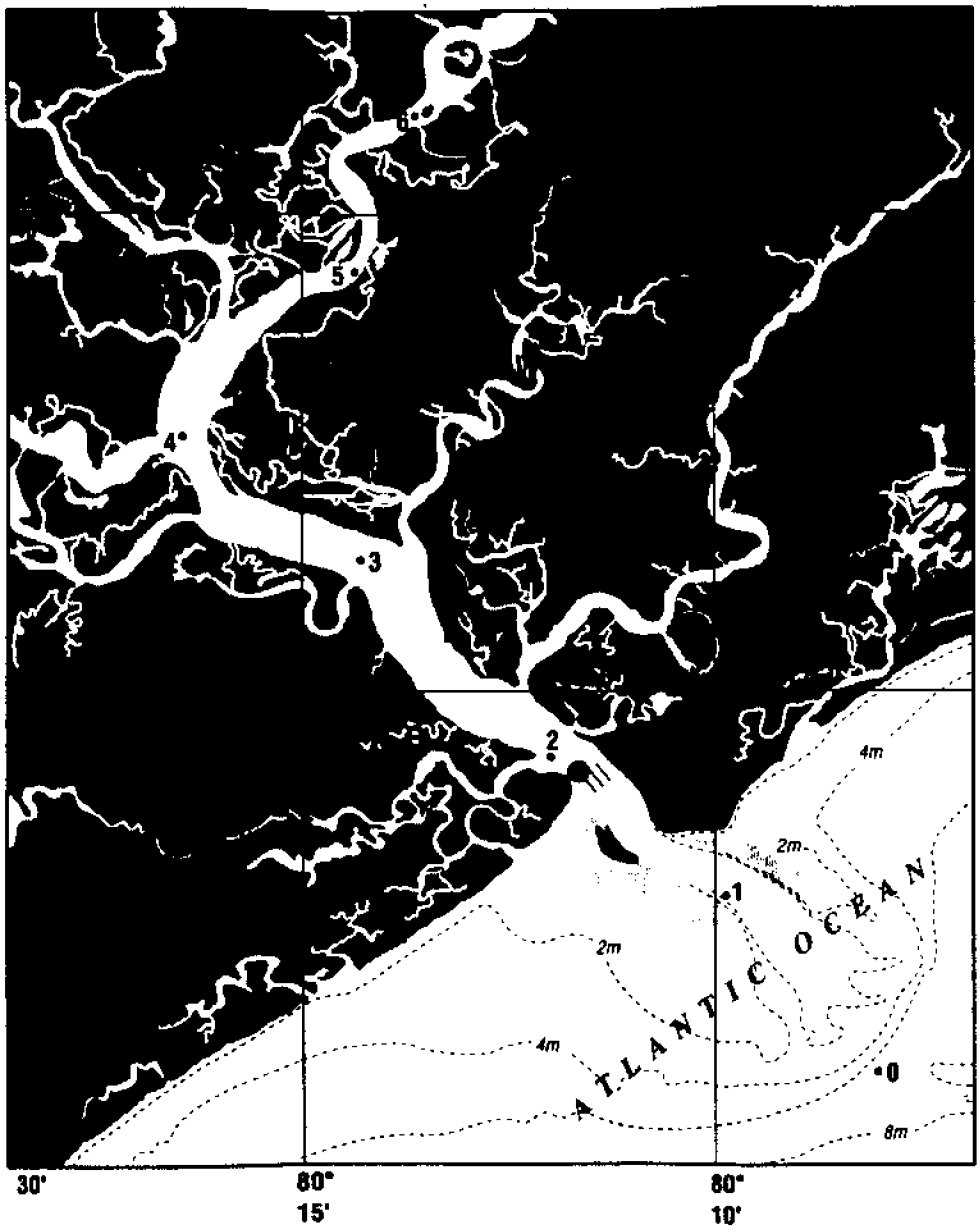

Figure 1B

NORTH EDISTO MOORINGS

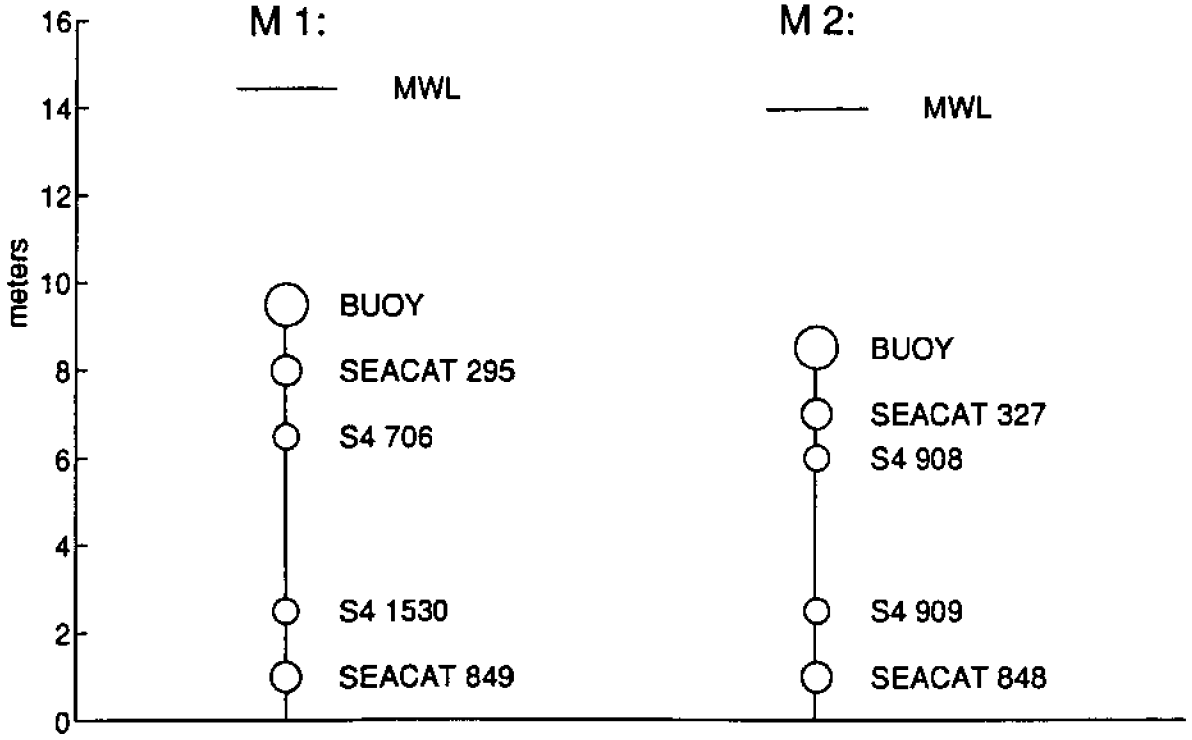

Figure 2

Figure 3

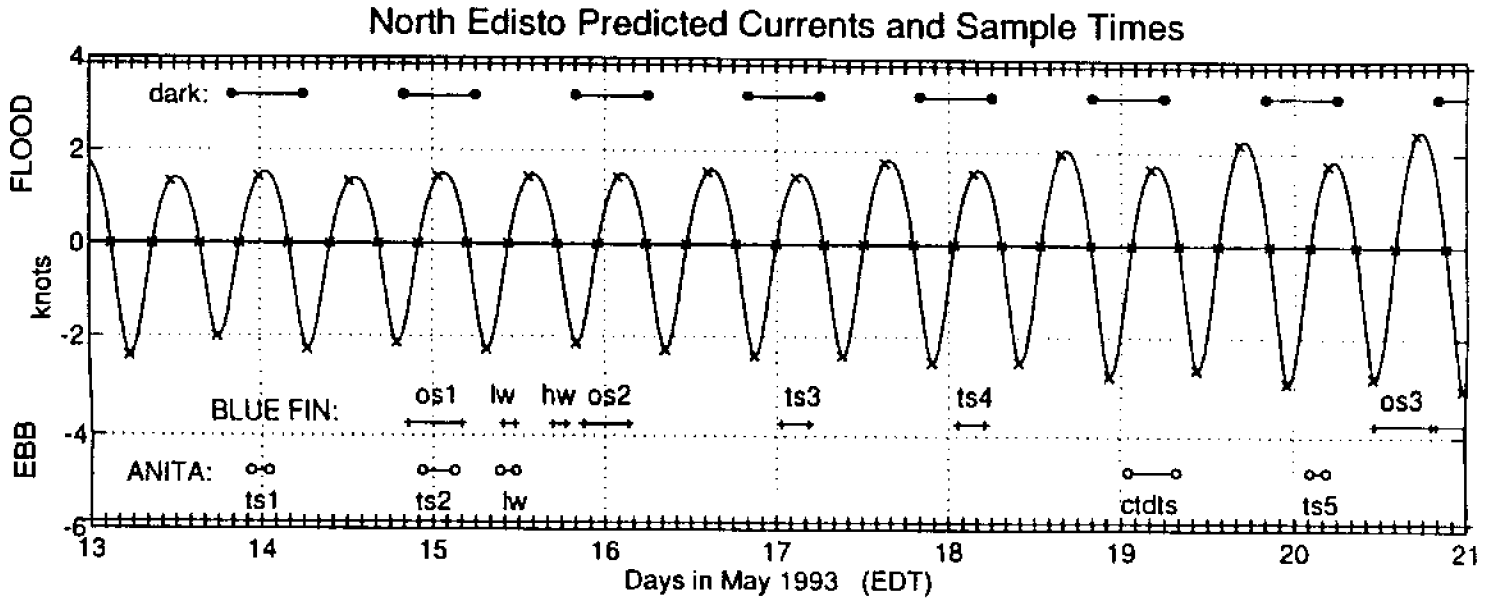
North Edisto Predicted Currents and Sample Times
FLOOD
knots
EBB
dark:
BLUE FIN:
os1
lw
hw
os2
ts3
ts4
os3
ANITA:
ts1
ts2
lw
ctdts
ts5
Days in May 1993 (EDT)

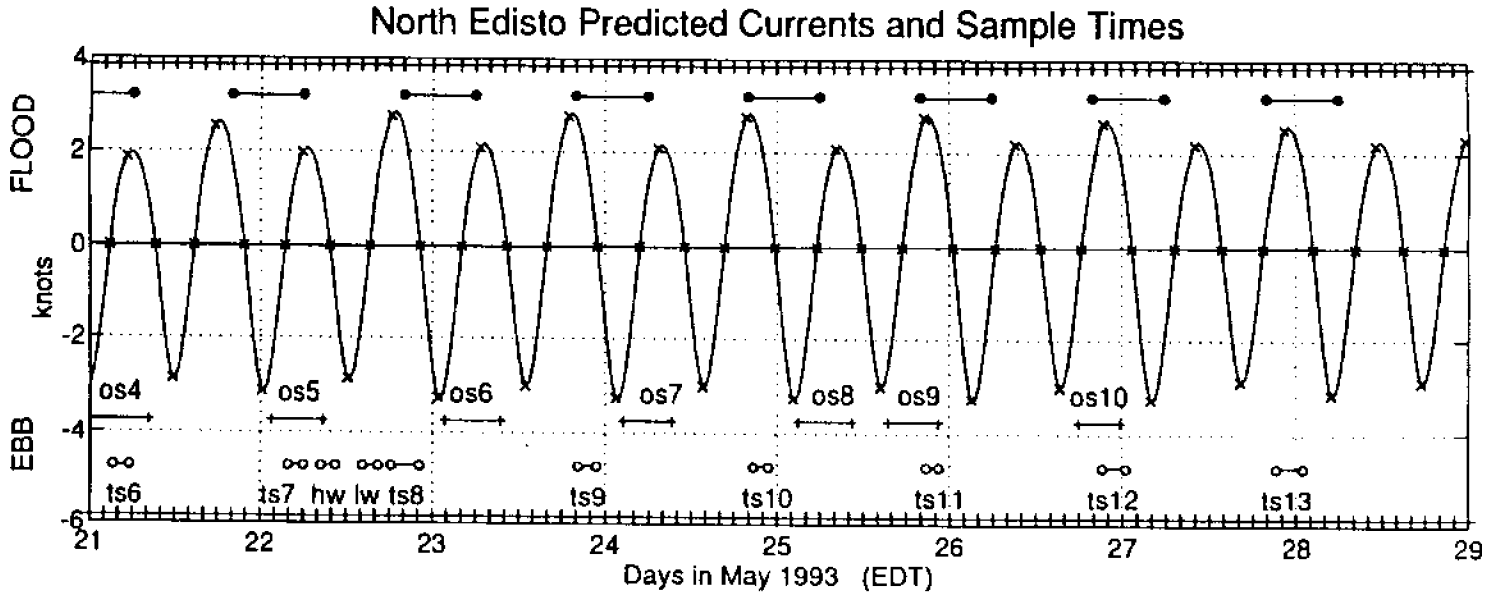
North Edisto Predicted Currents and Sample Times
FLOOD
knots
EBB
os4
os5
os6
os7
os8
os9
os10
ts6
ts7
hw
lw
ts8
ts9
ts10
ts11
ts12
ts13
Days in May 1993 (EDT)

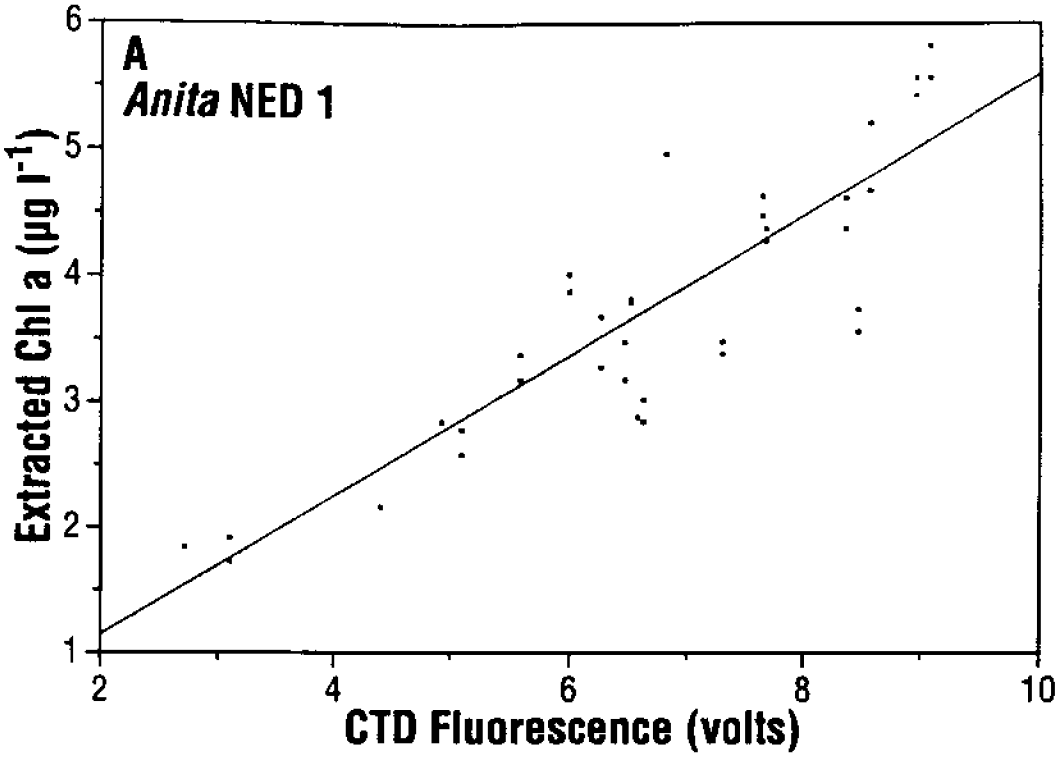
A
Anita NED 1
Extracted Chl a (µg l^{-1})
CTD Fluorescence (volts)
1
2
3
4
5
6
2
4
6
8
10

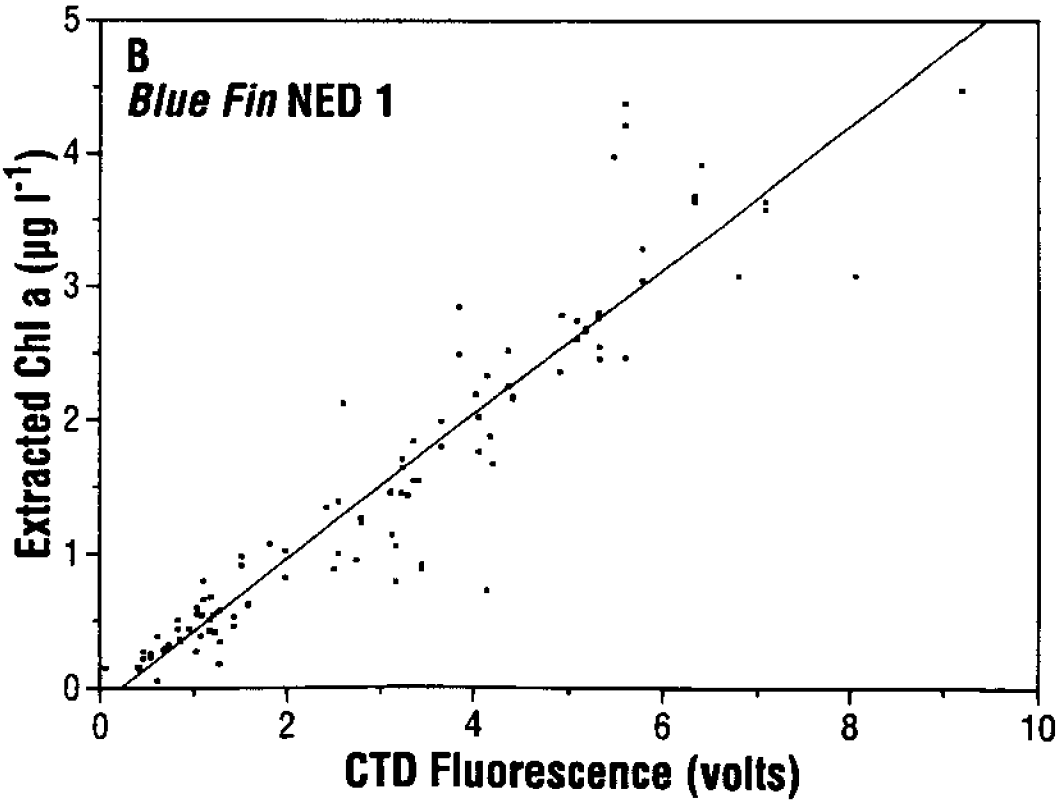
B
Blue Fin NED 1
Extracted Chl a (µg l^{-1})
CTD Fluorescence (volts)
0
1
2
3
4
5
0
2
4
6
8
10

Figure 4

Figure 5

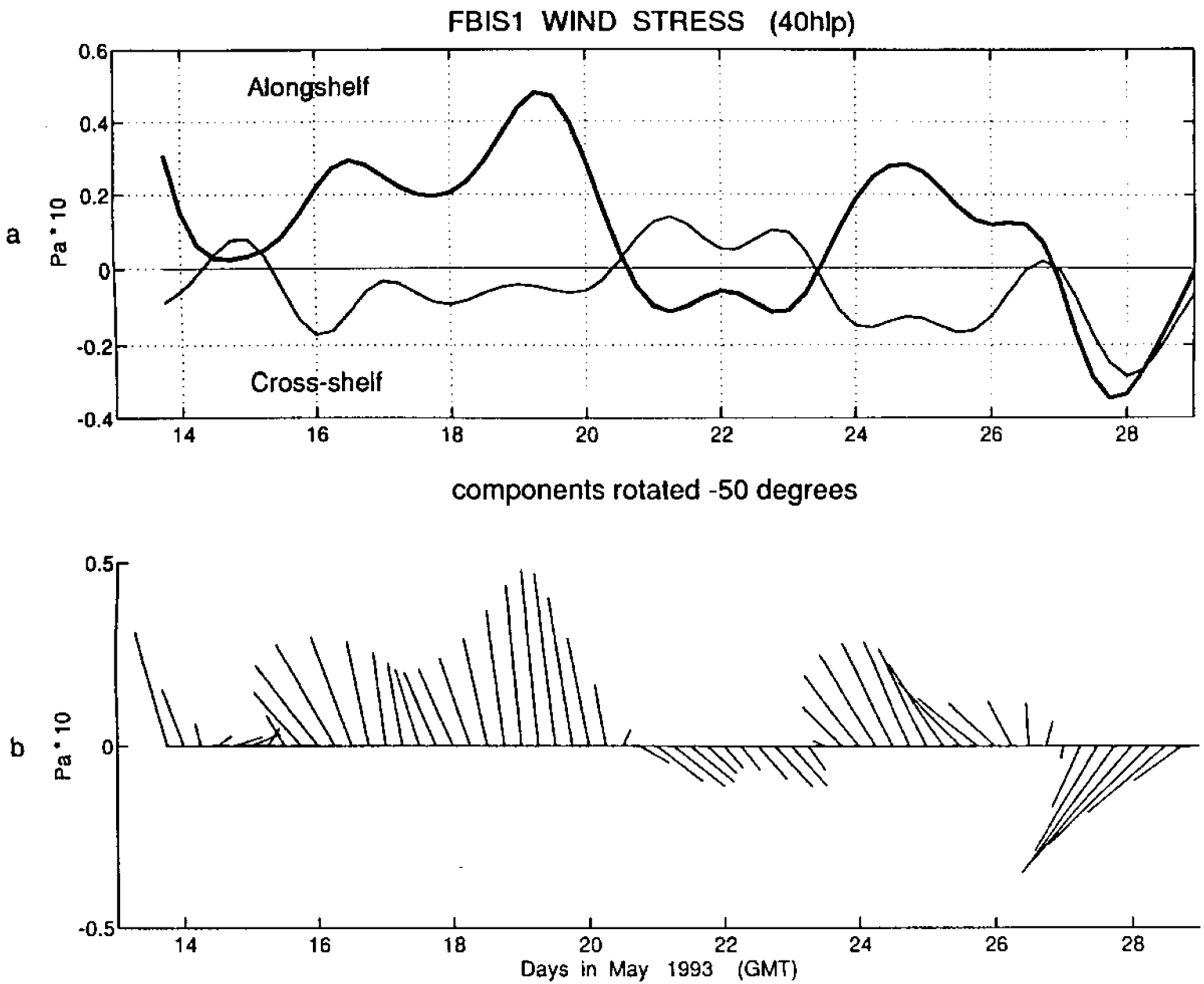
FBIS1 WIND STRESS (40hlp)
a
Alongshelf
Cross-shelf
Pa * 10
0.6
0.4
0.2
0
-0.2
-0.4
14
16
18
20
22
24
26
28
components rotated -50 degrees
b
Pa * 10
0.5
0
-0.5
Days in May 1993 (GMT)

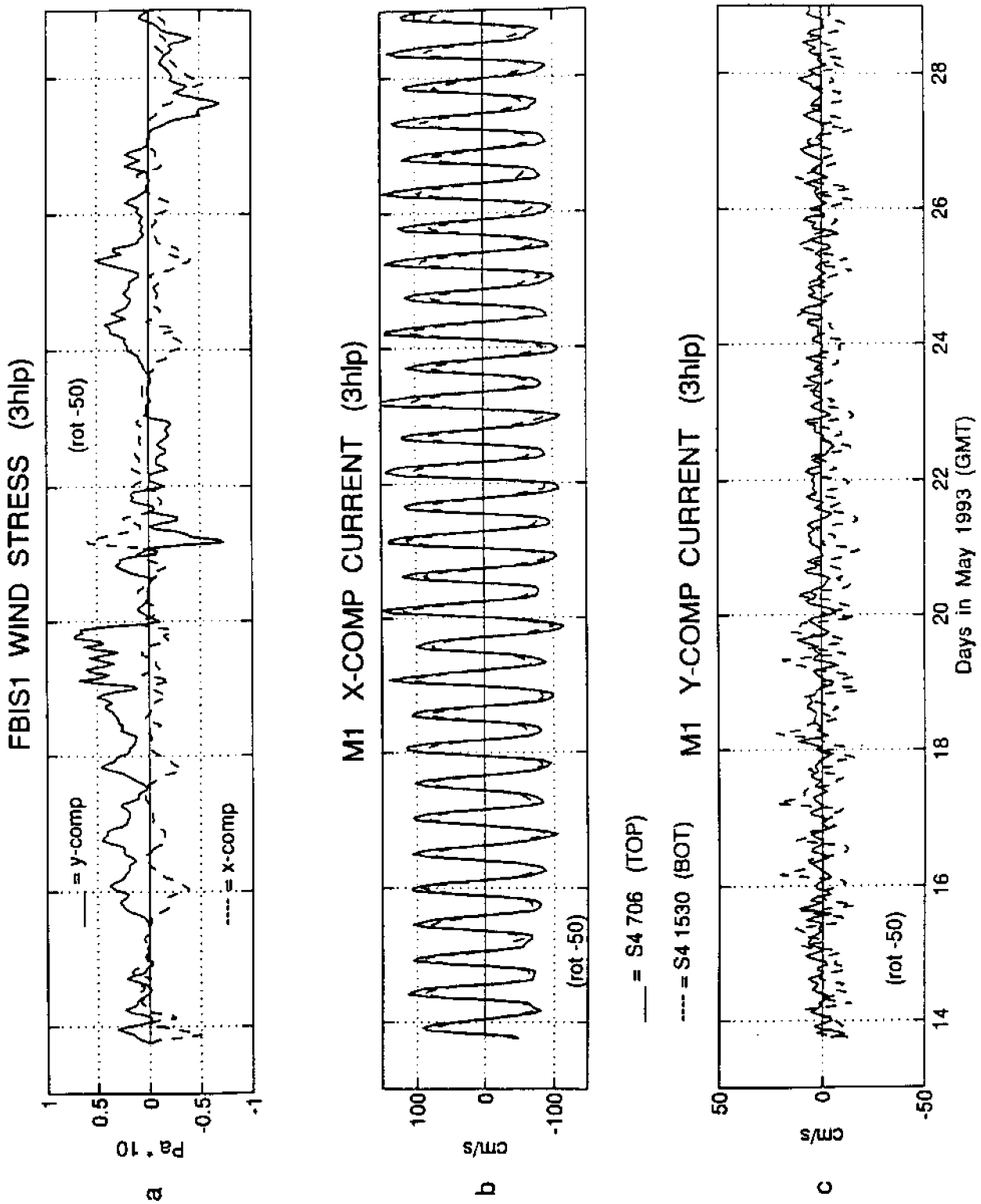
FBIS1 WIND STRESS (3hlp)
(rot -50)
___ = y-comp
---- = x-comp
Pa * 10
1
0.5
0
-0.5
-1
a
M1 X-COMP CURRENT (3hlp)
(rot -50)
cm/s
100
0
-100
b
M1 Y-COMP CURRENT (3hlp)
___ = S4 706 (TOP)
--- = S4 1530 (BOT)
(rot -50)
cm/s
50
0
-50
c
14
16
18
20
22
24
26
28
Days in May 1993 (GMT)

Figure 6

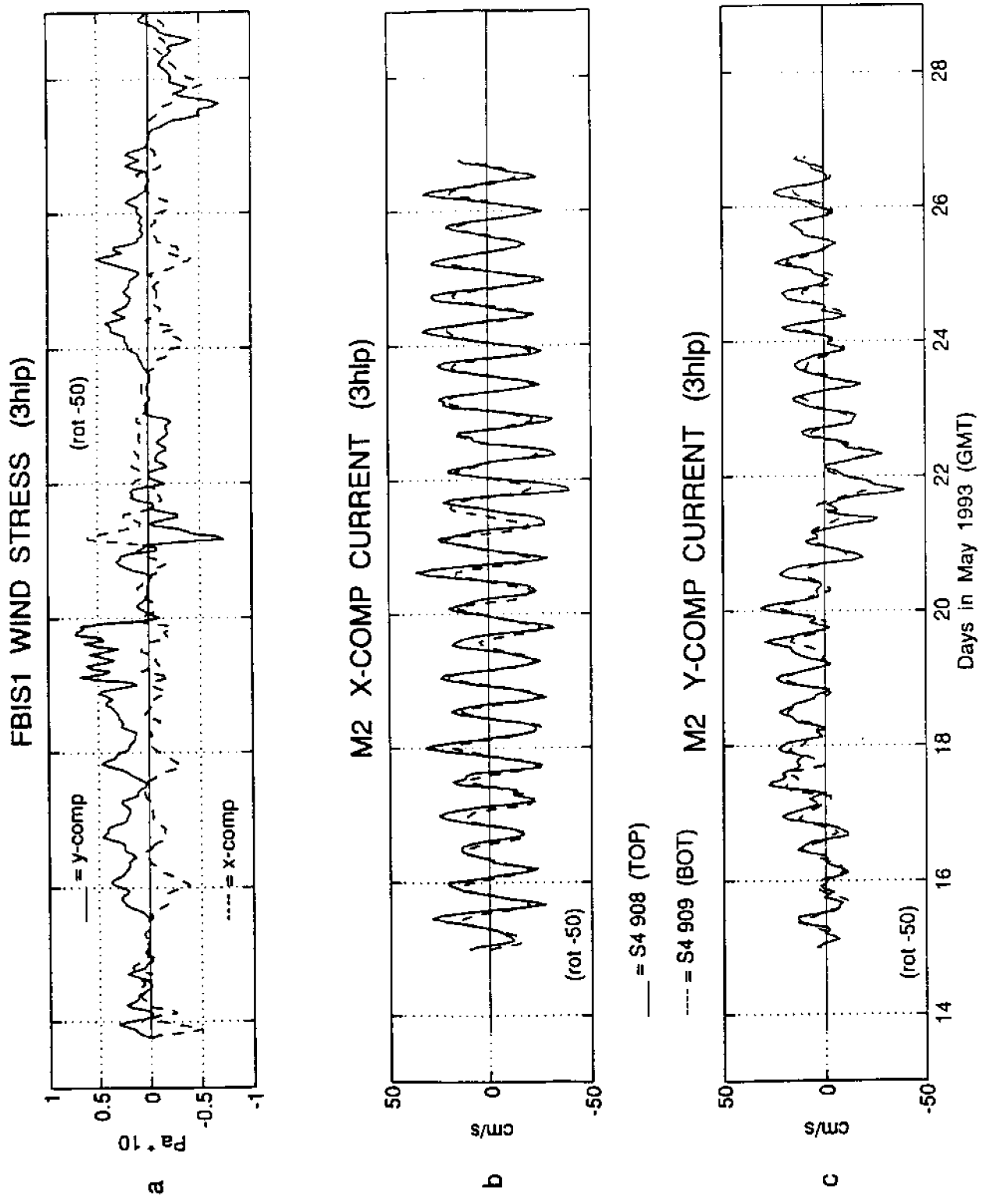
FBIS1 WIND STRESS (3hlp)
(rot -50)
___ = y-comp
---- = x-comp
Pa * 10
1
0.5
0
-0.5
-1
a
M2 X-COMP CURRENT (3hlp)
(rot -50)
cm/s
50
0
-50
b
___ = S4 908 (TOP)
---- = S4 909 (BOT)
M2 Y-COMP CURRENT (3hlp)
(rot -50)
cm/s
50
0
-50
c
14
16
18
20
22
24
26
28
Days in May 1993 (GMT)

Figure 7

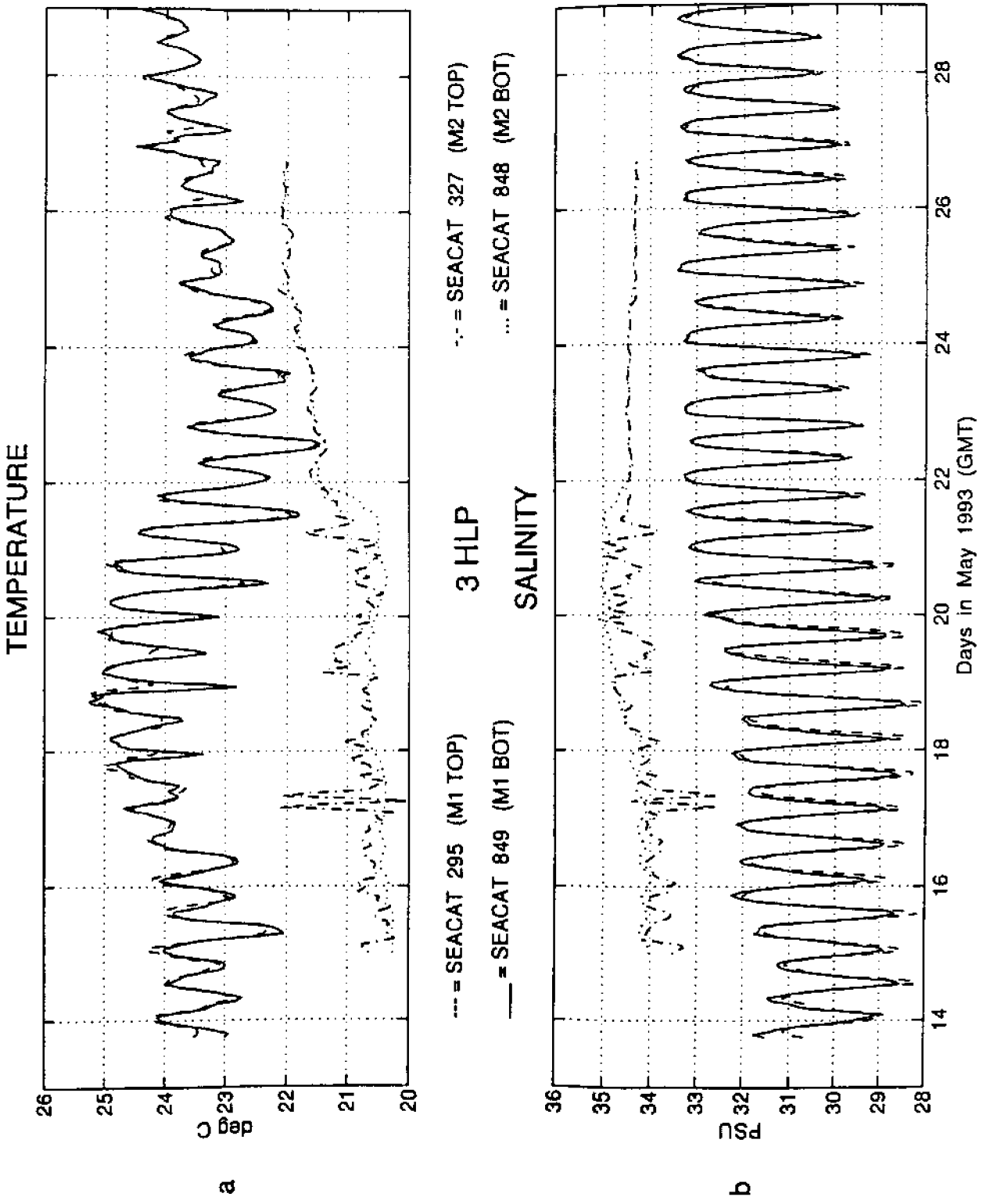
TEMPERATURE
deg C
a
3 HLP
--- = SEACAT 295 (M1 TOP)
___ = SEACAT 849 (M1 BOT)
-·- = SEACAT 327 (M2 TOP)
... = SEACAT 848 (M2 BOT)
SALINITY
PSU
b
Days in May 1993 (GMT)

Figure 8 (a & b)

Figure 8 (c & d)

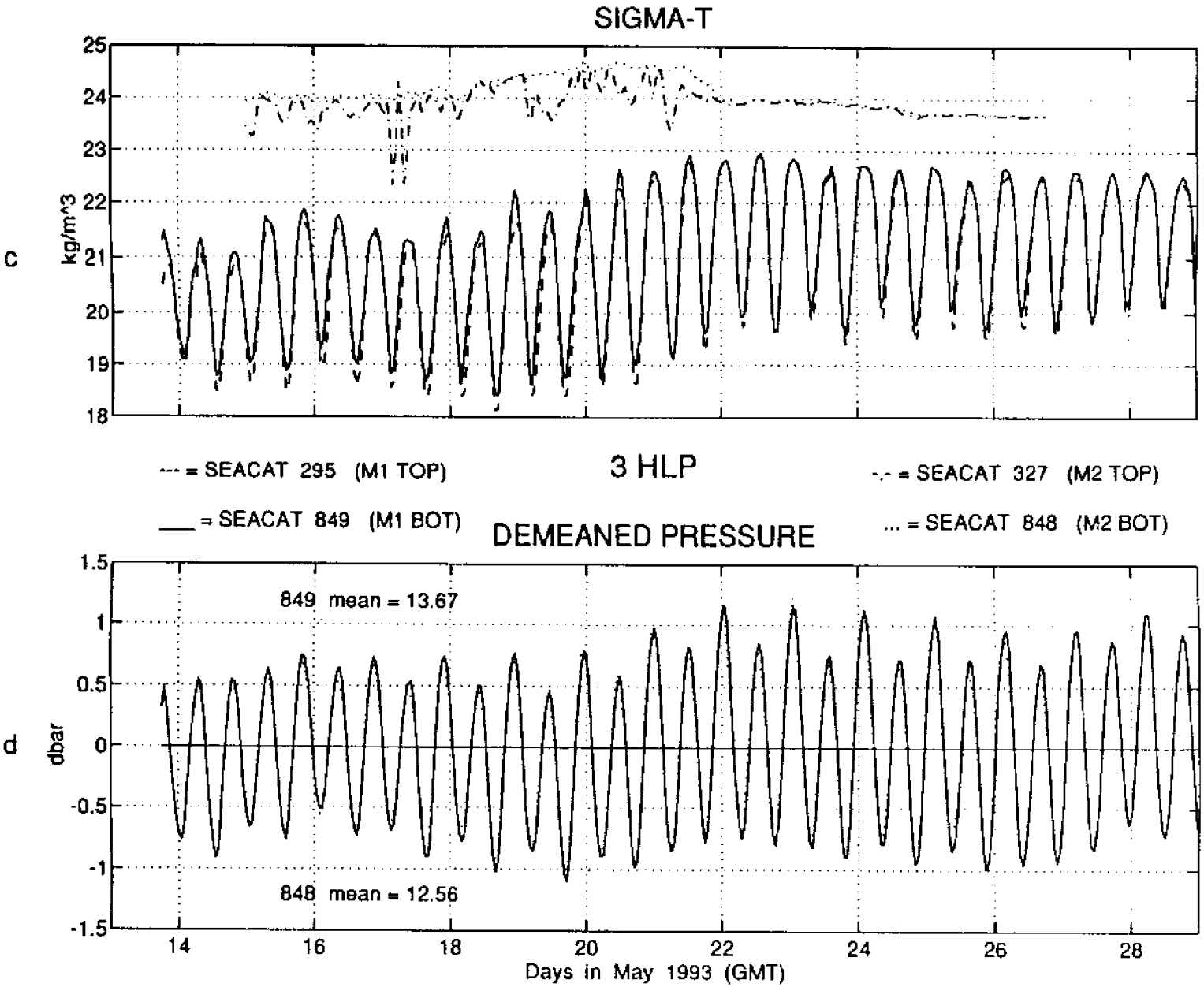
SIGMA-T
c
kg/m^3
25
24
23
22
21
20
19
18
--- = SEACAT 295 (M1 TOP)
-.- = SEACAT 327 (M2 TOP)
___ = SEACAT 849 (M1 BOT)
... = SEACAT 848 (M2 BOT)
3 HLP
DEMEANED PRESSURE
d
dbar
849 mean = 13.67
848 mean = 12.56
1.5
1
0.5
0
-0.5
-1
-1.5
14
16
18
20
22
24
26
28
Days in May 1993 (GMT)

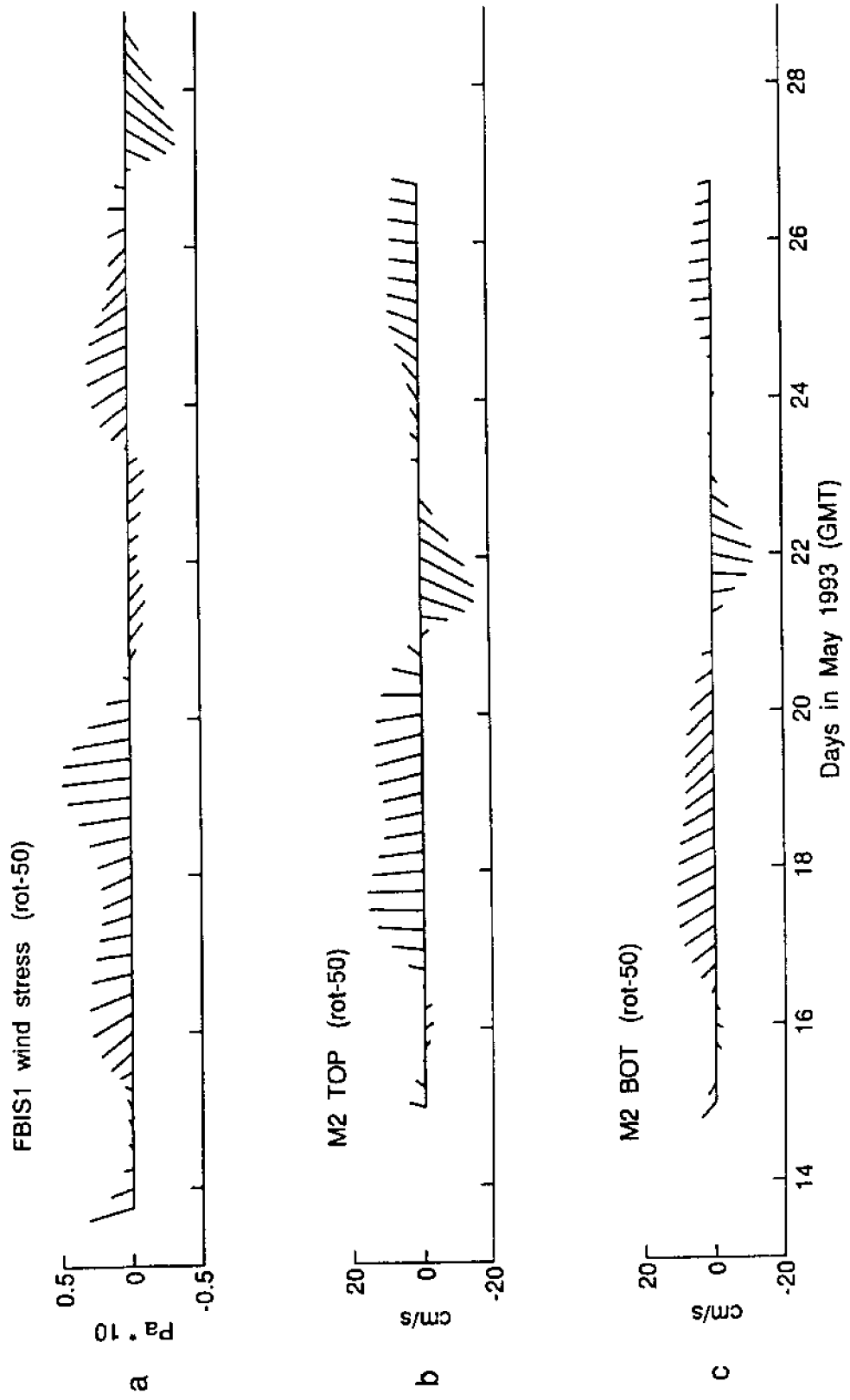
Wind Stress and Current Vectors (40hlp)
FBIS1 wind stress (rot-50)
0.5
0
-0.5
Pa * 10
a
M2 TOP (rot-50)
20
0
-20
cm/s
b
M2 BOT (rot-50)
20
0
-20
cm/s
c
14
16
18
20
22
24
26
28
Days in May 1993 (GMT)

Figure 9

Figure 10

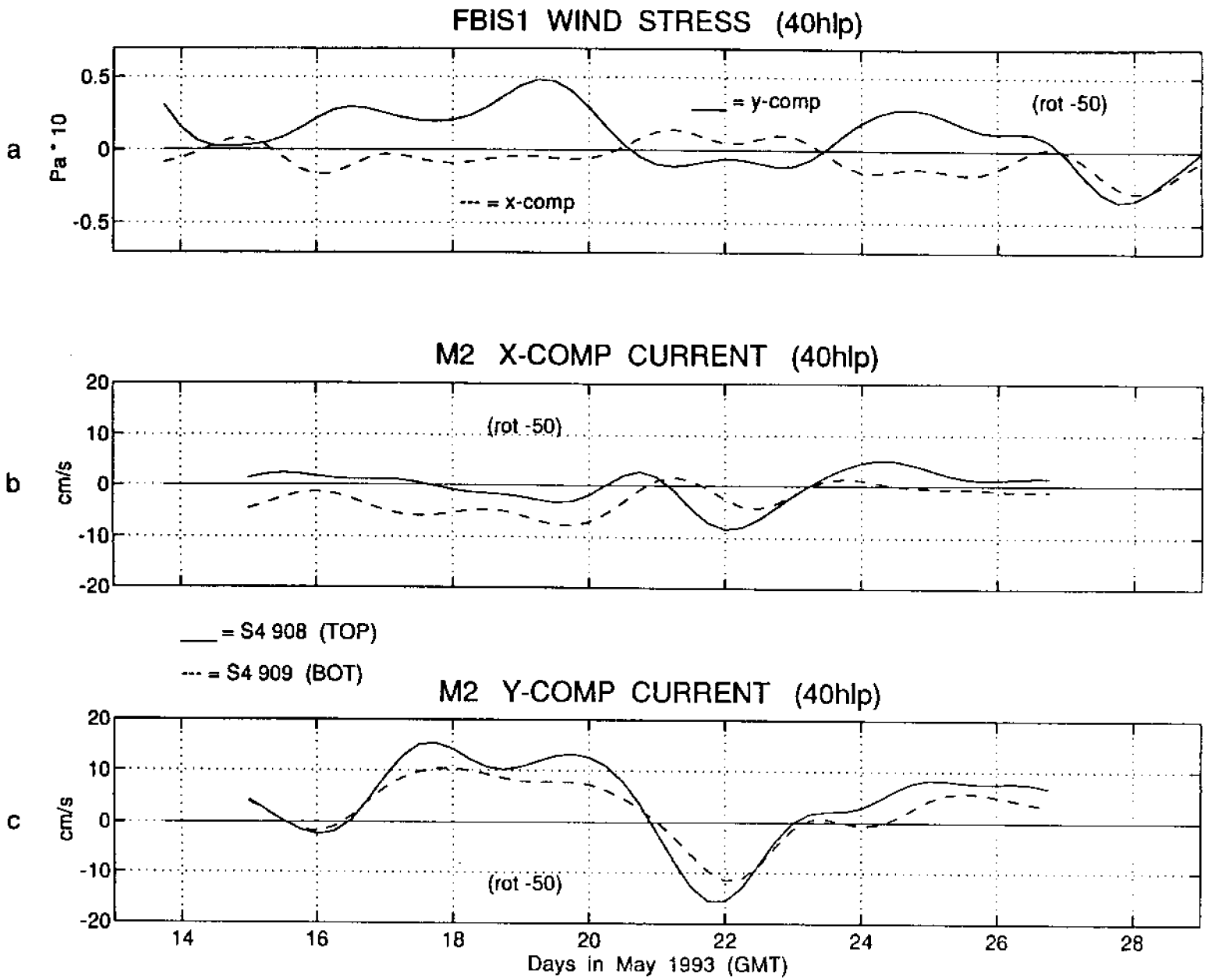
FBIS1 WIND STRESS (40hlp)
a
Pa * 10
0.5
0
-0.5
= y-comp
(rot -50)
--- = x-comp
M2 X-COMP CURRENT (40hlp)
b
cm/s
20
10
0
-10
-20
(rot -50)
___ = S4 908 (TOP)
--- = S4 909 (BOT)
M2 Y-COMP CURRENT (40hlp)
c
cm/s
20
10
0
-10
-20
(rot -50)
14
16
18
20
22
24
26
28
Days in May 1993 (GMT)

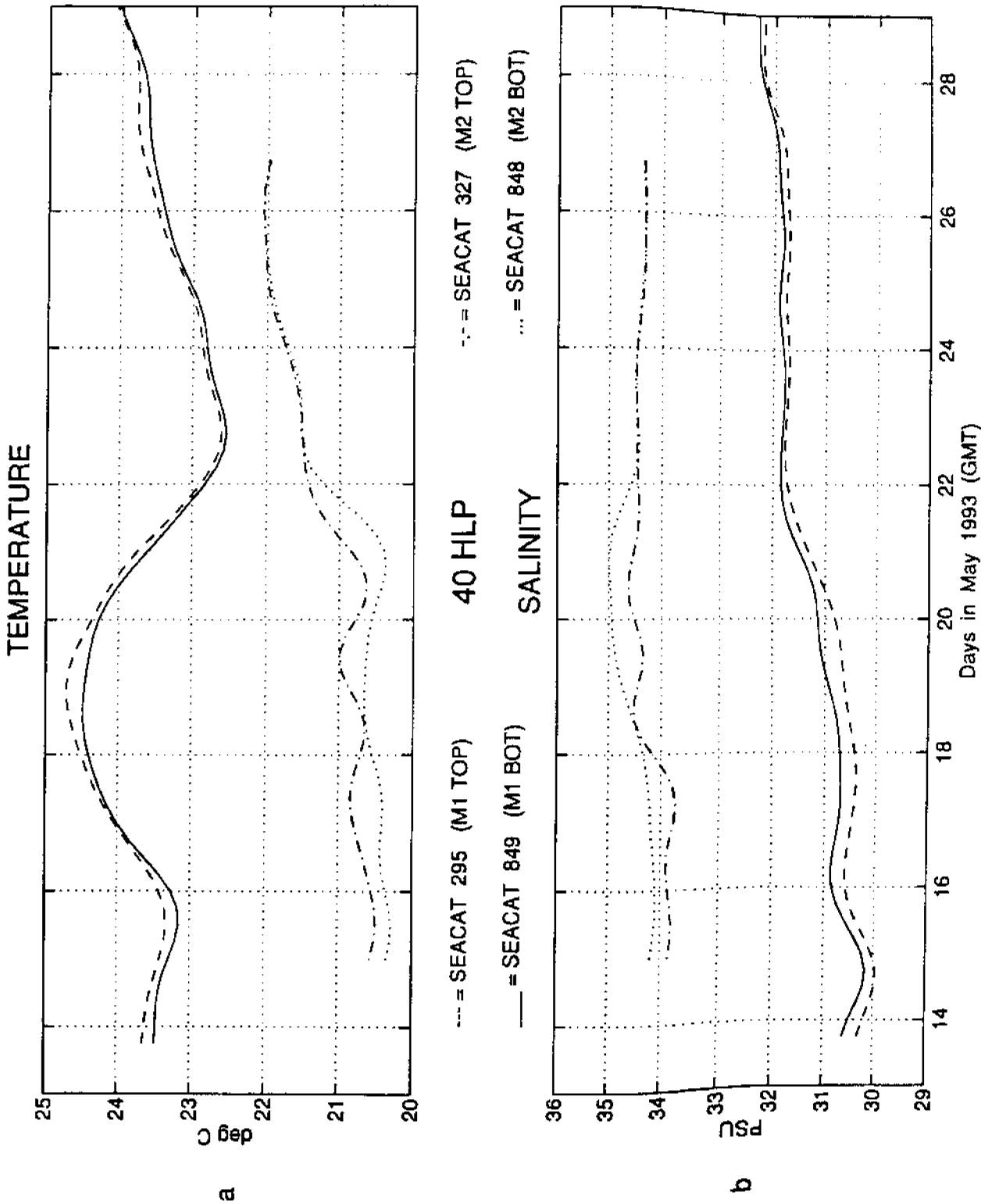
TEMPERATURE
deg C
25
24
23
22
21
20
a
40 HLP
--- = SEACAT 295 (M1 TOP)
___ = SEACAT 849 (M1 BOT)
-.- = SEACAT 327 (M2 TOP)
... = SEACAT 848 (M2 BOT)
SALINITY
PSU
36
35
34
33
32
31
30
29
14
16
18
20
22
24
26
28
Days in May 1993 (GMT)
b

Figure 11 (a & b)

Figure 11 (c & d)

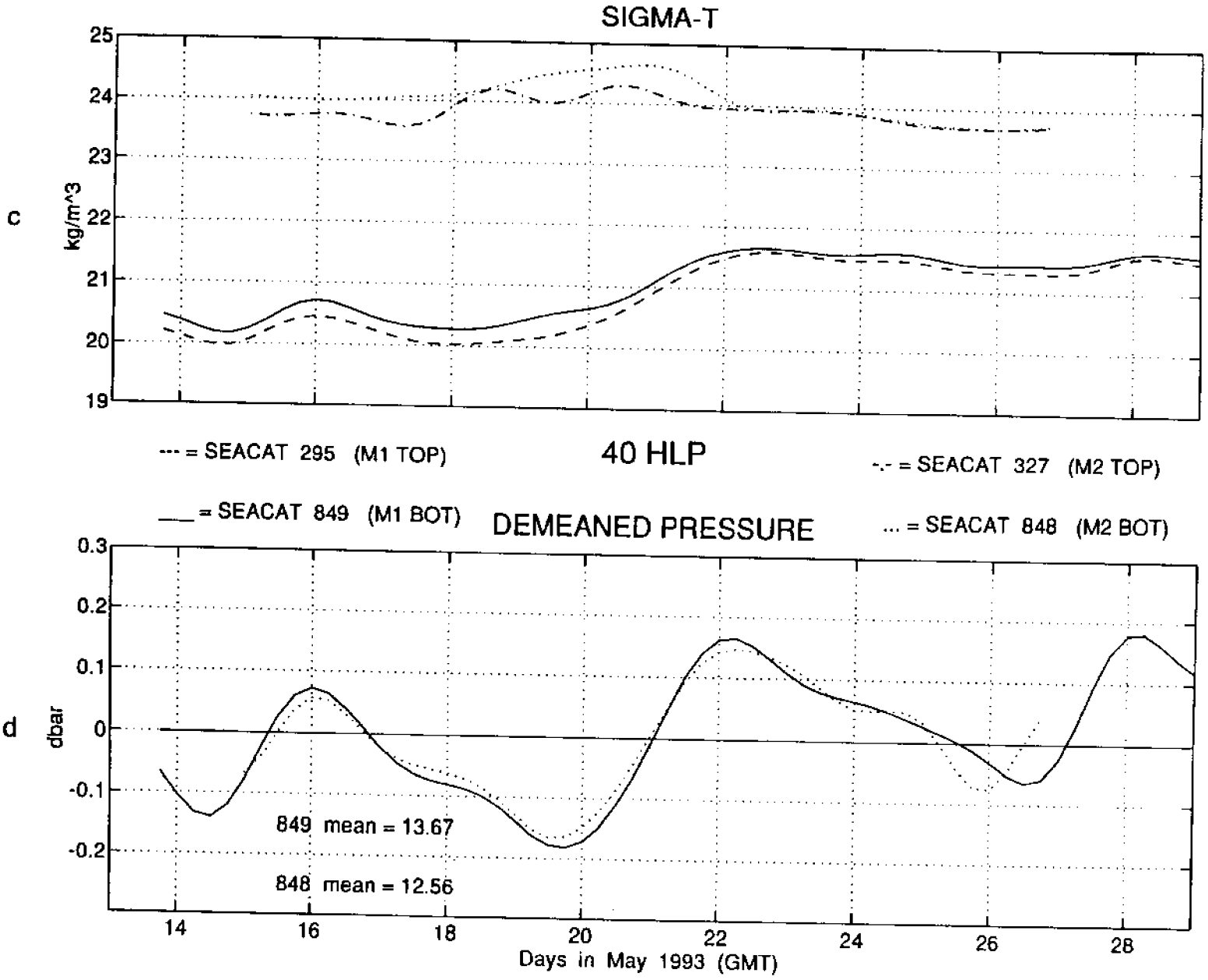
c
SIGMA-T
kg/m^3
25
24
23
22
21
20
19
--- = SEACAT 295 (M1 TOP)
40 HLP
-.- = SEACAT 327 (M2 TOP)
___ = SEACAT 849 (M1 BOT)
DEMEANED PRESSURE
... = SEACAT 848 (M2 BOT)
d
dbar
0.3
0.2
0.1
0
-0.1
-0.2
849 mean = 13.67
848 mean = 12.56
14
16
18
20
22
24
26
28
Days in May 1993 (GMT)

NED1 Offshore Survey Number 1
14-15 May 1993

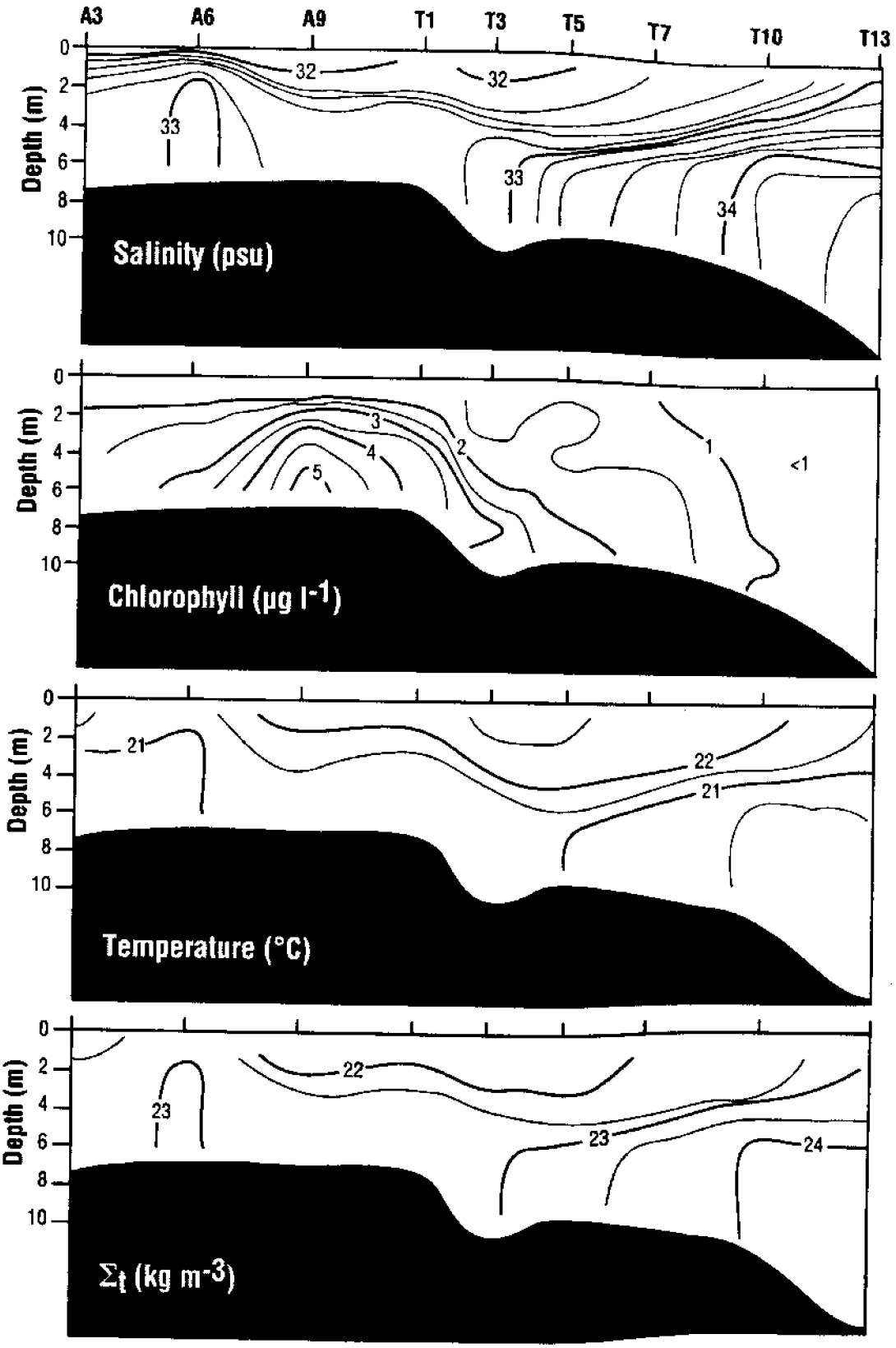

Figure 12

NED1 Offshore Survey Number 2
15-16 May 1993

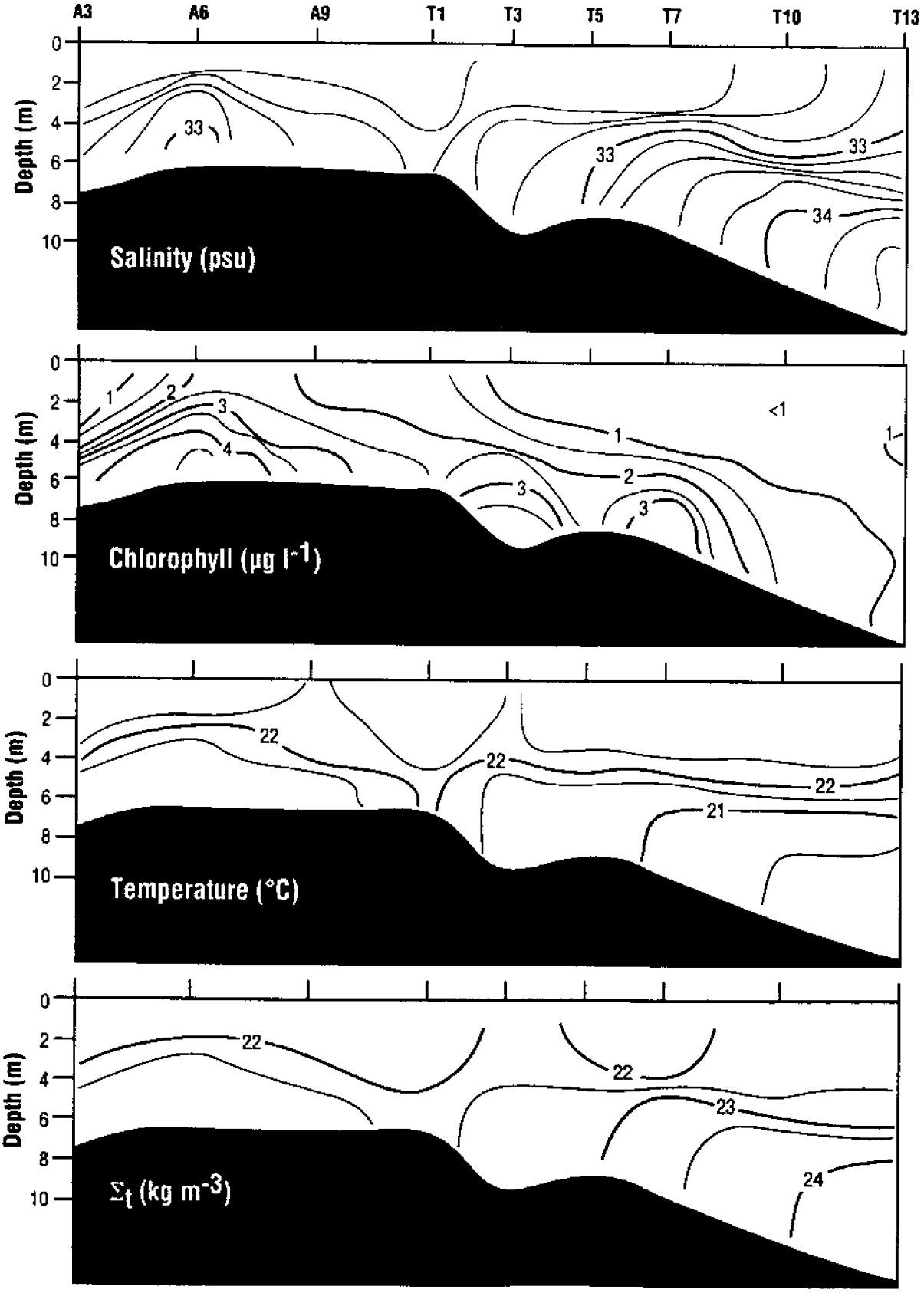

Figure 13

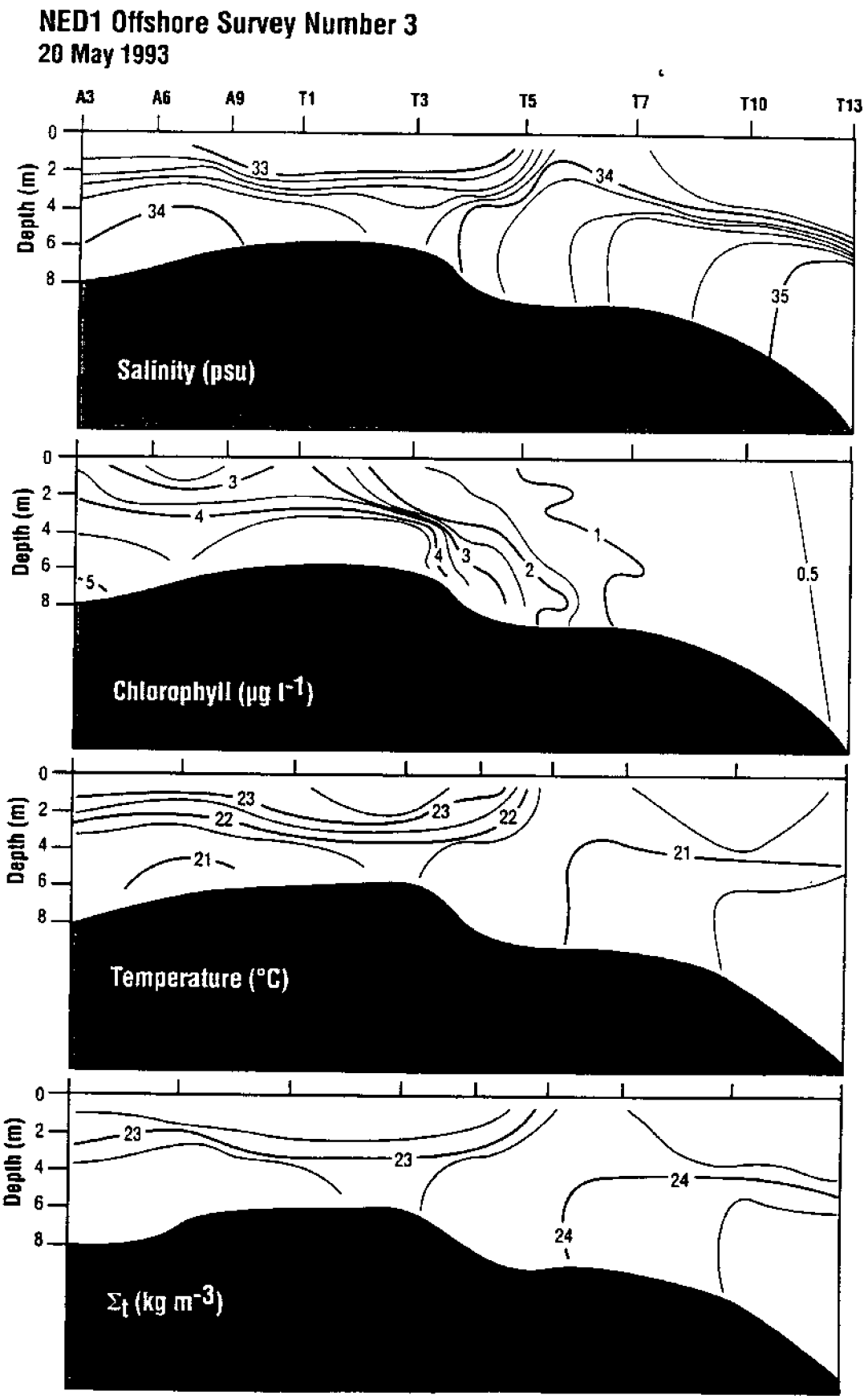
NED1 Offshore Survey Number 3
20 May 1993
A3
A6
A9
T1
T3
T5
T7
T10
T13
Depth (m)
0
2
4
6
8
33
34
34
35
Salinity (psu)
3
4
5
4
3
2
1
0.5
Chlorophyll (µg l-1)
23
22
23
22
21
21
Temperature (°C)
23
23
24
24
Σt (kg m-3)

Figure 14

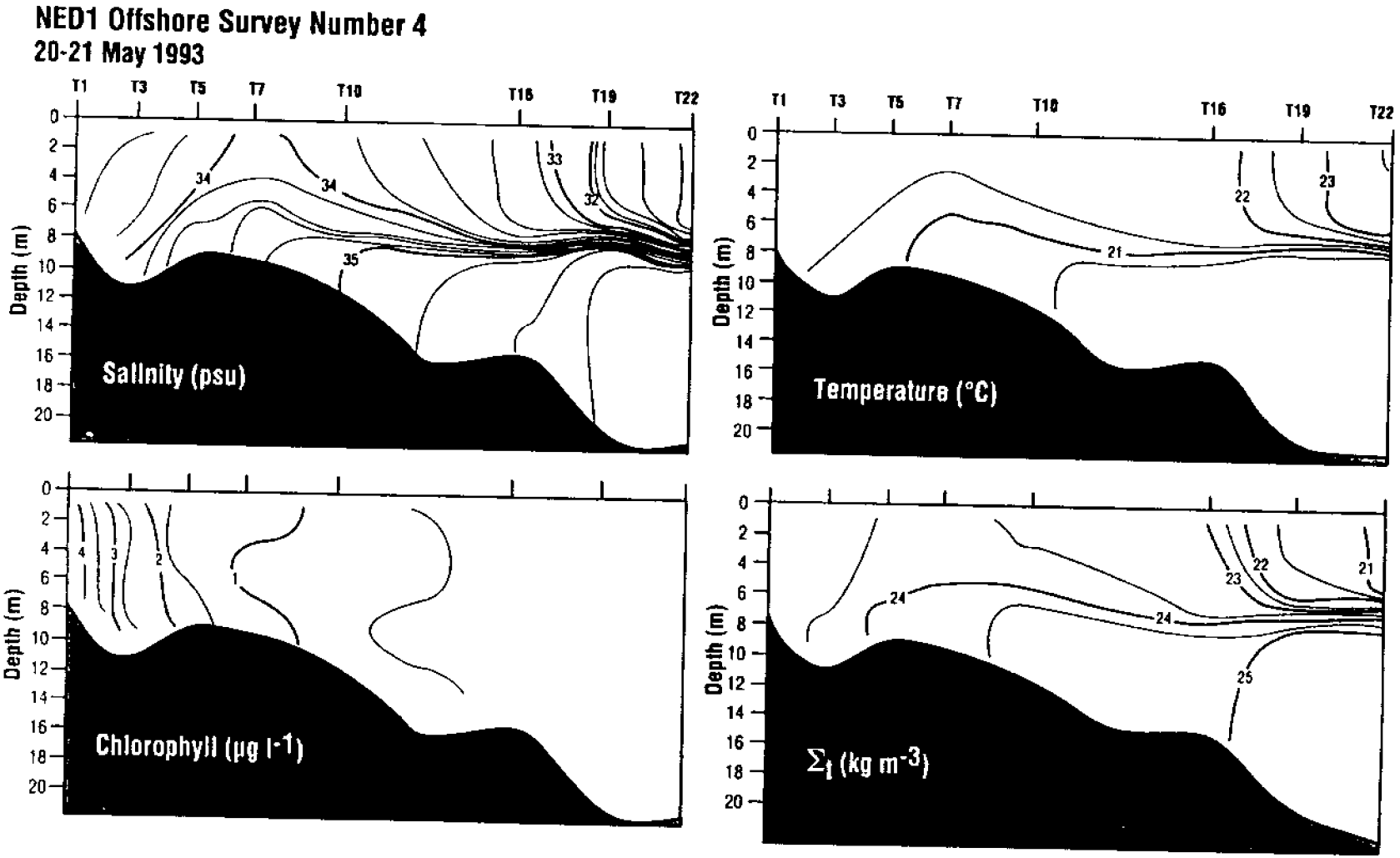
NED1 Offshore Survey Number 4
20-21 May 1993
T1
T3
T5
T7
T10
T16
T19
T22
Depth (m)
Salinity (psu)
Temperature (°C)
Chlorophyll (µg l-1)
Σt (kg m-3)

Figure 15

NED1 Offshore Survey Number 5
22 May 1993

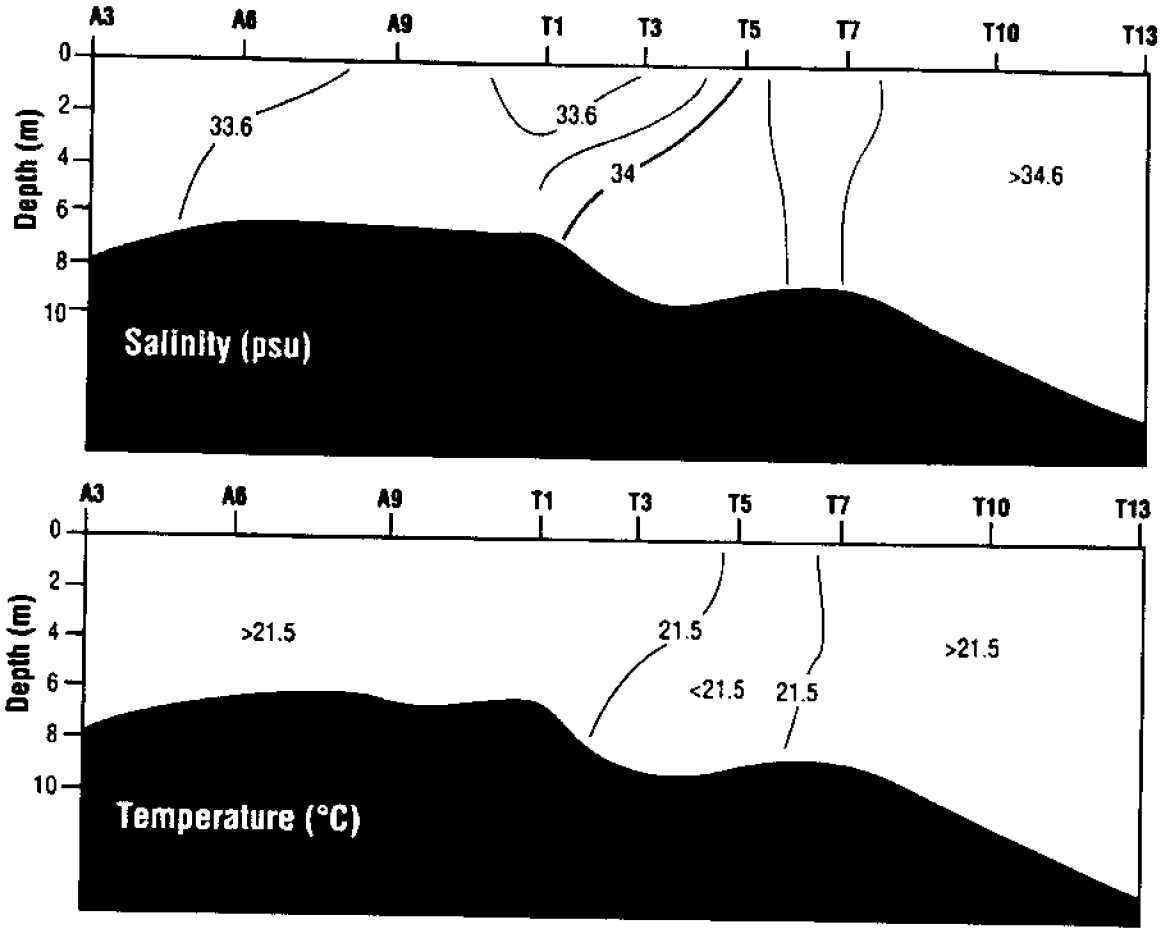

Figure 16

NED1 Offshore Survey Number 6
23 May 1993

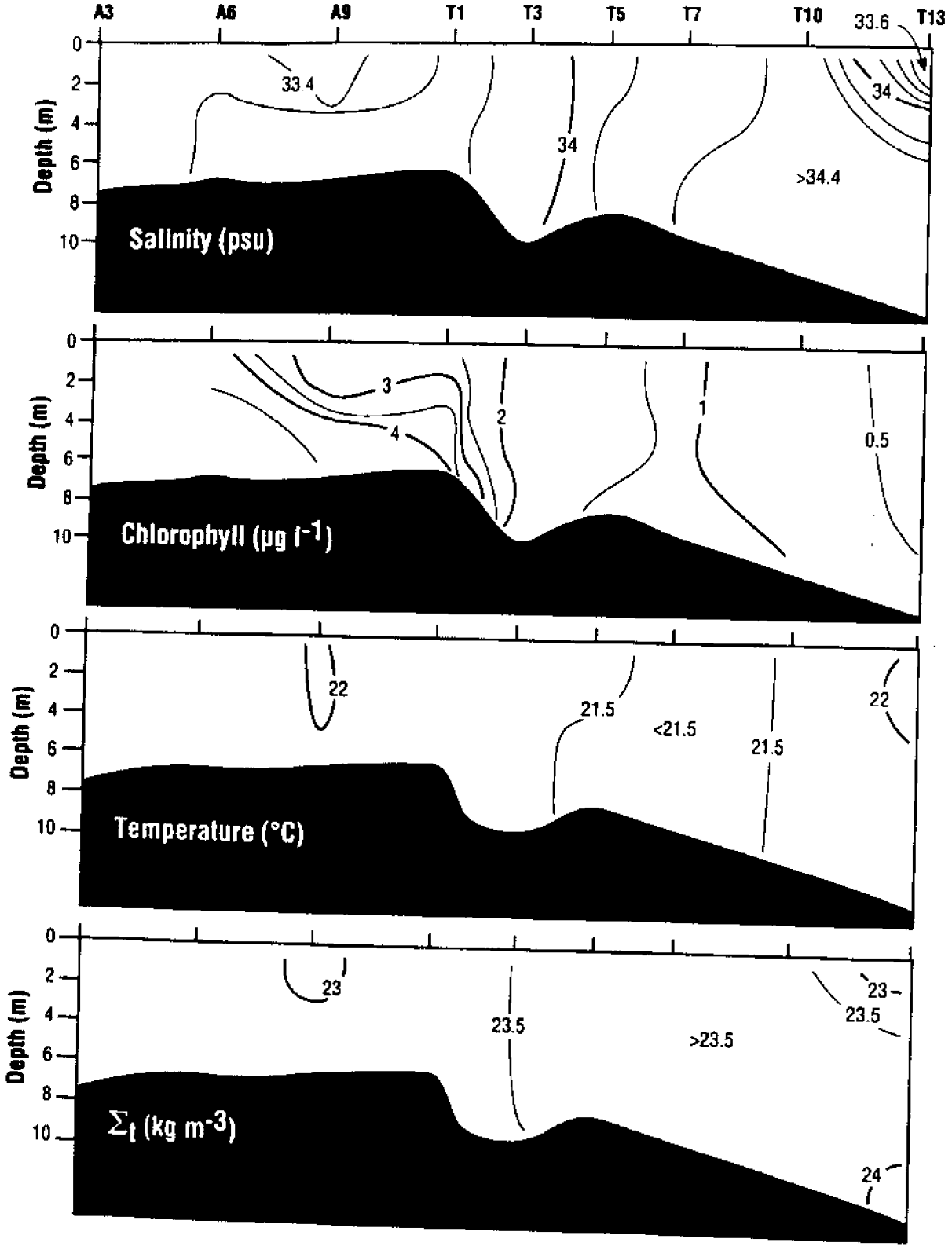

Figure 17

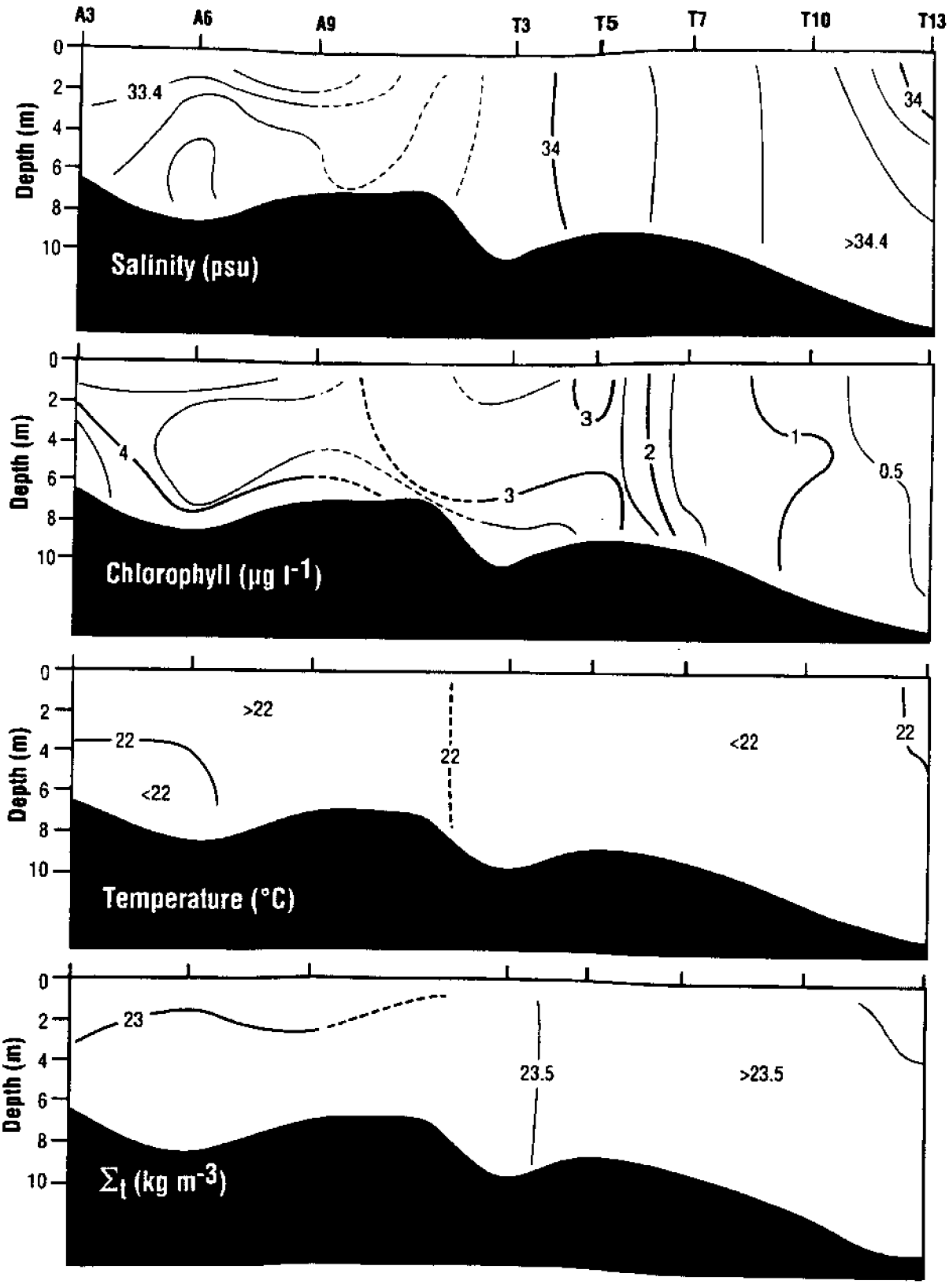
NED1 Offshore Survey Number 7
24 May 1993
A3
A6
A9
T3
T5
T7
T10
T13
Depth (m)
33.4
34
34
>34.4
Salinity (psu)
4
3
2
1
0.5
Chlorophyll (µg l-1)
>22
22
22
<22
<22
Temperature (°C)
23
23.5
>23.5
Σt (kg m-3)

Figure 18

NED1 Offshore Survey Number 8
25 May 1993

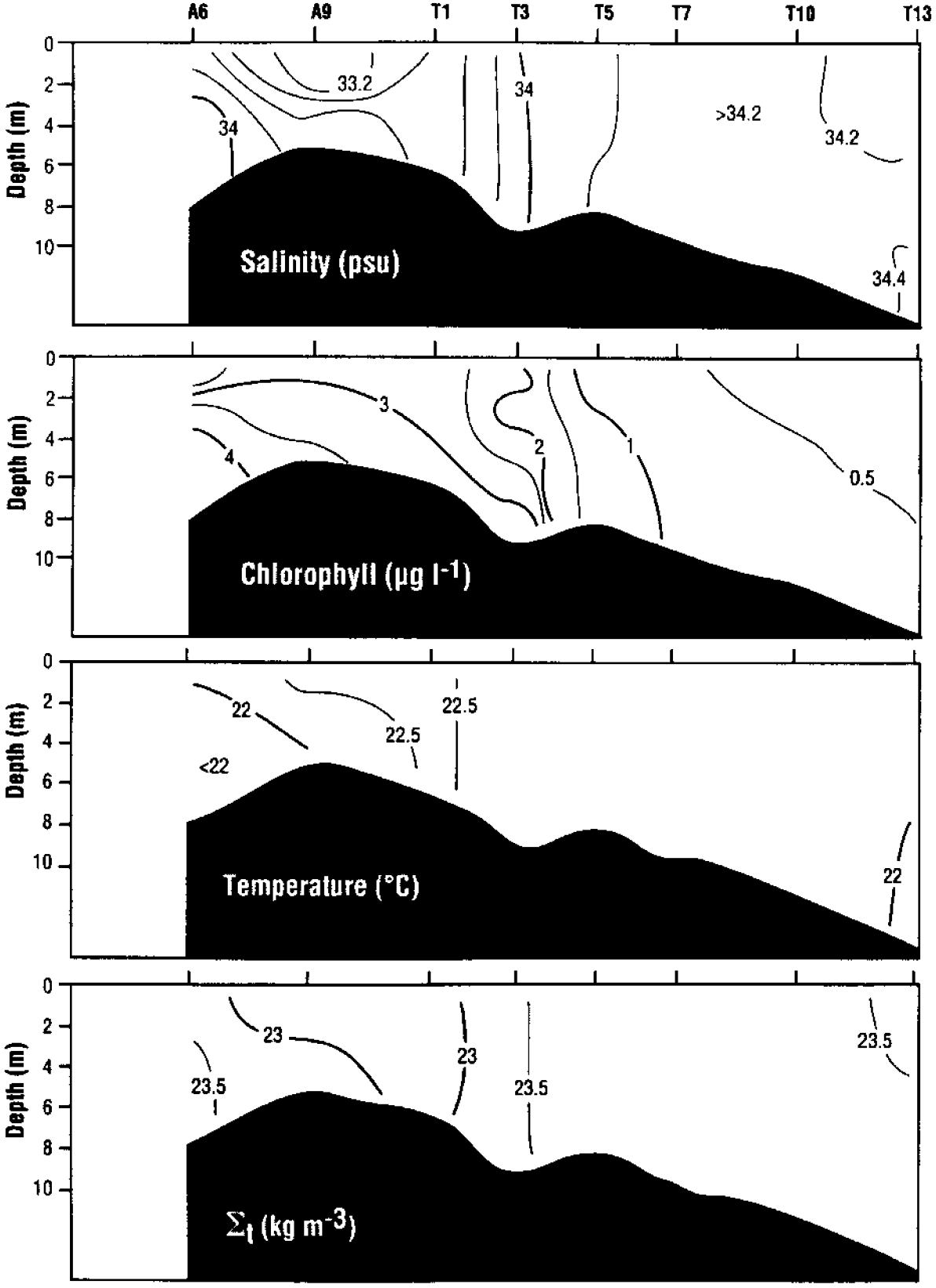

Figure 19

NED1 Offshore Survey Number 9
25 May 1993

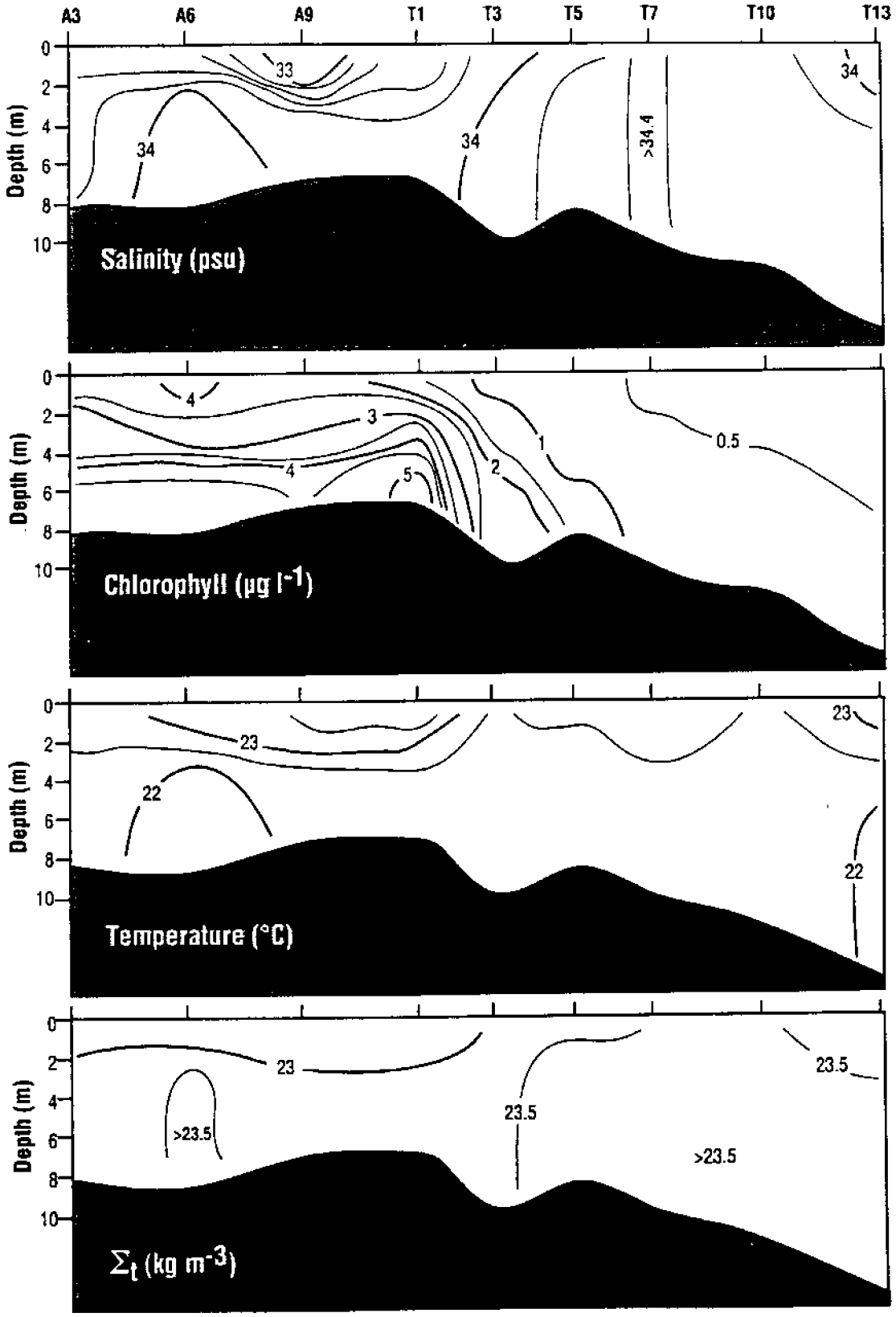

Figure 20

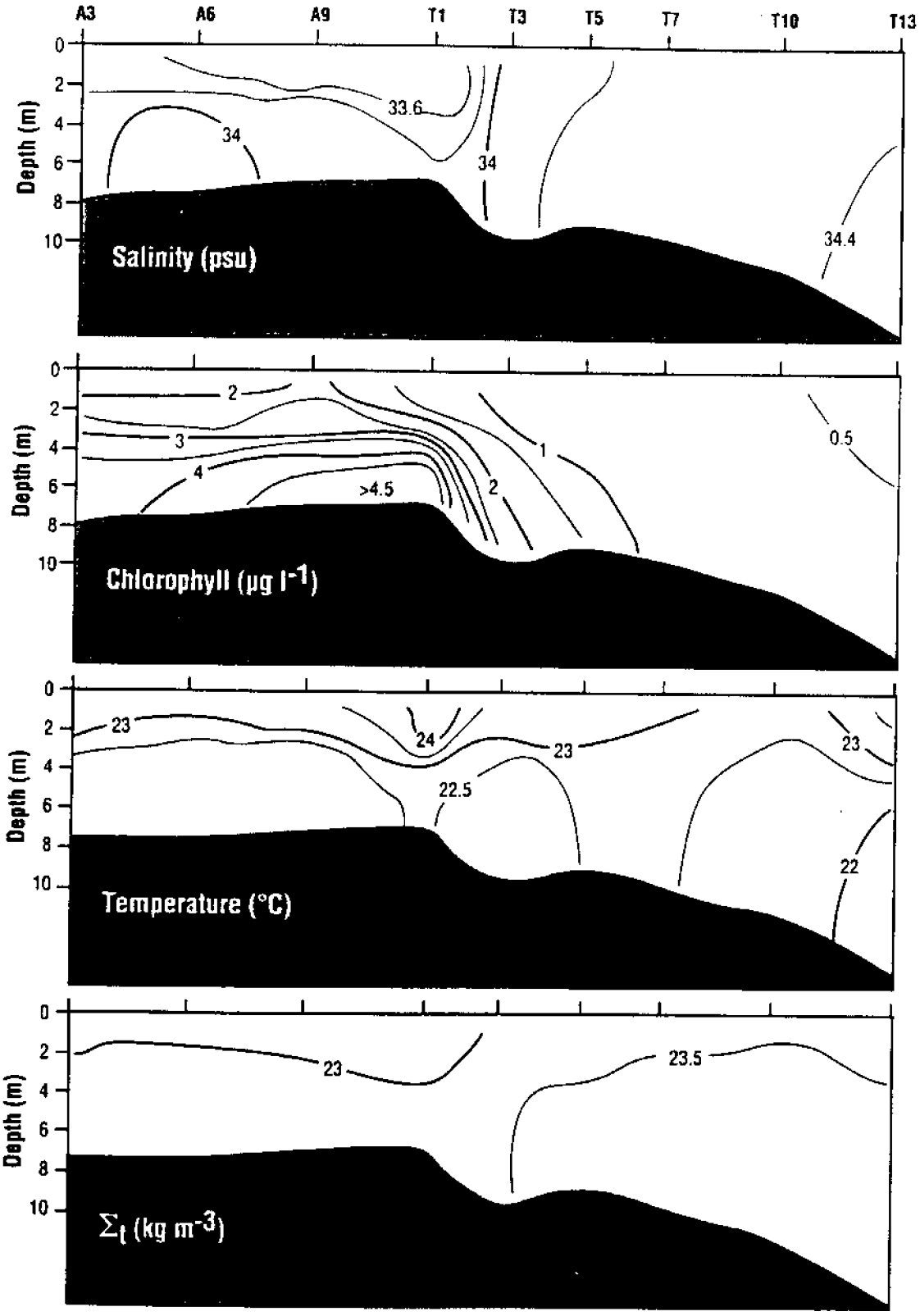
NED1 Offshore Survey Number 10
26 May 1993
A3
A6
A9
T1
T3
T5
T7
T10
T13
Depth (m)
0
2
4
6
8
10
33.6
34
34
34.4
Salinity (psu)
2
3
4
>4.5
2
1
0.5
Chlorophyll (µg l-1)
23
24
23
22.5
23
22
Temperature (°C)
23
23.5
Σt (kg m-3)

Figure 21

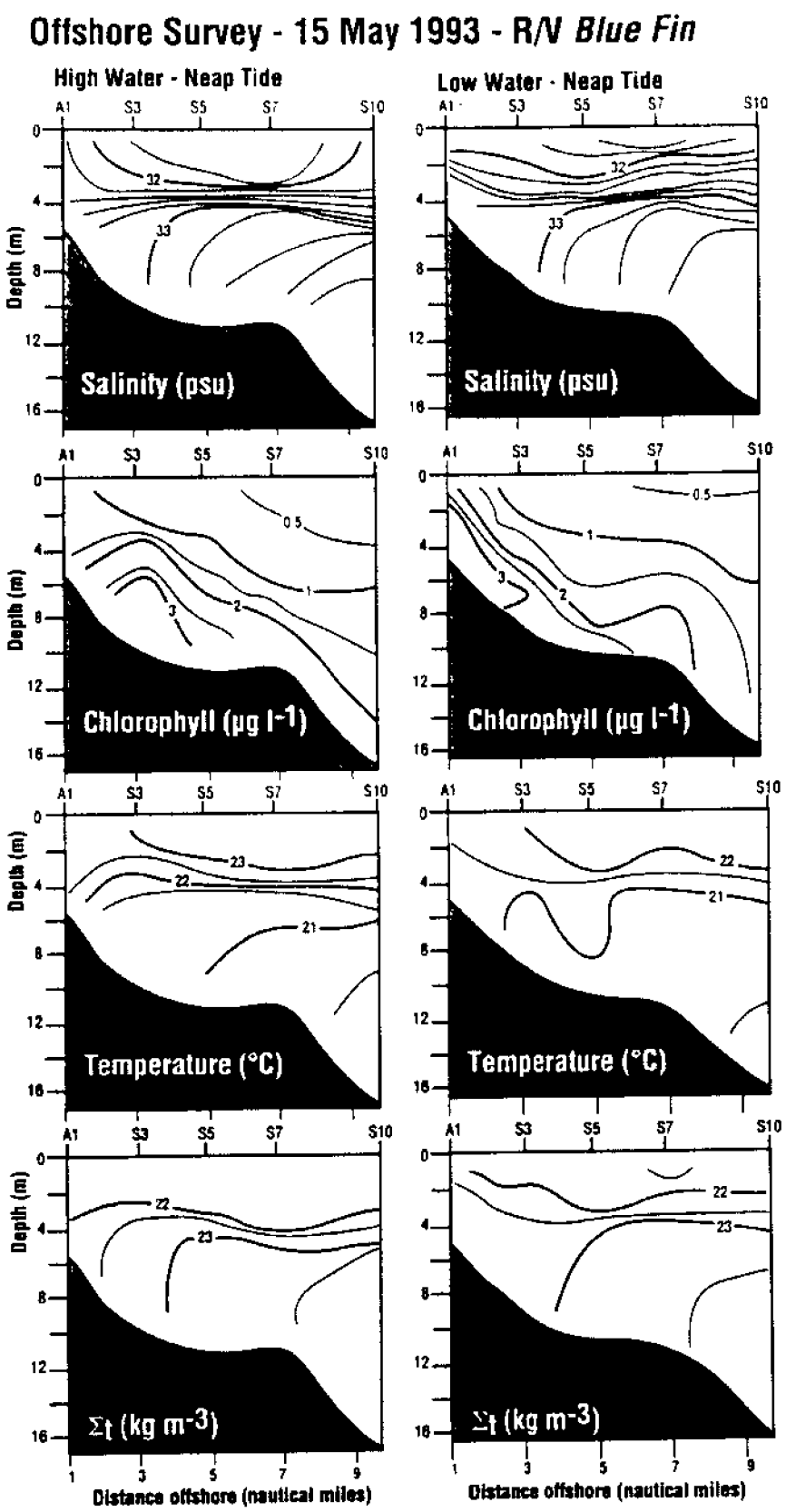
Offshore Survey - 15 May 1993 - R/V Blue Fin
High Water - Neap Tide
Low Water - Neap Tide
A1
S3
S5
S7
S10
Depth (m)
Salinity (psu)
Chlorophyll (µg l-1)
Temperature (°C)
Σt (kg m-3)
Distance offshore (nautical miles)

Figure 22

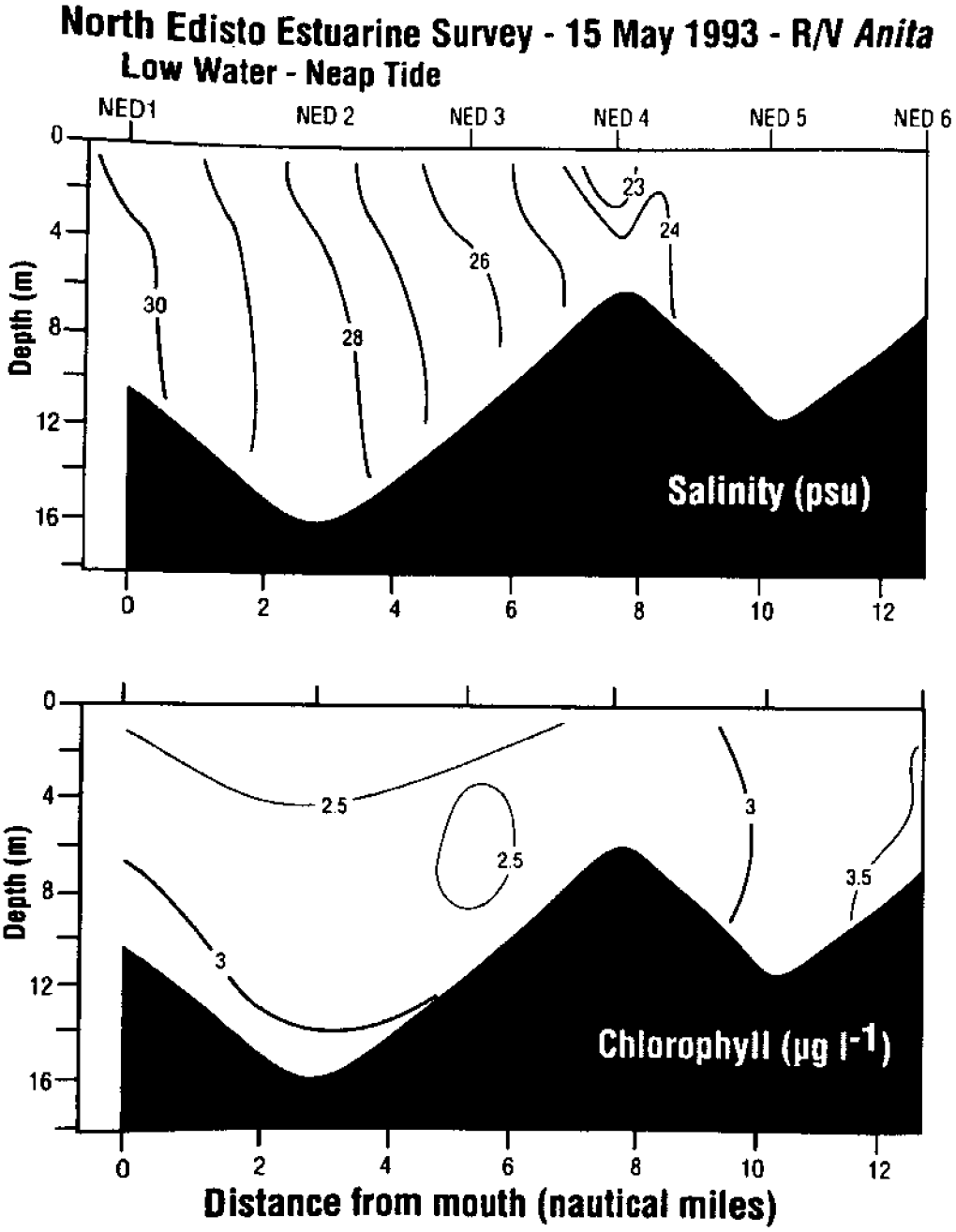
North Edisto Estuarine Survey - 15 May 1993 - R/V Anita
Low Water - Neap Tide
NED1
NED 2
NED 3
NED 4
NED 5
NED 6
Depth (m)
Salinity (psu)
Chlorophyll (µg l-1)
Distance from mouth (nautical miles)

Figure 23

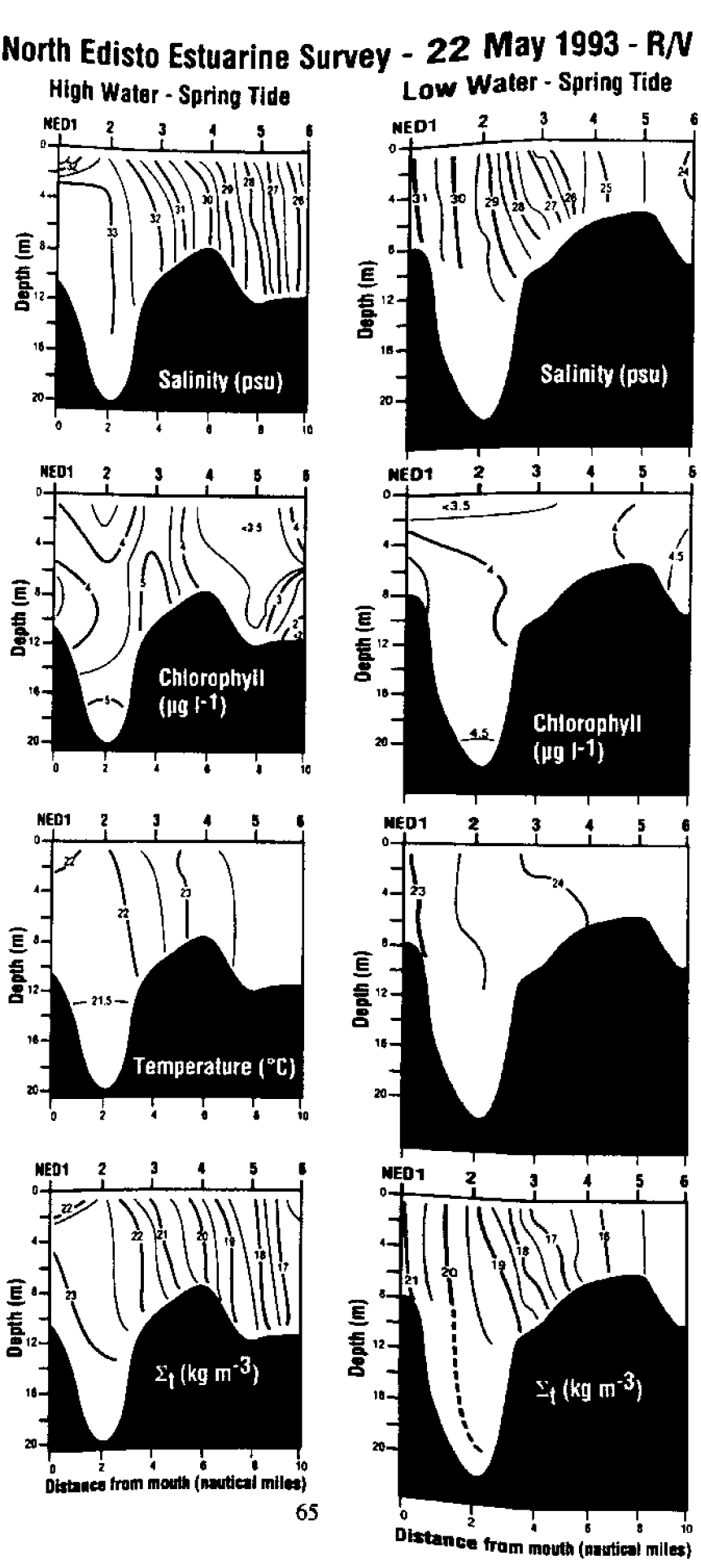
North Edisto Estuarine Survey - 22 May 1993 - R/V Anita
High Water - Spring Tide
Low Water - Spring Tide
NED1
Depth (m)
Salinity (psu)
Chlorophyll (µg l-1)
Temperature (°C)
Σt (kg m-3)
Distance from mouth (nautical miles)

Figure 24

Time versus Depth Plots during Maximum Flood Current in Throat of North Edisto Inlet

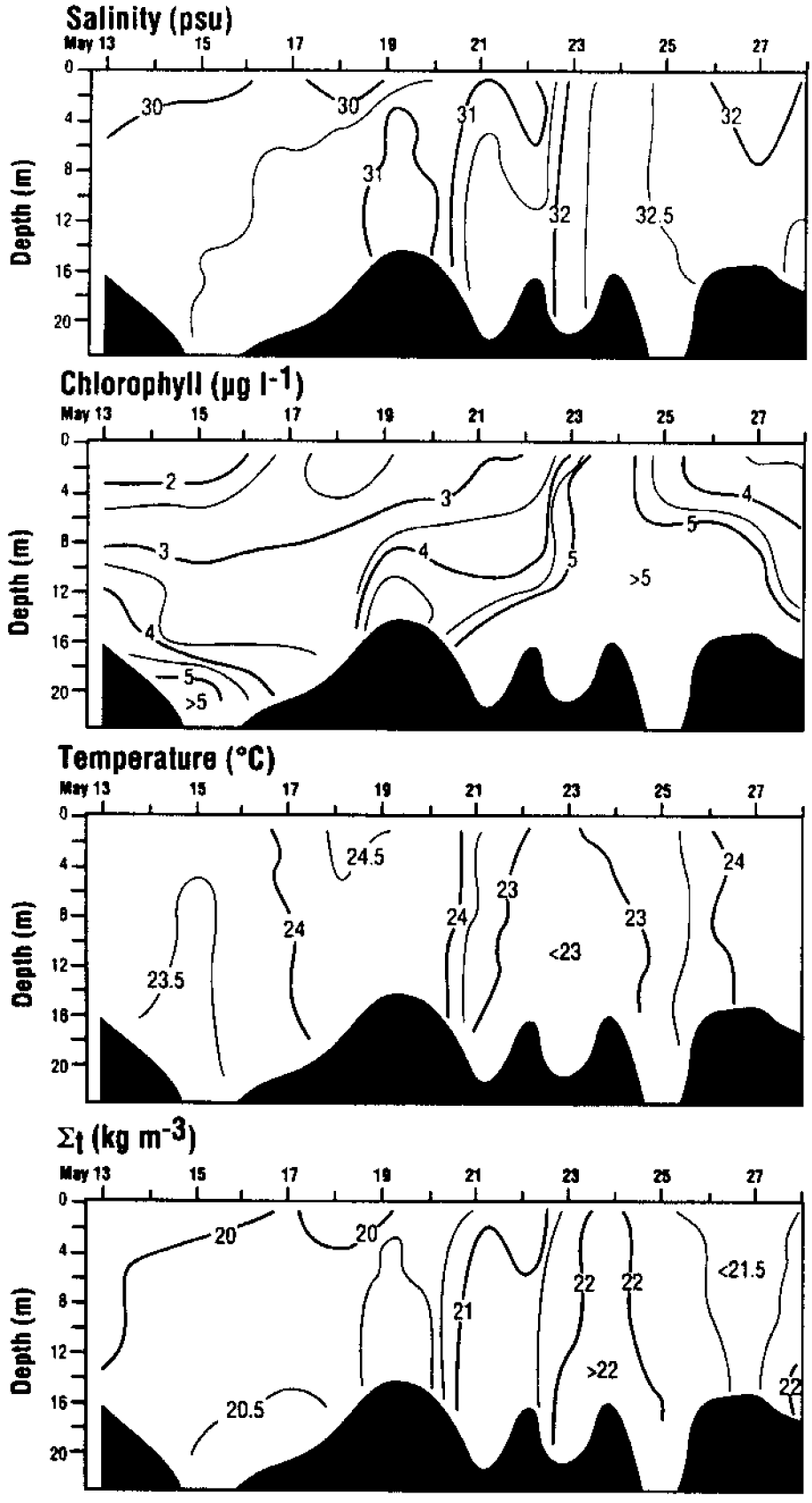

Figure 25

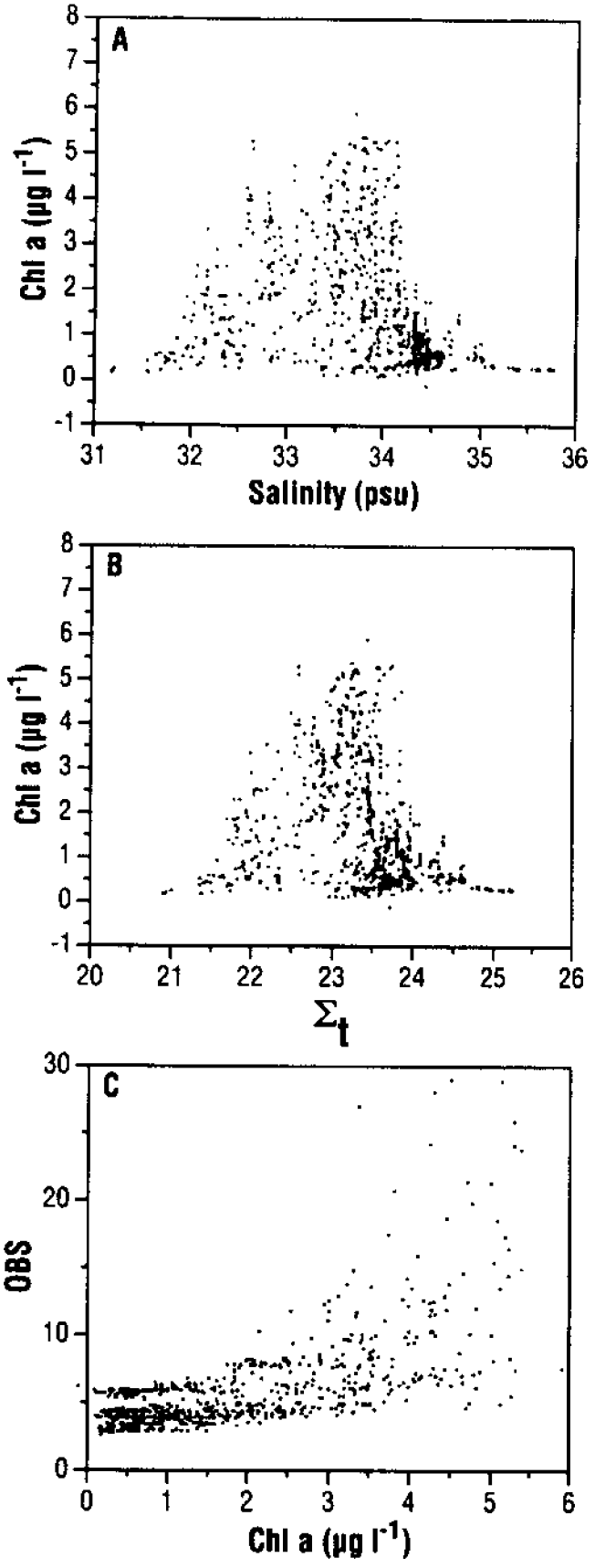

Figure 26

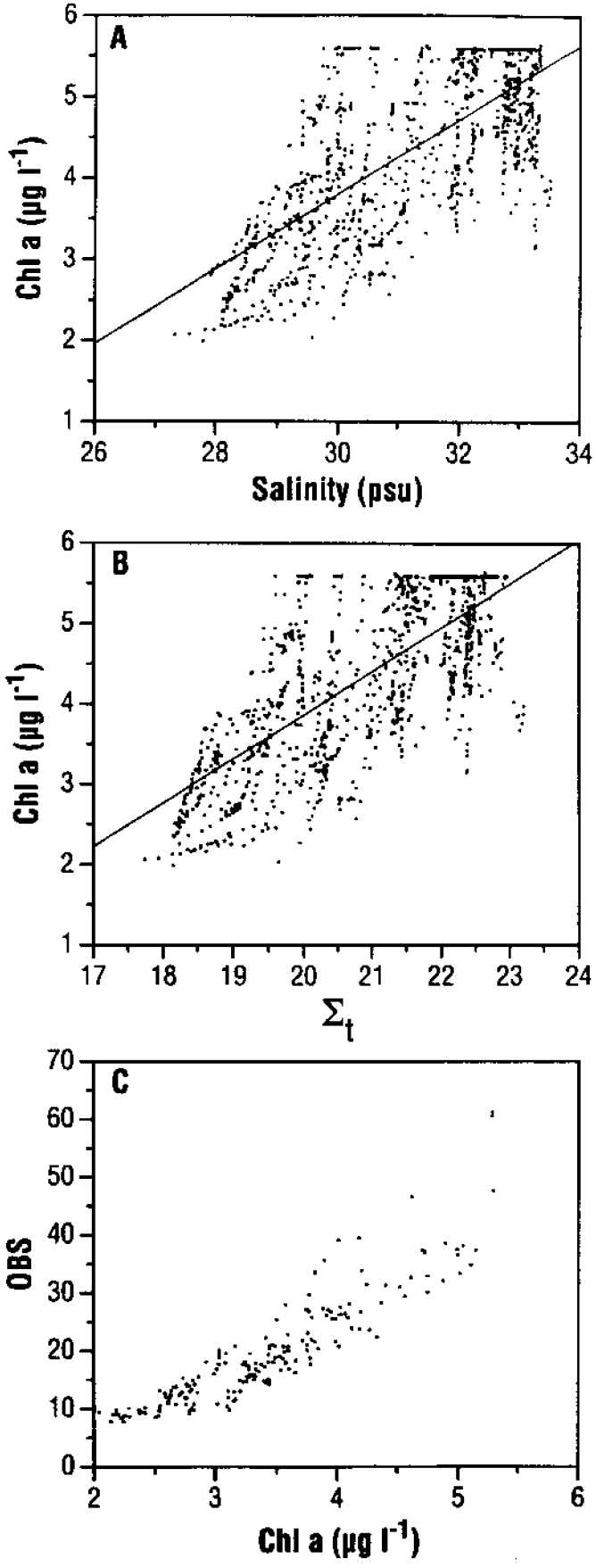

Figure 27

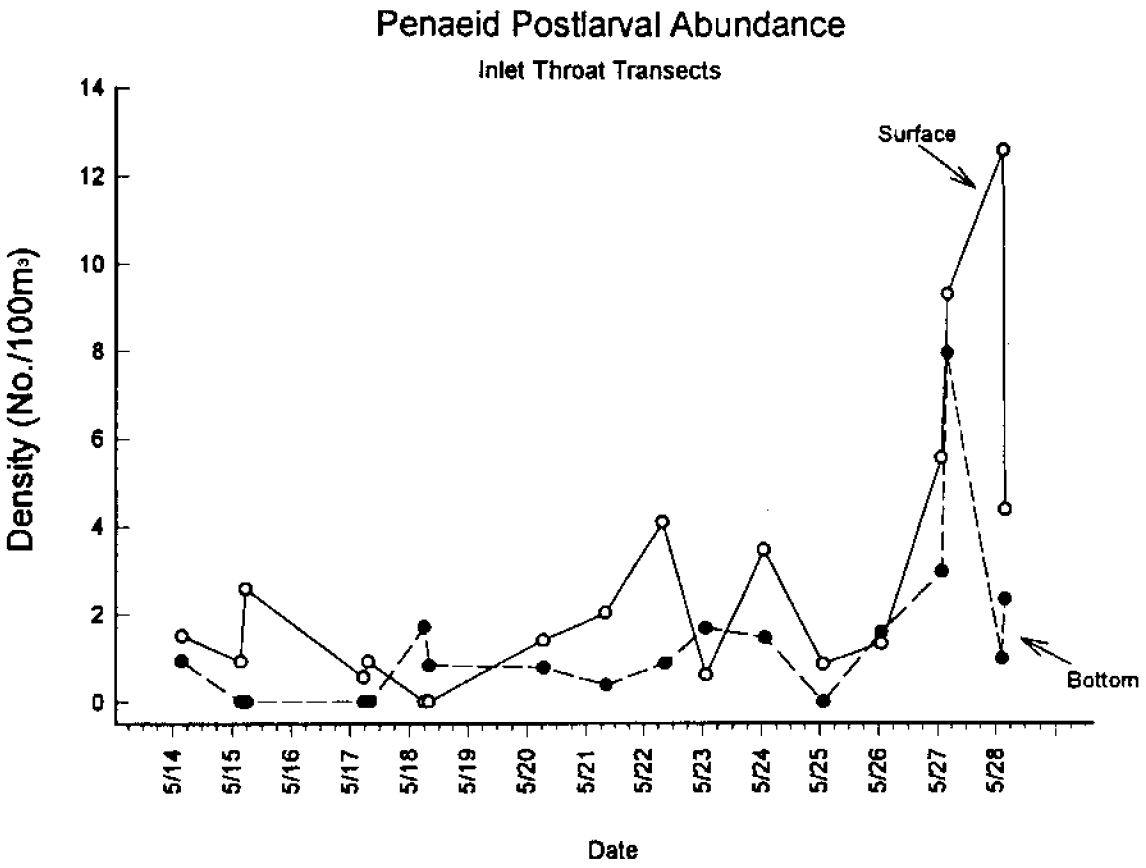
Penaeid Postlarval Abundance
Inlet Throat Transects
Density (No./100m³)
14
12
10
8
6
4
2
0
Surface
Bottom
5/14
5/15
5/16
5/17
5/18
5/19
5/20
5/21
5/22
5/23
5/24
5/25
5/26
5/27
5/28
Date

Figure 28

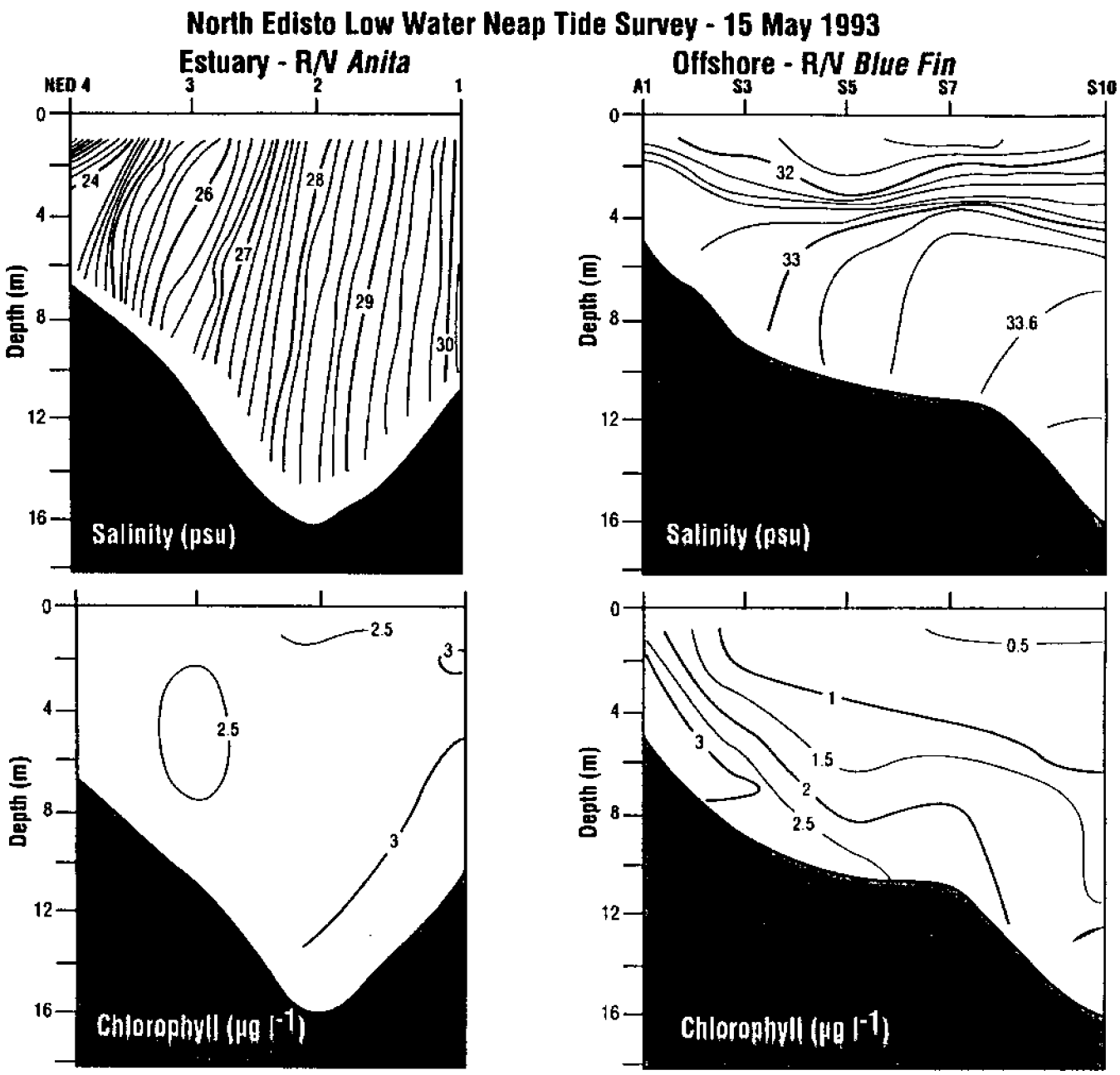
North Edisto Low Water Neap Tide Survey - 15 May 1993
Estuary - R/V Anita
Offshore - R/V Blue Fin
NED 4
3
2
1
A1
S3
S5
S7
S10
Depth (m)
0
4
8
12
16
24
26
27
28
29
30
32
33
33.6
Salinity (psu)
2.5
3
0.5
1
1.5
2
Chlorophyll (µg l-1)

Figure 29 (a & b)

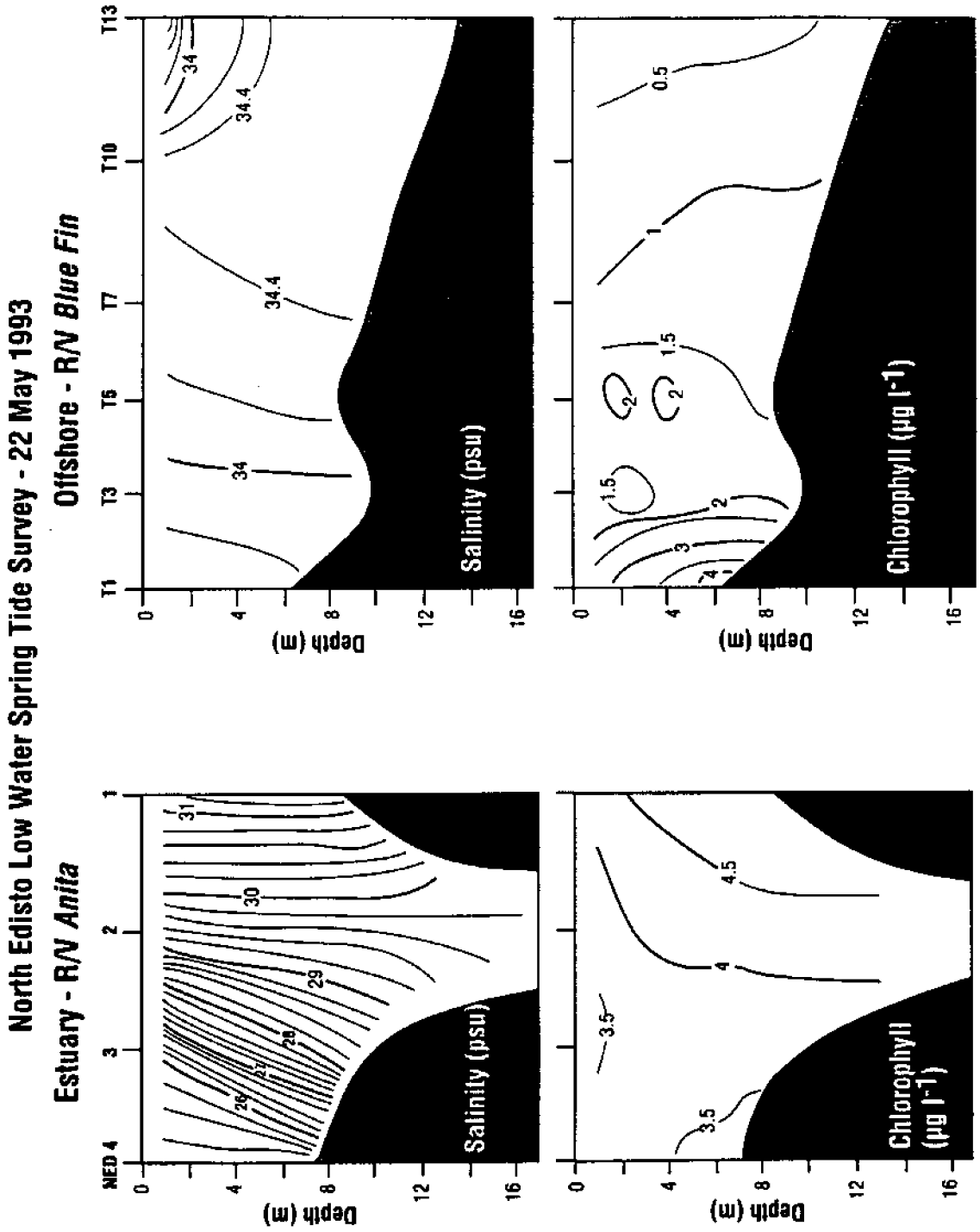
North Edisto Low Water Spring Tide Survey - 22 May 1993
Estuary - R/V Anita
Offshore - R/V Blue Fin
Salinity (psu)
Chlorophyll (µg l-1)
Depth (m)
NED 4
T1
T3
T5
T7
T10
T13

Figure 29 (c & d)

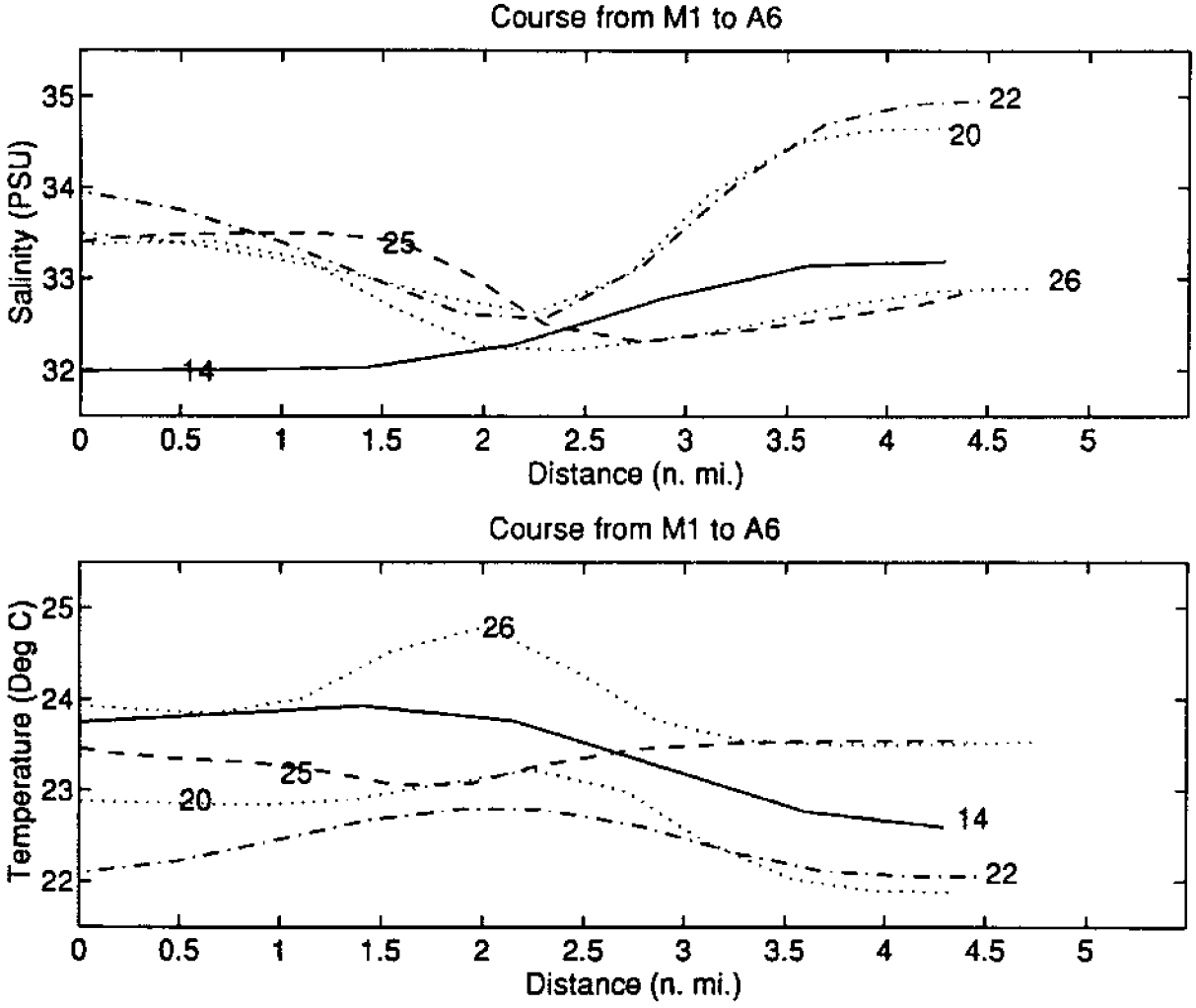
Course from M1 to A6
Salinity (PSU)
35
34
33
32
22
20
25
26
14
0
0.5
1
1.5
2
2.5
3
3.5
4
4.5
5
Distance (n. mi.)
Course from M1 to A6
Temperature (Deg C)
25
24
23
22
26
25
20
14
22
0
0.5
1
1.5
2
2.5
3
3.5
4
4.5
5
Distance (n. mi.)

Figure 30